



HAL
open science

Symmetric resonance based integrators and forest formulae

Yvonne Alama Bronsard, Yvain Bruned, Georg Maierhofer, Katharina Schratz

► **To cite this version:**

Yvonne Alama Bronsard, Yvain Bruned, Georg Maierhofer, Katharina Schratz. Symmetric resonance based integrators and forest formulae. 2024. <hal-04519788>

HAL Id: hal-04519788

<https://hal.science/hal-04519788v1>

Preprint submitted on 25 Mar 2024

HAL is a multi-disciplinary open access archive for the deposit and dissemination of scientific research documents, whether they are published or not. The documents may come from teaching and research institutions in France or abroad, or from public or private research centers.

L'archive ouverte pluridisciplinaire **HAL**, est destinée au dépôt et à la diffusion de documents scientifiques de niveau recherche, publiés ou non, émanant des établissements d'enseignement et de recherche français ou étrangers, des laboratoires publics ou privés.



HAL Authorization

Symmetric resonance based integrators and forest formulae

March 25, 2024

Yvonne Alama Bronsard¹, Yvain Bruned², Georg Maierhofer³, Katharina Schratz¹

¹ LJLL (UMR 7598), Sorbonne University

² IECL (UMR 7502), Université de Lorraine

³ DAMTP, University of Cambridge

Email: yvonne.alama-bronsard@sorbonne-universite.fr,

yvain.bruned@univ-lorraine.fr,

gam37@cam.ac.uk,

katharina.schratz@sorbonne-universite.fr.

Abstract

In the present work we introduce a unified framework that allows for the very first systematic construction of symmetric resonance-based integrators to approximate a wide class of nonlinear dispersive equations at low-regularity. The inclusion of symmetries in the construction of resonance-based schemes presents serious challenges and induces a need for a significant extension of prior approaches to allow for sufficient number of degrees of freedom in the resulting schemes while preserving the favorable low-regularity convergence properties of prior constructions. Motivated by recent work [15], we achieve this by introducing a novel formalism based on forest formulae that allows us to encode a wider range of possibilities of iterating Duhamel's formula and interpolatory approximations of lower order parts in the construction of these time-stepping methods. The forest formulae allow for a simple characterisation of symmetric schemes and provides a fascinating algebraic structure in its own right which echo those used in Quantum Field Theory for renormalising Feynman diagrams and those used for the renormalisation of singular SPDEs via the theory of Regularity Structures. Our constructions lead to the development of several new symmetric low-regularity integrators that exhibit remarkable structure preservation and convergence properties which are witnessed in numerical experiments.

Contents

1	Introduction	2
2	Main ideas of the derivation of symmetric resonance based schemes	8

3	Decorated trees and generalised resonance based schemes	15
3.1	Dominant part and polynomial interpolation	18
3.2	A forest formula for resonance based schemes	23
3.3	A more general forest formula	29
3.4	Midpoint general resonance based schemes	32
4	Symmetric schemes	39
4.1	Symmetric interpolation	39
4.2	Conditions for symmetry	42
4.3	Examples	46
5	Numerical Experiments	59
5.1	The Nonlinear Schrödinger equation	60
5.2	The Korteweg–de Vries equation	66
	References	68

1 Introduction

We consider a general class of dispersive differential equations of the form

$$\begin{aligned} i\partial_t u(t, x) + \mathcal{L}\left(\nabla, \frac{1}{\varepsilon}\right)u(t, x) &= |\nabla|^\alpha p(u(t, x), \bar{u}(t, x)), \\ u(0, x) &= v(x), \end{aligned} \quad (1.1)$$

equipped with periodic boundary conditions $x \in \mathbb{T}^d$. Throughout, we assume that p is a polynomial nonlinearity, and that the structure of (1.1) implies at least local well-posedness of the problem on a finite time interval $]0, T]$, $T < \infty$, in an appropriate functional space. This class of equations captures a number of physically important models, including the Korteweg de Vries (KdV) equation

$$\partial_t u - i\mathcal{L}(\nabla)u = \frac{1}{2}\partial_x u^2, \quad \mathcal{L}(\nabla) = i\partial_x^3, \quad |\nabla|^\alpha = \partial_x, \quad x \in \mathbb{T}, \quad (1.2)$$

and the nonlinear Schrödinger (NLS) equation,

$$i\partial_t u + \mathcal{L}(\nabla)u = |u|^2 u, \quad \mathcal{L}(\nabla) = \Delta, \quad x \in \mathbb{T}^d. \quad (1.3)$$

Like those two examples many physical equations in this class possess conservation laws, or are indeed integrable systems (for example the KdV equation is a completely integrable parity-time invariant system). It is known that symmetric numerical schemes have favourable long-time behaviour when applied to such reversible integrable systems, such as linear (slow) growth in error as a function of the integration time, and near conservation of first integrals over long times [35, 36, 8]. At the same time the numerical approximation of the Cauchy problem in low-regularity regimes requires the design of designated methods, amongst which resonance-based schemes have seen significant success over recent years. Firstly developed for specific equations, including the KdV equation [39, 63, 47], the NLS equation [55, 18, 4, 53, 54, 62, 6], the Gross–Pitaevskii equation [3] and the Navier–Stokes equations [46], more recent work has started to establish a more

general framework for resonance based low-regularity integrators [2, 1, 57]. The key idea of these schemes lies in embedding the underlying structure of resonances - triggered by the nonlinear frequency interactions between the leading differential operator $\mathcal{L}(\nabla, \frac{1}{\varepsilon})$ and the nonlinearity $p(u(t, x), \bar{u}(t, x))$ - into the numerical discretisation. These nonlinear interactions are in general neglected by classical approximation techniques such as Runge-Kutta methods, splitting methods or exponential integrators. While for smooth solutions these nonlinear interactions are indeed negligible, they do play a central role at low regularity and high oscillations. The accurate resolution of these interactions has been achieved in broad generality only in the recent few years in [15, 56, 2]. Yet, while the design of such schemes has seen a wide range of developments, prior work has focussed mostly on explicit schemes with desired convergence properties. A few recent results [7, 4, 29, 50] have introduced first or second order implicit symmetric integrators at low-regularity fitting the particular structure of the equation with better conservation properties. Nevertheless, a central question remained unanswered: *Can we systematically construct structure preserving resonance based schemes up to arbitrary order which preserve central symmetries of the underlying continuous equation?*

For ordinary differential equations (ODEs) the theory of *structure preservation* in numerical schemes is thoroughly established [36], specifically there is a extensive amount of literature on the characterisation of symmetric and symplectic Runge-Kutta methods [43, 59, 42] and, more broadly, B-series methods [9, 20]; on the favourable long-time behaviour of such methods when applied for finite-dimensional integrable reversible systems and Hamiltonian systems [35, 36, 8] respectively; and even on the limitations on types of structure that can be preserved with B-series methods [41]. Even though the long-time analysis of such methods in the case of PDEs is much less straightforward [28, 30], these favourable structure preservation properties have motived the study of symmetric methods for PDEs, for example in the classification of symmetric splitting methods [51] and symmetric exponential integrators [19].

In general, resonance based schemes are *not* structure preserving and do not preserve the symmetries in the system. We can consider for example the second order resonance based scheme introduced by [15, Section 5.1.2], referred to henceforth as ‘Bruned & Schratz 2022’, and given by

$$\begin{aligned} u^{n+1} = & e^{i\tau\Delta} u^n - i\tau e^{i\tau\Delta} \left((u^n)^2 (\varphi_1(-2i\tau\Delta) - \varphi_2(-2i\tau\Delta)) \bar{u}^n \right) \\ & - i\tau (e^{i\tau\Delta} u^n)^2 \varphi_2(-2i\tau\Delta) (e^{i\tau\Delta} \bar{u}^n) - \frac{\tau^2}{2} e^{i\tau\Delta} (|u^n|^4 u^n), \end{aligned} \quad (1.4)$$

where $\varphi_1(\sigma) = \frac{e^\sigma - 1}{\sigma}$ and $\varphi_2(\sigma) = \frac{e^\sigma - \varphi_1(\sigma)}{\sigma}$. Symmetry of a numerical scheme is defined by considering its adjoint method: For a given method $u^n \mapsto u^{n+1} = \Phi_\tau(u^n)$ its adjoint method is defined as $\widehat{\Phi}_\tau := \Phi_{-\tau}^{-1}$.

Definition 1 (See for example Definition V.1.4 in [36]) *The method Φ_τ is called symmetric if $\Phi_\tau = \widehat{\Phi}_\tau$.*

The scheme (1.4) is not symmetric in the sense of definition 1 because the adjoint method is given by

$$\begin{aligned} u^{n+1} = & e^{i\tau\Delta}u^n - i\tau\left((u^{n+1})^2(\varphi_1(2i\tau\Delta) - \varphi_2(2i\tau\Delta))\overline{u^{n+1}}\right) \\ & - i\tau e^{i\tau\Delta}\left((e^{-i\tau\Delta}u^{n+1})^2\varphi_2(2i\tau\Delta)(e^{-i\tau\Delta}\overline{u^{n+1}})\right) \\ & + \frac{\tau^2}{2}\left(|u^{n+1}|^4u^{n+1}\right), \end{aligned}$$

which is implicit as opposed to the original scheme (1.4), which is explicit.

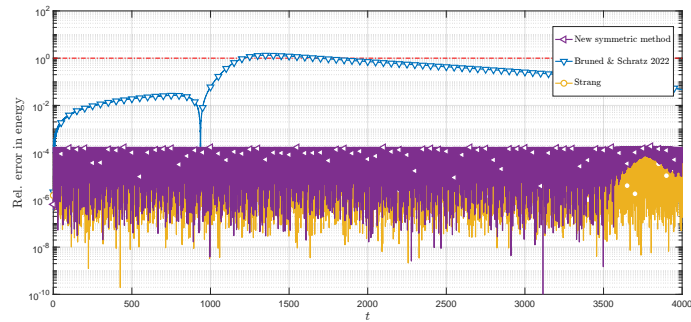
The derivation of new schemes which are structure preserving and at the same time allow for low-regularity approximations was first addressed in the specific case of the KdV, the Klein-Gordon (KG), the NLS equation and the isotropic Landau–Lifschitz equation in the recent work of [50], [61], [4] and [7] respectively. A further symmetric low-regularity integrator with good long time behaviour was introduced in [29]; see also [50] for the construction of symplectic resonance-based schemes. Let us also highlight the work [62] which was the first low regularity method which allowed for high order mass conservation (for fixed time). However, all these results are yet again tailored to the particular structure of the equation, and bespoke calculations made on individual resonance structure of the equation at hand. Furthermore, they are restricted to second order and not always optimal in the sense of regularity.

This motivates the study of systematic constructions of symmetric resonance based schemes that we address in the present work. In particular, we develop a unified framework of symmetric resonance based schemes which preserve central symmetries of the system (1.1) while allowing for good approximation in the regimes treated by [15]. We extend the resonance decorated trees approach introduced in [15] to a richer framework by exploring different ways of iterating Duhamel’s formula, capturing the dominant parts while interpolating the lower parts of the resonances in a symmetric manner. This gives a range of new numerical schemes with more degrees of freedom than the original framework from [15]. Our new framework allows us to recover previously constructed low-regularity symmetric schemes such as [4], but also introduce new symmetric low regularity schemes which are optimal in the sense of regularity - in the spirit of [15]. An example of such a method introduced in the present work is (4.18) matching the regularity obtained for the non-symmetric scheme given in [15]. In addition, as opposed to the previous works [15, 1, 2] the schemes we introduce here do not need to be accompanied by well-chosen filter functions in order to obtain stability of the scheme. Indeed, our construction based on interpolation rather than Taylor series expansion of the non-dominant parts of the nonlinear frequency interactions directly leads to stable schemes, see also [56, 3].

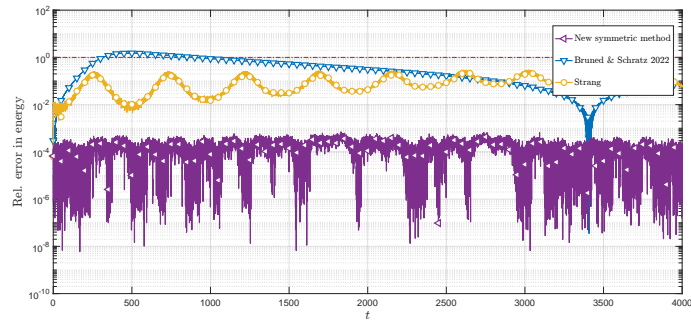
Our main result is the new general resonance based scheme presented in Definition 3.13, with its error structure given in Theorem 3.19, the latter of which is a consequence of [15]. We show that this scheme is symmetric in Theorem 4.3 and

that it is contained within a forest formula in Theorem 3.15. Our general framework is illustrated on concrete examples in Section 4.3 and simulations show the better structure preserving properties as well as the convergence properties of the scheme. This was only possible through a significant extension of the algebraic structures proposed in [15] by introducing new forest formulae in Theorem 3.6 and Theorem 3.8. These formulae are used for finding new symmetric schemes and have their own interest by providing a new parametrisation of low regularity schemes allowing for implicitness in the schemes and thus resembling more closely the formulation of classical schemes such as Runge–Kutta methods or exponential integrators. We derive conditions on the coefficients of these formulae for having a symmetric scheme, see Proposition 4.7.

Remark 1.1 Up to now we were faced with a choice between structure preservation and low-regularity approximation properties. This is exhibited in Figure 1 where we study the cubic NLS equation and compare the preservation of energy of the Strang splitting (a symmetric splitting method) against previous resonance based integrators (Bruned & Schratz 2022 [15]) for smooth C^∞ and H^2 data.



(a) Smooth data, $u_0 \in C^\infty$ and $M = 64$.



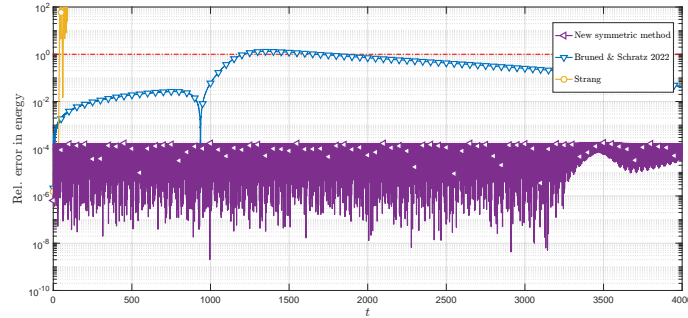
(b) Low regularity data, $u_0 \in H^2$ and $M = 64$.

Figure 1: Long-time relative error in the energy of the NLS equation with time-step $\tau = 0.02$.

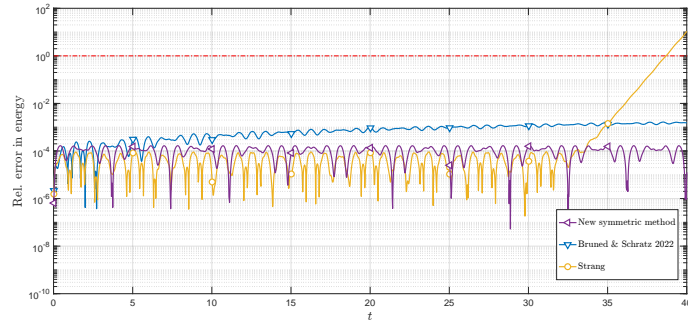
The Strang splitting almost preserves the energy over long times for smooth solutions, but suffers from numerical energy blow up for rougher data. The

resonance based integrator Bruned & Schratz 2022 [15] on the other hand only achieves approximate energy preservation up to short times (for both smooth and rougher data). Our novel resonance based midpoint method (4.18) bridges this gap allowing for numerical long-time approximate energy conservation even at low regularity, see Figure 1b.

Let us now take a closer look at smooth solutions, where we find a surprising additional characteristic of our new scheme (4.18). Note that long-time structure preservation properties apply only subject to a CFL condition for Strang splitting methods applied to the NLS equation. More precisely the time step size τ has to be chosen such that $\tau \lesssim M^{-2}$ where M is the number of degrees of freedom in the spatial discretisation, see for instance [28] and references therein for a detailed discussion. This step size restriction is not only a theoretical technicality, but also observed in numerical experiments. The long-time energy preservation in the Strang splitting drastically breaks down if we start to increase the number of Fourier modes M , i.e., move from “ODE to PDE”, see Figure 1a versus Figure 2, where we double the Fourier modes in our discretisation. A very interesting feature of our new resonance-based constructions appears to be that in numerical experiments the long-time behaviour of the method seemingly does not depend on the number M of spatial modes used.

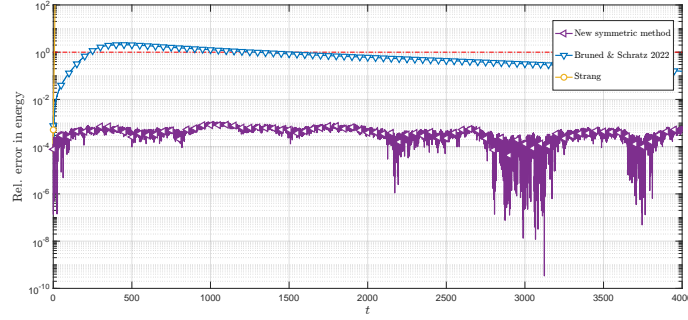


(a) Long time interval $t \in [0, 4000]$, smooth data $u_0 \in C^\infty$ and $M = 256$.

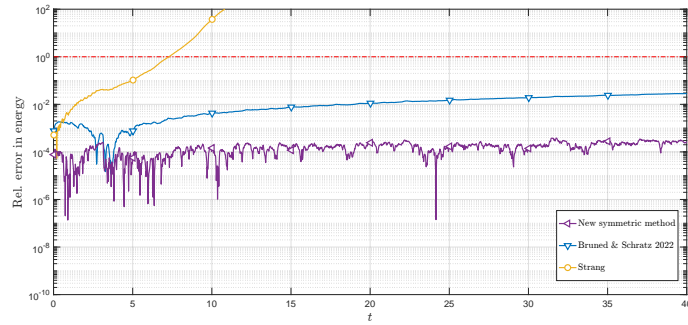


(b) Zoom on time interval $t \in [0, 40]$, smooth data $u_0 \in C^\infty$ and $M = 256$.

Figure 2: Long-time relative error in the energy of the NLS equation with time-step $\tau = 0.02$.



(a) Long time interval $t \in [0, 4000]$, low-regularity data $u_0 \in H^2$ and $M = 256$.



(b) Zoom on time interval $t \in [0, 40]$, low-regularity data $u_0 \in H^2$ and $M = 256$.

Figure 3: Long-time relative error in the energy of the NLS equation with time-step $\tau = 0.02$.

In summary, the long-time dynamics shown in Figures 1-3 is representative of the behaviour of these methods and is observed in a large number of numerical experiments. Namely, we have that the Strang splitting is able to approximately preserve the energy over long times only for a small number of spatial discretisation points and for smooth initial data ($M \ll \tau^{-1/2}$). In contrast, our proposed symmetric low-regularity integrators can achieve this feat even for low regularity solutions and with a large number of spatial discretisation points.

Outline of the article

The remainder of this manuscript is structured as follows. To begin with, in section 2, we outline the main ideas in the construction of symmetric resonance based schemes, before formalising those ideas more rigorously in the subsequent sections. In particular, in section 3 we firstly recall the decorated tree framework introduced in [15] for non-symmetric resonance based schemes. We then generalise this framework in order to capture a broader class of resonance based integrators allowing for polynomial interpolation of lower order parts in the approximation (cf. section 3.1). This leads to a general framework taking the form of a forest formula that can capture a wide class of implicit and explicit resonance based schemes and which is introduced in section 3.2 followed by a generalisation in section 3.3.

This forest formula motivates our consideration of a particular way of iterating Duhamel’s formula to generate a subclass of resonance based schemes described by this general framework in section 3.4 which turns out to be sufficiently general to allow us to find symmetric resonance based schemes of arbitrary order in this class. In section 4 we then describe how symmetric interpolation in the construction from section 3.4 leads to symmetric schemes before classifying all symmetric schemes captured by the general forest formula in section 4.2. We conclude the section with examples of the new symmetric resonance based integrators that can be found using our novel framework in section 4.3. In section 5, we provide numerical experiments demonstrating the favorable practical performance of the new symmetric resonance based schemes that we were able to develop using our formalism.

Acknowledgements

K. S. and Y. A. B. received financial support from the European Research Council (ERC) under the European Union’s Horizon 2020 research and innovation programme (grant agreement No. 850941). Y. B. received financial support from the European Research Council (ERC) (ERC Starting Grant grant agreement No. 101075208) and from the ANR via the project LoRDeT (Dynamiques de faible régularité via les arbres décorés) from the projects call T-ERC_STG. G. M. gratefully acknowledges funding from the European Union’s Horizon Europe research and innovation programme under the Marie Skłodowska–Curie grant agreement No. 101064261.

2 Main ideas of the derivation of symmetric resonance based schemes

Before diving into a more abstract construction of the algebraic structures describing our novel resonance based schemes let us begin by outlining the main assumptions on the type of equation we consider as well as the blueprint for the construction of implicit (and specifically symmetric) resonance based integrators for equations of the form (1.1).

Assumptions

We impose periodic boundary conditions, i.e. $x \in \mathbf{T}^d$. We assume that the differential operator \mathcal{L} is real and that the differential operators $\mathcal{L}(\nabla)$ and $|\nabla|^\alpha$ shall cast in Fourier space into the form

$$\mathcal{L}(\nabla)(k) = k^\sigma + \sum_{\gamma:|\gamma|<\sigma} a_\gamma \prod_j k_j^{\gamma_j}, \quad |\nabla|^\alpha(k) = \sum_{\gamma:|\gamma|\leq\alpha} \prod_{j=1}^d k_j^{\gamma_j} \quad (2.1)$$

for some $\alpha \in \mathbf{R}$, $\sigma \in \mathbf{N}$, $\gamma \in \mathbf{Z}^d$ and $|\gamma| = \sum_i \gamma_i$, where for $k = (k_1, \dots, k_d) \in \mathbf{Z}^d$ and $m = (m_1, \dots, m_d) \in \mathbf{Z}^d$ we set

$$k^\sigma = k_1^\sigma + \dots + k_d^\sigma, \quad k \cdot m = k_1 m_1 + \dots + k_d m_d.$$

Construction of implicit resonance based schemes

We first rewrite (1.1) in Duhamel's form

$$u(t, x) = e^{it\mathcal{L}} v(0, x) - ie^{it\mathcal{L}} \int_0^t e^{-is\mathcal{L}} |\nabla|^\alpha p(u(s, x), \bar{u}(s, x)) ds$$

where we have used $\mathcal{L} = \mathcal{L}(\nabla, \frac{1}{\varepsilon})$ as a short hand notation. Then, if we move to Fourier space by denoting u_k and v_k the k -th Fourier coefficients of u and v , one obtains:

$$u_k(t) = e^{it\mathcal{L}(k)} v_k(0) - ie^{it\mathcal{L}(k)} \int_0^t e^{-is\mathcal{L}(k)} |\nabla|^\alpha(k) p_k(u(s, x), \bar{u}(s, x)) ds \quad (2.2)$$

where $\mathcal{L}(k)$ and $|\nabla|^\alpha(k)$ are the differential operators \mathcal{L} and $|\nabla|^\alpha$ mapped in Fourier space. The term $p_k(u(s, x), \bar{u}(s, x))$ stands for the Fourier transform of the product. For example, in the case of NLS we have $\alpha = 0$, $\mathcal{L} = \Delta$, and $p(u, \bar{u}) = u^2 \bar{u}$. The equation (2.2) becomes

$$u_k(t) = e^{-itk^2} v_k(0) - ie^{-itk^2} \int_0^t e^{isk^2} \left(\sum_{k=-k_1+k_2+k_3} \bar{u}_{k_1}(s) u_{k_2}(s) u_{k_3}(s) \right) ds.$$

The product $|u|^2 u$ becomes a convolution on the coefficients in Fourier space, where we note that the minus pre-multiplying k_1 is due to the conjugate. We have also used the fact that the Fourier transform of $e^{it\Delta}$ is e^{-itk^2} . The first step in the construction of resonance based schemes consists in iterating (2.2) inside the nonlinearity which produces a sum of oscillatory integrals that can be described by decorated trees as introduced in [15]. Namely, in [15] we iterate only with (2.2) which corresponds to a left end point iteration, meaning that given a time step τ , we always take the left end point approximation in the linear part $\exp(-itk^2)v_k(0)$ on the interval $[0, \tau]$. Hence, in general we do not obtain a symmetric scheme. Indeed, one has the possibility to write Duhamel's formula around any point in the interval $[0, \tau]$. In particular, if we set for $s \in [0, \tau]$

$$\begin{aligned} I(k, u, s, t) &= e^{i(t-s)\mathcal{L}(k)} u_k(s) \\ &\quad - ie^{it\mathcal{L}(k)} \int_s^t e^{-i\tilde{s}\mathcal{L}(k)} |\nabla|^\alpha(k) p_k(u(\tilde{s}, x), \bar{u}(\tilde{s}, x)) d\tilde{s} \end{aligned} \quad (2.3)$$

then we have the identity:

$$u_k(t) = I(k, u, v, s, t).$$

From the identity (2.3), we will obtain implicit schemes. We can take a weighted sum of the various Duhamel's iterations (2.3) ultimately to arrive at schemes with a large number of additional degrees of freedom. The sum that we will use for a large part of this paper is the midpoint rule, that is:

$$u_k(t) = \frac{1}{2} (I(k, u, 0, t) + I(k, u, \tau, t)). \quad (2.4)$$

For example, to construct a symmetric resonance based scheme of a desired order we can start the first iteration for $u_k(\tau)$ with the left end point Duhamel's formula and then we iterate the midpoint rule (2.4). We can express this iteration in terms of the following tree series

$$U_{\text{mid},k}^r(\tau) = e^{i\tau\mathcal{L}} u_k(0) + \sum_{T \in \mathcal{V}_k^r} \frac{\Upsilon_{\text{mid}}^p(T)(u, \tau)}{S(T)} (\Pi_{\text{mid}} T)(\tau) \quad (2.5)$$

where \mathcal{V}_k^r is a set of decorated trees of size at most $r + 1$ which incorporate the frequency k . These trees encode via $(\Pi_{\text{mid}} T)(\tau)$, iterated integrals of depth at most $r + 1$. The coefficient $S(T)$ is the symmetry factor associated to the tree T and $\Upsilon_{\text{mid}}^p(T)(u, \tau)$ is the coefficient appearing in the iteration of Duhamel's formulation depending on the nonlinearity p . The coefficients $\Upsilon_{\text{mid}}^p(T)(u, \tau)$ depend on τ as with our midpoint iteration, we finish always on terms of the form:

$$\frac{1}{2} \left(e^{is\mathcal{L}} u_{k_j}(0) + e^{i(s-\tau)\mathcal{L}} u_{k_j}(\tau) \right) = e^{is\mathcal{L}} \frac{1}{2} \left(u_{k_j}(0) + e^{-i\tau\mathcal{L}} u_{k_j}(\tau) \right).$$

It is natural to absorb the term $e^{is\mathcal{L}}$ in the definition of $(\Pi_{\text{mid}} T)(\tau)$ and

$$\frac{1}{2} \left(u_{k_j}(0) + e^{-i\tau\mathcal{L}} u_{k_j}(\tau) \right)$$

into the definition of $\Upsilon_{\text{mid}}^p(T)(u, \tau)$. These aforementioned quantities are described in detail in Section 3.4. The sum (2.5) can be viewed as a first numerical approximation by keeping only the iterated integrals of order below r of the infinite series describing formally the solution of (1.1). In Proposition 4.1, we show that (2.5) is a symmetric scheme.

In order for the scheme to have a suitable local error when applied to low-regularity solutions, it is necessary to replace each oscillatory integral $(\Pi_{\text{mid}} T)(\tau)$ appearing in the finite sum (2.5) by a low regularity approximation that embeds the resonance structure into the numerical discretization. Our novel approach is to try and perform this approximation in a symmetric manner. Let us explain briefly how it works. Suppose we aim to discretise an oscillatory integral of the form

$$\int_0^t e^{is\mathcal{L}} ds, \quad \mathcal{L} = \mathcal{L}_{\text{dom}} + \mathcal{L}_{\text{low}},$$

where we have split the operator into a dominant part \mathcal{L}_{dom} that we will integrate exactly and a lower part \mathcal{L}_{low} that we will approximate (cf. section 3.1 for a definition of these quantities). A typical example arising in the case of NLS is

$$\mathcal{L} = k^2 + k_1^2 - k_2^2 - k_3^2, \quad \mathcal{L}_{\text{dom}} = 2k_1^2 \quad \mathcal{L}_{\text{low}} = -2k_1(k_2 + k_3) + 2k_2k_3,$$

where $k = -k_1 + k_2 + k_3$. We see that the exact integration of

$$\int_0^t e^{is\mathcal{L}_{\text{dom}}} ds = \frac{e^{2isk_1^2} - 1}{2ik_1^2}$$

can be mapped back to physical space as $1/k^2$ corresponds to Δ^{-1} . This property of being able to write the scheme in physical space is crucial for efficient numerical implementation: If we have an expression in physical space the differential operators can be computed quickly in *frequency* space using the Fast Fourier Transform (FFT) while any polynomial-type nonlinear term can be computed quickly in *physical* space since it corresponds to a local operation on the function values on a grid. Now, it remains to approximate the lower part. For this task, we use a polynomial interpolation with $m + 1$ points on $[0, \tau]$ denoted by $a_j \tau$. We note that the error incurred by this polynomial interpolation will be one of the determining factors of the convergence order of our overall numerical scheme, and thus we highlight that this interpolation can be done to any given order. We take $r + 1$ distinct interpolation points $0 \leq a_0 < a_1 < \dots < a_r \leq 1$ which are symmetrically distributed such that $a_j = 1 - a_{r-j}$, $j = 0, \dots, r$. Let us denote the corresponding nodal polynomials by $p_{j,r}$ such that

$$p_{j,r}(a_m \tau) = \delta_{j,m}.$$

Then, we define the following approximation

$$\tilde{p}_r(f, \xi) = \sum_{j=0}^r f(a_j) p_{j,r}(\xi), \quad f(a_j) = e^{ia_j \tau \mathcal{L}_{\text{low}}}.$$

We have the following local error

$$f(\xi) - \tilde{p}_r(f, \xi) = \mathcal{O}\left(\prod_{j=0}^r (\xi - a_j \tau) (i\mathcal{L}_{\text{low}})^{r+1}\right) \quad (2.6)$$

which requires less regularity than if we had chosen to base our approximation on \mathcal{L} instead of \mathcal{L}_{low} as classical schemes do.

In order to arrive at a numerical scheme, we will in the following introduce the low-regularity symmetric approximation operator of Π_{mid} denoted by $\Pi_{\text{mid}}^{n,r}$. Here, r corresponds to the order of the discretization and n is the a priori regularity assumed on the initial data v . Namely, we assume $v \in H^n$, where H^n is a Sobolev space. The general scheme then takes the form:

$$U_{\text{mid},k}^{n,r}(\tau, u) = \sum_{T \in \mathcal{T}_k^r} \frac{\Upsilon_{\text{mid}}^p(T)(u, \tau)}{S(T)} (\Pi_{\text{mid}}^{n,r} T)(\tau). \quad (2.7)$$

We will show in Theorem 4.3 that this scheme is symmetric. The local error structure for each approximated iterated integral is given by

$$(\Pi_{\text{mid}} T - \Pi_{\text{mid}}^{n,r} T)(\tau) = \mathcal{O}\left(\tau^{r+2} \mathcal{L}_{\text{low}}^r(T, n)\right), \quad (2.8)$$

where $\mathcal{L}_{\text{low}}^r$ involves only lower order derivatives. Its proof is exactly the same as in [15]. The local error does not depend on the choice of Duhamel's iteration

and polynomial interpolations. The form of the scheme draws its inspiration from the treatment of singular stochastic partial differential equations (SPDEs) via Regularity Structures in [33, 12, 10, 13]. These decorated tree expansions are generalization of the B-series widely used for ordinary differential equations, we refer to [17, 19, 36, 52] and tree series used for dispersive equations [25, 31, 32, 48, 38]. In the end, one obtains an approximation of u under much lower regularity assumptions than classical methods (e.g., splitting methods, exponential integrators [21, 28, 36, 37, 40, 44, 49, 45, 51, 58]) require, which in general introduce the local error

$$\mathcal{O}(\tau^{r+2}\mathcal{L}^r(T, n)) \quad (2.9)$$

involving the full high order differential operator \mathcal{L}^r . Indeed, denoting by $\mathcal{D}(\cdot)$ the domain of a given operator, we have that $\mathcal{D}(\mathcal{L}_{\text{low}}) \supset \mathcal{D}(\mathcal{L})$, meaning that the local error structure (2.8) allows us to deal with a rougher class of solutions than the classical error bound (2.9). Let us mention that the local error analysis can be nicely understood via a Birkhoff factorisation of the character $\Pi_{\text{mid}}^{n,r}$ (see [15, 11]) that involves a deformed Butcher-Connes-Kreimer coproduct (see [17, 23, 24, 15, 14]). In the present work, we push further the algebraic perspective by writing several forest formulae that can be used to represent a larger class of low regularity schemes. These forest formulae take the following form:

$$\begin{aligned} u_k^{\ell+1} &= e^{i\tau\mathcal{L}}u_k^\ell + e^{i\tau\mathcal{L}} \sum_{T \in \tilde{\mathcal{T}}_k^r} \sum_{\mathbf{a} \in [0,1]^{\tilde{E}_T}} \sum_{\chi \in \{0,1\}^{L_T}} \sum_{T_0 \cdot T_1 \dots T_m \subset T} C_T \\ & b_{\mathbf{a}, \chi, T, T_0 \dots T_m}(\tau, i\tau \mathcal{F}_{\text{dom}}(T_j), j \in \{0, \dots, m\}) \\ & \prod_{e \in \tilde{E}_{T_j}} e^{i\tau a_e \mathcal{F}_{\text{low}}(T_j^e)} \frac{\Upsilon_\chi^p(T)(u_{k_v}^{\ell+\chi_v}, v \in L_T, \tau)}{S(T)}. \end{aligned} \quad (2.10)$$

Below, we give a brief description of the notation of this forest formula before introducing each term in full detail in section 3. Here, \mathcal{L} is the full operator of (1.1), $\tilde{\mathcal{T}}_k^r$ is a finite set of decorated trees, \tilde{E}_T denotes the edges of T that correspond to a time integration. These time integrals are discretised with a low regularity approximation. Therefore, we have to use a map \mathbf{a} on these edges that specifies which interpolation points have been used. This corresponds to the following term

$$\prod_{e \in \tilde{E}_{T_j}} e^{i\tau a_e \mathcal{F}_{\text{low}}(T_j^e)}$$

Here $\mathcal{F}_{\text{low}}(T_j^e)$ denote the lower part of the various discretisations where T_j^e is included into T_j . The set L_T are the leaves of T associated to some u_{k_u} and the map χ specifies if they are evaluated at the right ($u_{k_u}^\ell$) or left end point ($u_{k_u}^{\ell+1}$). The coefficients $\Upsilon_\chi^p(T)(u_{k_v}^{\ell+\chi_v}, v \in L_T, \tau)$ depend on the structure of the equation and the way one iterates Duhamel's formula. One essential choice of this forest

formula is the splitting of T into a forest $T_0 \cdot \dots \cdot T_m$ where the T_i are decorated trees. This allows us to encode all the lower parts of the resonances $\mathcal{F}_{\text{low}}(T_j^e)$ and all their dominant parts $\mathcal{F}_{\text{dom}}(T_j)$ that appear in the low regularity discretisation. As we shall see below, this forest splitting is a crucial novelty necessary for the construction and classification of symmetric low-regularity integrators. For the splitting, one can use a Butcher-Connes-Kreimer coproduct (see Section 3.2) or a deformed Butcher-Connes-Kreimer coproduct used for the local error analysis (see Section 3.3). The difference between the two is that one provides more terms in the deformed forest formula (deformed Butcher-Connes-Kreimer coproduct) and therefore more degrees of freedom for finding new schemes. In our applications so far, the forest formula without deformation is enough for finding symmetric schemes. We derive a condition on the coefficients $b_{\mathbf{a}, \chi, T, T_0 \dots T_m}$ in Proposition 4.7 that allows to find symmetric schemes. The coefficients $b_{\mathbf{a}, \chi, T, T_0 \dots T_m}$ do not depend on the frequencies that are node decorations of the trees T, T_j . One can see them only as functions of the dominant parts of the various operators encountered during the discretisation. The term C_T is a structure term depending on the frequencies that encode the various operators that appear in the iterated integral given by T . We conclude this section with a few remarks concerning the structures introduced and the properties of the resulting low-regularity schemes.

Remark 2.1 The forest formula appear in the BPHZ algorithm [16, 34, 64] for renormalising Feynman diagrams and was later used for renormalising singular SPDEs in [12, 22] with an extension of the algebraic structure.

Remark 2.2 The scheme (2.7) has been generalized to non-polynomial nonlinearities and to parabolic equations in [2] with the use of nested commutators first introduced in [56]. The Birkhoff factorisation discovered in [15] is not available in this case. It is also not obvious to translate forest formulae into this context. Indeed, due to the fact that the formula is written in Fourier space, there is no order on the operators written in Fourier space. This is not the case in physical space. But one can repeat the construction of the scheme $U_k^{n,r}$ in this context and this scheme should be symmetric as the recursive proofs in Section 4.1 seem robust to this case.

Remark 2.3 The schemes presented in [15] have been adapted to a probabilistic setting by proposing a low regularity approximation [1] of the second moment of the Fourier coefficient of the solution, i.e. $\mathbb{E}(|u(v^\eta, \tau)|^2)$ where v^η is a random initial data. In this context, one has to work with paired decorated trees. It possible to write symmetric schemes for approximating this second moment using our approach. Also, one can set up an equivalent forest formula on these paired decorated trees. One open direction is to understand the connection between the algebraic tools developed for these numerical schemes and the tools used for the rigorous derivation of the wave kinetic equation (WKE) for NLS is performed in [27, 26, 5]

Remark 2.4 The central novelty of the present work is the structured understanding of implicit and, in particular, symmetric low-regularity integrators. The local error

bounds we use in this paper often rely on the previous local error derivations first introduced in [15]. Indeed, the scheme $U_k^{n,r}(\tau, u)$ is of the form (2.10) but the local error analysis comes from the fact that it is defined recursively via the character $\Pi_{\text{mid}}^{n,r}$ and therefore the tools from [15] are available. If one found a new scheme by choosing the coefficients $b_{\mathbf{a}, \chi, T, T_0, \dots, T_m}$, it is not clear how to get directly the local error analysis and check that the scheme is optimal in terms of regularity.

We also make the important remark that given that we derive schemes which are of implicit nature, an additional fixed-point argument needs to be performed on the numerical flow in order to rigorously buckle the local error bounds, we refer to the works of [50, 4] where this analysis is made in detail.

Remark 2.5 On this forest formula, we have identified symmetric schemes and, in addition, we have provided a general recursive mechanism to derive symmetric schemes for a large class of PDEs. One can wonder if such an approach could be repeated for other symmetries. Indeed, we believe that our techniques are fairly general. The degrees of freedom offered by different Duhamel's iterations and interpolations should allow us to capture other symmetries at low regularity using variants of the recursive scheme $U_k^{n,r}(\tau, u)$. One degree of freedom which has not been used in full generality is the splitting of the operator into dominant and lower part :

$$\mathcal{L} = \mathcal{L}_{\text{dom}} + \mathcal{L}_{\text{low}}.$$

Right now, it is governed by Definition 3.1 that guarantees to get a resonance-based scheme and a scheme which can be written in physical space. For symplectic schemes, one expects to have symmetries between the frequencies of \mathcal{L}_{dom} and those \mathcal{L}_{low} . One should have the possibility of refining this splitting for encapsulating some symmetries as has been done for the 1D NLSE and the KdV equation in recent work [50]. The rest of the construction of the scheme remains unchanged. Consequently, a natural line of future research is the study of such symmetries (ϱ -reversibility, preservation of quadratic invariants, etc.) directly on a structured tree or forest expansion of the numerical schemes comparable to the use of B-series in the study of structure preservation properties of methods for ODEs. We believe that the forest formulae presented in the current work take a first step in this direction.

Remark 2.6 Let us close this section with an interesting, but crucial observation: In the context of ODEs it is well known that symmetric methods are of even order (cf. [36, Theorem IX.2.2]). In general this is, however, *not* the case for PDEs as the rate of convergence depends intrinsically on the regularity of the solution, and hence convergence at even order only holds if sufficient regularity requirements are met by the solution. For instance, the resonance based midpoint method for the NLS

equation takes the form (see Section 4.3.1 below for its derivation)

$$\begin{aligned} u^{n+1} &= e^{i\tau\Delta} u^n \\ &\quad - i \frac{\tau}{16} e^{i\tau\Delta} \left((u^n + e^{-i\tau\Delta} u^{n+1})^2 \varphi_1(-2i\tau\Delta) \left(\overline{u^n} + e^{i\tau\Delta} \overline{u^{n+1}} \right) \right) \\ &\quad - i \frac{\tau}{16} \left((e^{i\tau\Delta} u^n + u^{n+1})^2 \varphi_1(2i\tau\Delta) \left(e^{-i\tau\Delta} \overline{u^n} + \overline{u^{n+1}} \right) \right). \end{aligned} \quad (2.11)$$

This scheme is symmetric and first order with optimal local error structure in the sense of [15], as its first order local error structure $\mathcal{O}(\tau^2 \nabla u)$ does not require more regularity on the solution than the asymmetric first order resonance based schemes of [15, 55]. As the scheme (2.11) is symmetric it is, for C^∞ solutions, naturally of even order, hence, not only of order one, but also of order two. However, a closer look shows that its second order convergence is only attained for sufficiently regular solutions: With a similar error analysis as introduced in [4] one can show that at second order the symmetric scheme (2.11) introduces a local error of type $\mathcal{O}(\tau^3 \nabla \Delta u)$ which requires the boundedness of three additional derivatives in order to attain second order convergence. For initial data in lower order spaces than H^3 , one can obtain fractional convergence of order *less than two*, see [4]. We make the additional remark that in view of [15], requiring a local error of $\mathcal{O}(\tau^3 \nabla \Delta u)$ is not optimal in the sense of regularity. Indeed, we recall that the second-order non-symmetric resonance based integrators [15] obeys the favourable error structure $\mathcal{O}(\tau^3 \Delta u)$, hence asking for one less derivative on the solution.

3 Decorated trees and generalised resonance based schemes

The main object of this manuscript is to formalise the construction of symmetric resonance based schemes as outlined in section 2. To achieve this we resort to a new, generalised tree formalism which has already seen (in much simpler version) significant success in the construction of explicit (asymmetric) resonance based schemes (cf. [15]). In the present section we will begin by recalling some of the main definitions in this framework before generalising the construction to incorporate the possibility of implicit low-regularity integrators before ultimately culminating in a forest formula (3.16) & (3.23) which captures a broad class of resonance based numerical schemes in such way that we can later characterise those schemes in this class which are symmetric in the sense of definition 1.

We recall briefly the structure of decorated trees introduced in [15, Sec. 2]. Let \mathcal{L} a finite set and frequencies $k_1, \dots, k_m \in \mathbf{Z}^d$. We suppose we are given a fixed time step $\tau > 0$. The set \mathcal{L} parametrizes a set of differential operators with constant coefficients, whose symbols are given by the polynomials $(P_l)_{l \in \mathcal{L}}$. These operators are given in Fourier space and therefore the polynomials will be evaluated in the frequencies k_j . We define the set of decorated trees $\hat{\mathcal{T}}$ as elements of the form $T_\epsilon^{n,0} = (T, \mathbf{n}, \sigma, \epsilon)$ where

- T is a non-planar rooted tree with root ρ_T , node set N_T and edge set E_T . We denote the leaves of T by L_T . T must also be a planted tree which means that

there is only one edge connecting the root to the rest of the tree.

- the map $\epsilon : E_T \rightarrow \mathcal{L} \times \{0, 1\}$ are edge decorations. The set $\{0, 1\}$ encodes the action of taking the conjugate, and determines the sign of the frequencies at the top of this edge. Namely, we have that 1 corresponds to a conjugate and to multiplying by (-1) the frequency on the node above and adjacent to this edge.
- the map $\mathfrak{n} : N_T \setminus \{\varrho_T\} \rightarrow \mathbf{N}^2$ are node decorations. For every inner node v , this map encodes a monomial of the form $\xi^{\mathfrak{n}_1(v)} \tau^{\mathfrak{n}_2(v)}$ where ξ is a free time variable belonging to $[0, \tau]$. This is a novelty from [15] where we do not have factors in τ . We need it as in the sequel, we will consider integrals of the form $\int_{\tau}^{\xi} \dots ds$.
- the map $\mathfrak{o} : N_T \setminus \{\varrho_T\} \rightarrow \mathbf{Z}^d$ are node decorations. These decorations are frequencies that satisfy for every inner node u :

$$(-1)^{\mathfrak{p}(e_u)} \mathfrak{o}(u) = \sum_{e=(u,v) \in E_T} (-1)^{\mathfrak{p}(e)} \mathfrak{o}(v) \quad (3.1)$$

where $\epsilon(e) = (\mathfrak{t}(e), \mathfrak{p}(e))$ is the edge decoration of e with $\mathfrak{t}(e) \in \mathcal{L}$ and $\mathfrak{p}(e) \in \{0, 1\}$ and e_u is the unique edge outgoing from u which is part of the path connecting u to the root. We denote this edge by (v, u) . From this definition, one can see that the node decorations at the leaves $(\mathfrak{o}(u))_{u \in L_T}$ determine the decoration of the inner nodes. One can call this identity Kirchhoff's law. We assume that the node decorations at the leaves are linear combinations of the k_i with coefficients in $\{-1, 0, 1\}$.

- we assume that the root of T has no decoration.

When the node decoration \mathfrak{n} is zero, we will denote the decorated trees $T_{\epsilon}^{\mathfrak{n}, \mathfrak{o}}$ as $T_{\epsilon}^{\mathfrak{o}} = (T, \mathfrak{o}, \epsilon)$. The set of decorated trees satisfying such a condition is denoted by $\hat{\mathcal{T}}_0$. We set \hat{H} (resp. \hat{H}_0) the (unordered) forests composed of trees in $\hat{\mathcal{T}}$ (resp. $\hat{\mathcal{T}}_0$) with linear spans $\hat{\mathcal{H}}$ and $\hat{\mathcal{H}}_0$. The forest product is denoted by \cdot , the empty forest by $\mathbf{1}$. Elements in $\hat{\mathcal{T}}$ are abstract representation of iterated time integrals and elements in \hat{H} are a product of them.

We now introduce how one can represent uniquely decorated trees by using symbolic notations. We denote by \mathcal{F}_o , an edge decorated by $o = (\mathfrak{t}, \mathfrak{p}) \in \mathcal{L} \times \{0, 1\}$. We introduce the operator $\mathcal{F}_o(\lambda_k^{\ell} \cdot) : \hat{\mathcal{H}} \rightarrow \hat{\mathcal{H}}$ that merges all the roots of the trees composing the forest into one node decorated by $(\ell, k) \in \mathbf{N}^2 \times \mathbf{Z}^d$. The new decorated tree is then grafted onto a new root with no decoration. If the condition (3.1) is not satisfied on the argument then $\mathcal{F}_o(\lambda_k^{\ell} \cdot)$ gives zero. If $\ell = 0$, then the term λ_k^{ℓ} is denoted by λ_k as a short hand notation for λ_k^0 . The forest product between $\mathcal{F}_{o_1}(\lambda_{k_1}^{\ell_1} F_1)$ and $\mathcal{F}_{o_2}(\lambda_{k_2}^{\ell_2} F_2)$ is given by:

$$\mathcal{F}_{o_1}(\lambda_{k_1}^{\ell_1} F_1) \mathcal{F}_{o_2}(\lambda_{k_2}^{\ell_2} F_2) := \mathcal{F}_{o_1}(\lambda_{k_1}^{\ell_1} F_1) \cdot \mathcal{F}_{o_2}(\lambda_{k_2}^{\ell_2} F_2).$$

The right hand side of the previous equality could be understood as a set where we can repeat elements and the forest product is the disjoint union of these sets. Any decorated tree T is uniquely represented as

$$T = \mathcal{F}_o(\lambda_k^{\ell} F), \quad F \in \hat{H}.$$

Given an iterated integral, its size is given by the number of integrations in time. Therefore, we suppose we are given a subset \mathcal{L}_+ of \mathcal{L} that encodes edge decorations which correspond to time integrals that we have to approximate.

Example 2 We illustrate the definitions introduced above with decorated trees coming from the NLS equation. We consider the following decorated tree:

$$T = \mathcal{F}_{(t_1,0)} \left(\lambda_k \mathcal{F}_{(t_2,0)} (\lambda_k \mathcal{F}_{(t_1,1)} (\lambda_{k_1}) \mathcal{F}_{(t_1,0)} (\lambda_{k_2}) \mathcal{F}_{(t_1,0)} (\lambda_{k_3})) \right) = \begin{array}{c} \textcircled{k_2} \\ | \\ \textcircled{k_1} \text{---} \textcircled{k_3} \\ | \\ \text{---} \\ | \\ \text{---} \end{array},$$

where $k = -k_1 + k_2 + k_3$, $\mathcal{L} = \{t_1, t_2\}$, $\mathcal{L}_+ = \{t_2\}$, $P_{t_1}(\lambda) = -\lambda^2$ and $P_{t_2}(\lambda) = \lambda^2$. We put the frequency decorations only on the leaves as those on the inner nodes are uniquely determined by them. In the table below, we explain the coding of the edges

Edge	Decoration	Operator
	$(t_1, 0)$	$e^{itP_{t_1}(k)} = e^{-itk^2}$
⋮	$(t_1, 1)$	$e^{-itP_{t_1}(k)} = e^{itk^2}$
	$(t_2, 0)$	$-i \int_0^t e^{i\xi P_{t_2}(k)} \dots d\xi = -i \int_0^t e^{i\xi k^2} \dots d\xi$
⋮	$(t_2, 1)$	$-i \int_0^t e^{-i\xi P_{t_2}(k)} \dots d\xi = -i \int_0^t e^{-i\xi k^2} \dots d\xi$

In the end, T is an abstract version of the following integral:

$$-ie^{-itk^2} \int_0^t e^{i\xi k^2} e^{i\xi k_1^2} e^{-i\xi k_2^2} e^{-i\xi k_3^2} d\xi.$$

The next combinatorial structure which we recall from [15] encodes abstract versions of a discretization of an oscillatory integral. We denote by \mathcal{T} the set of decorated trees $T_{\mathfrak{e},r}^{n,0} = (T, n, \mathfrak{o}, \mathfrak{e}, r)$ where

- $T_{\mathfrak{e}}^{n,0} \in \hat{\mathcal{T}}$.
- The decoration of the root is given by $r \in \mathbf{Z}$, $r \geq -1$ such that

$$r + 1 \geq \deg(T_{\mathfrak{e}}^{n,0}) \quad (3.2)$$

where \deg is defined recursively by

$$\begin{aligned} \deg(\mathbf{1}) &= 0, \quad \deg(F_1 \cdot F_2) = \max(\deg(F_1), \deg(F_2)), \\ \deg(\mathcal{F}_{(t,p)}(\lambda_k^\ell F_1)) &= |\ell| + \mathbf{1}_{\{t \in \mathcal{L}_+\}} + \deg(F_1) \end{aligned}$$

where $\ell = (\ell_1, \ell_2)$, $|\ell| = \ell_1 + \ell_2$, F_1, F_2 are forests composed of trees in \mathcal{T} . The quantity $\deg(T_{\mathfrak{e}}^{n,0})$ is the maximum number of edges with type in \mathcal{L}_+ , corresponding to time integrations, and of node decorations n lying on the same path from one leaf to the root.

We call decorated trees in \mathcal{T} *approximated* decorated trees. The order of the approximation is encoded by a new decoration at the root r . We denote by \mathcal{H} the vector space spanned by forests composed of trees in \mathcal{T} and λ^ℓ , $\ell \in \mathbf{N}^2$ where λ^ℓ is the tree with one node decorated by ℓ . When the decoration ℓ is equal to zero we identify this tree with the empty forest: $\lambda^0 = \mathbf{1}$. We now define the symbol $\mathcal{F}_o^r(\lambda_k^\ell \cdot) : \mathcal{H} \rightarrow \mathcal{H}$, as the same as $\mathcal{F}_o(\lambda_k^\ell \cdot)$, with the added adjunction of the decoration r which constrains the time-approximations to be of order r . It is given by:

$$\mathcal{F}_o^r(\lambda_k^\ell (\prod_j \lambda^{m_j} \prod_i \mathcal{F}_{o_i}^{r_i}(\lambda_{k_i}^{\ell_i} F_i))) := \mathcal{F}_o^r(\lambda_k^{\ell + \sum_j m_j} (\prod_i \mathcal{F}_{o_i}(\lambda_{k_i}^{\ell_i} F_i))).$$

We define a projection operator \mathcal{D}^r which depends on r and which is used during the construction of the numerical schemes in order to only retain the terms of order at most r . We define the map $\mathcal{D}^r : \hat{\mathcal{H}} \rightarrow \mathcal{H}$ which assigns r to the root of a decorated tree. This implies a projection along the identity (3.2). It is given by

$$\mathcal{D}^r(\mathbf{1}) = \mathbf{1}_{\{0 \leq r+1\}}, \quad \mathcal{D}^r(\mathcal{F}_o(\lambda_k^\ell F)) = \mathcal{F}_o^r(\lambda_k^\ell F) \quad (3.3)$$

and we extend it multiplicatively to any forest in $\hat{\mathcal{H}}$.

Example 3 We illustrate the action of the map \mathcal{D}_r on the decorated tree T introduced in Example 2. One has:

$$\deg(T) = 1, \quad \mathcal{D}_r(T) = 0, \quad r > 1, \quad \mathcal{D}_r(T) = \begin{array}{c} \textcircled{k_2} \\ | \\ \textcircled{k_1} \textcircled{k_3} \\ | \\ r \end{array}$$

3.1 Dominant part and polynomial interpolation

Let us now introduce the operations used when approximating integrals represented by tree formalism as described above. We first recall [15, Def.2.2] that select higher degree terms in a polynomial of the frequencies.

Definition 3.1 Let $P(k_1, \dots, k_n)$ a polynomial in the k_i . If the highest-degree monomials of P are of the form

$$a \sum_{i=1}^n (a_i k_i)^m, \quad a_i \in \{0, 1\}, \quad a \in \mathbf{Z},$$

then we define $\mathcal{P}_{\text{dom}}(P)$ as

$$\mathcal{P}_{\text{dom}}(P) = a \left(\sum_{i=1}^n a_i k_i \right)^m. \quad (3.4)$$

Otherwise, it is zero.

This definition is used for splitting an operator between a lower part and a dominant part. Indeed, if we consider the polynomial

$$P(k_1, k_2, k_3) = k^2 + k_1^2 - k_2^2 - k_3^2, \quad k = -k_1 + k_2 + k_3.$$

coming from the NLS equation, we observe that P can be rewritten into the form:

$$P(k_1, k_2, k_3) = 2k_1^2 - 2k_1(k_2 + k_3) + 2k_2k_3.$$

Then, we set

$$\mathcal{L}_{\text{dom}} = \mathcal{P}_{\text{dom}}(P) = 2k_1^2, \quad \mathcal{L}_{\text{low}} = (\text{id} - \mathcal{P}_{\text{dom}})(P).$$

We note that \mathcal{L}_{dom} asks for boundedness of two derivatives due to the factor k_1^2 and \mathcal{L}_{low} only one because the latter consists only of cross products $k_i k_j$, $i \neq j$. Another main reason for this splitting is to be able to map back to physical space the following integral:

$$\int_0^t e^{is\mathcal{L}_{\text{dom}}} ds = \frac{e^{it\mathcal{L}_{\text{dom}}} - 1}{i\mathcal{L}_{\text{dom}}}.$$

We observe that it is essential to map back to physical space the term $\frac{1}{\mathcal{L}_{\text{dom}}}$ equal to $\frac{1}{2k_1^2}$. Such a term is given by Δ^{-1} in physical space.

The next definition extracted from [15, Def. 2.6] allows us to compute recursively the various frequency interactions by extracting dominant and lower parts. Such a definition is required for the local error analysis and the forest formula given in the sequel.

Definition 3.2 We recursively define $\mathcal{F}_{\text{dom}}, \mathcal{F}_{\text{low}} : \hat{H}_0 \rightarrow \mathbb{R}[\mathbf{Z}^d]$ as:

$$\begin{aligned} \mathcal{F}_{\text{dom}}(\mathbf{1}) &= 0 & \mathcal{F}_{\text{dom}}(F \cdot \bar{F}) &= \mathcal{F}_{\text{dom}}(F) + \mathcal{F}_{\text{dom}}(\bar{F}) \\ \mathcal{F}_{\text{dom}}(\mathcal{J}_{(t,p)}(\lambda_k F)) &= \begin{cases} \mathcal{P}_{\text{dom}}(P_{(t,p)}(k) + \mathcal{F}_{\text{dom}}(F)), & \text{if } t \in \mathcal{L}_+, \\ P_{(t,p)}(k) + \mathcal{F}_{\text{dom}}(F), & \text{otherwise} \end{cases} \\ \mathcal{F}_{\text{low}}(\mathcal{J}_{(t,p)}(\lambda_k F)) &= (\text{id} - \mathcal{P}_{\text{dom}})(P_{(t,p)}(k) + \mathcal{F}_{\text{dom}}(F)), \end{aligned}$$

where we recall that \mathcal{L}_+ is a subset of \mathcal{L} that encodes edge decorations which correspond to time integrals. We extend these two maps to \hat{H} by ignoring the node decorations n .

In a nutshell the above recursive definition means that in the set $\mathcal{L} \setminus \mathcal{L}_+$, i.e. operators that do not correspond to integration, we collect all frequency contributions, and in the set \mathcal{L}_+ , i.e. operators that correspond to integration, we extract the dominant frequencies of the full integrand.

Example 4 We illustrate the previous definition on a simple decorated tree coming from the NLS equation.

$$T = \begin{array}{c} \textcircled{k_1} \quad \textcircled{k_2} \quad \textcircled{k_3} \\ \vdots \quad \vdots \quad \vdots \\ \cdot \end{array} = \mathcal{J}_{(t_2,0)}(\lambda_k F), \quad F = \mathcal{J}_{(t_1,1)}(\lambda_{k_1}) \mathcal{J}_{(t_1,0)}(\lambda_{k_2}) \mathcal{J}_{(t_1,0)}(\lambda_{k_3}).$$

with $k = -k_1 + k_2 + k_3$. One has

$$\mathcal{F}_{\text{dom}}(T) = \mathcal{P}_{\text{dom}}(P_{(t_2,0)}(k) + \mathcal{F}_{\text{dom}}(F))$$

because $t_2 \in \mathcal{L}_+$. Then, we use the fact that

$$P_{(t_2,0)}(k) = k^2, \quad P_{(t_1,0)}(k) = -k^2, \quad P_{(t_1,1)}(k) = k^2$$

and

$$\begin{aligned} \mathcal{F}_{\text{dom}}(F) &= \mathcal{F}_{\text{dom}}(\mathcal{J}_{(t_1,1)}(\lambda_{k_1})) + \mathcal{F}_{\text{dom}}(\mathcal{J}_{(t_1,0)}(\lambda_{k_2})) + \mathcal{F}_{\text{dom}}(\mathcal{J}_{(t_1,0)}(\lambda_{k_3})) \\ &= P_{(t_2,1)}(k_1) + P_{(t_2,0)}(k_2) + P_{(t_2,0)}(k_3) \\ &= k_1^2 - k_2^2 - k_3^2. \end{aligned}$$

Therefore,

$$\begin{aligned} \mathcal{F}_{\text{dom}}(T) &= \mathcal{P}_{\text{dom}}(k^2 + k_1^2 - k_2^2 - k_3^2) \\ &= \mathcal{P}_{\text{dom}}(2k_1^2 - 2k_1(k_2 + k_3) + 2k_2k_3) \\ &= 2k_1^2 \end{aligned}$$

One observes that the projection \mathcal{P}_{dom} projects to zero the cross terms $k_i k_j$ with $i \neq j$.

A central novel idea which we introduce in our present work is that we proceed to interpolate the exponential of the lower part of the operator in place of a direct Taylor series expansion. The advantage of this procedure is firstly that it allows us to immediately arrive at stable schemes without the need for filter functions (the spectrum of $i\mathcal{P}_{\text{low}} = i\mathcal{P} - i\mathcal{P}_{\text{dom}}$ typically lies on the imaginary axis so terms involving the exponential of the operator are all bounded). Secondly, through this interpolation process we are able to arrive at numerical schemes whose adjoint has the same functional form which is essential in the construction of symmetric methods. Classical Taylor expansion for the lower part gives:

$$e^{i\xi\mathcal{L}_{\text{low}}} = \sum_{\ell \leq r} \frac{\xi^\ell}{\ell!} (i\mathcal{L}_{\text{low}})^\ell + \mathcal{O}(\xi^{r+1} (i\mathcal{L}_{\text{low}})^{r+1})$$

Now, for reasons of stability, we would like to use a polynomial interpolation that will give the same local error analysis. We suppose given $r + 1$ distinct interpolation

points $0 \leq a_0 < a_1 < \dots < a_r \leq 1$ associated to the polynomials $p_{j,r}(\cdot, \tau)$ such that

$$p_{j,r}(a_m \tau, \tau) = \delta_{j,m}.$$

Then, we define the following approximation

$$\tilde{p}_r(f, \xi) = \sum_{j=0}^r f(a_j \tau) p_{j,r}(\xi, \tau), \quad f(a_j \tau) = e^{ia_j \tau \mathcal{L}_{\text{low}}}, j = 0, \dots, r,$$

where we have suppressed the implicit τ -dependency of $\tilde{p}_r(f, \xi)$ for notational simplicity. One has the following local error

$$f(\xi) - \tilde{p}_r(f, \xi) = \mathcal{O} \left(\prod_{j=0}^r (\xi - a_j \tau) (i \mathcal{L}_{\text{low}})^{r+1} \right). \quad (3.5)$$

In the sequel, we will write the polynomial interpolation as:

$$\tilde{p}_r(f, \xi) = \sum_{j=0}^r \hat{p}_{j,r}(f, \tau) \xi^j \quad (3.6)$$

where the $\hat{p}_{j,r}(f, \tau)$ are bounded in τ because they correspond to linear combinations of terms of the form $\exp(ia_j \tau \mathcal{L}_{\text{low}})$. We provide below one example with two points 0 and τ

$$\tilde{p}_1(f, \xi) = 1 + \frac{s}{\tau} \left(e^{is \mathcal{L}_{\text{low}}} - 1 \right), \quad (3.7)$$

and

$$\begin{aligned} \hat{p}_{0,1}(f, \tau) &= 1, & \hat{p}_{1,1}(f, \tau) &= \frac{e^{is \mathcal{L}_{\text{low}}} - 1}{\tau}, \\ p_{0,1}(f, \xi) &= \frac{\tau - s}{\tau}, & p_{1,1}(f, \xi) &= \frac{s}{\tau} e^{is \mathcal{L}_{\text{low}}}. \end{aligned}$$

When $r = 0$ we can, for example, pick

$$p_0(f, \xi) = \hat{p}_{0,0}(f, \tau) = p_{0,0}(f, \xi) = f\left(\frac{\tau}{2}\right).$$

In practice, we will also consider

$$\hat{p}_{0,0}(f, \xi) = \frac{f(0) + f(\xi)}{2}.$$

The next definition is a slight modification of [15, Def. 3.1] where Taylor expansions around zero are replaced by an interpolation on the interval $[0, \tau]$ and we take into account monomials in τ for the discretisation.

Definition 3.3 Assume that $G : \xi \mapsto \tau^m \xi^q e^{i\xi P(k_1, \dots, k_n)}$ where P is a polynomial in the frequencies k_1, \dots, k_n and let $o_2 = (t_2, p) \in \mathfrak{L}_+ \times \{0, 1\}$ and $r \in \mathbf{N}$. Let k be a linear combination of k_1, \dots, k_n using coefficients in $\{-1, 0, 1\}$ and

$$\begin{aligned} \mathcal{L}_{\text{dom}} &= \mathcal{P}_{\text{dom}}(P_{o_2}(k) + P), & \mathcal{L}_{\text{low}} &= \mathcal{P}_{\text{low}}(P_{o_2}(k) + P) \\ f(\xi) &= e^{i\xi \mathcal{L}_{\text{dom}}}, & g(\xi) &= e^{i\xi \mathcal{L}_{\text{low}}}, & \tilde{g}(\xi) &= e^{i\xi(P_{o_2}(k)+P)}. \end{aligned}$$

Then, we define for $n \in \mathbf{N}$, $r \geq q$, $\tilde{r} = r - q - m$ and $\bar{n} = \deg(\mathcal{L}_{\text{dom}}^{r+1}) + \alpha$

$$\mathcal{H}_{o_2}^{k,r}(G, n)(s) = \begin{cases} -i|\nabla|^\alpha(k) \sum_{\ell \leq \tilde{r}} \hat{p}_{\ell, \tilde{r}}(\tilde{g}, \tau) \int_0^s \tau^m \xi^{q+\ell} d\xi, & \text{if } n \geq \bar{n}, \\ -i|\nabla|^\alpha(k) \sum_{\ell \leq \tilde{r}} \tau^m \hat{p}_{\ell, \tilde{r}}(g, \tau) \Psi_{n,q}^r(\mathcal{L}_{\text{dom}}, \ell)(s), & \text{otherwise.} \end{cases} \quad (3.8)$$

Thereby we set for $(r - q - m - \ell + 1) \deg(\mathcal{L}_{\text{dom}}) + \ell \deg(\mathcal{L}_{\text{low}}) + \alpha > n$

$$\Psi_{n,q}^r(\mathcal{L}_{\text{dom}}, \ell)(s) = \int_0^s \xi^{q+\ell} f(\xi) d\xi. \quad (3.9)$$

Otherwise,

$$\Psi_{n,q}^r(\mathcal{L}_{\text{dom}}, \ell)(s) = \sum_{j \leq \hat{r}} \hat{p}_{j, \hat{r}}(f, \tau) \int_0^s \xi^{q+\ell+j} d\xi. \quad (3.10)$$

Here $\hat{r} = r - q - m - \ell$, $\deg(\mathcal{L}_{\text{dom}})$ and $\deg(\mathcal{L}_{\text{low}})$ denote the degree of the polynomial \mathcal{L}_{dom} and \mathcal{L}_{low} , respectively and $|\nabla|^\alpha(k) = \prod_{\alpha = \sum \gamma_j < \deg(\mathcal{L})} k_j^{\gamma_j}$. If $r < q + m$, the map $\mathcal{H}_{o_2}^{k,r}(G, n)(s)$ is equal to zero.

We perform an example to illustrate the polynomial interpolation.

Example 5 We consider $P_{t_2}(\lambda) = -\lambda^2$, $p = 0$, $\alpha = 0$, $k = -k_1 + k_2 + k_3$ and

$$G(\xi) = \xi e^{i\xi(k_1^2 - k_2^2 - k_3^2)}.$$

With the notation of Definition 3.3 we observe that

$$\mathcal{L}_{\text{dom}} = 2k_1^2, \quad \mathcal{L}_{\text{low}} = -2k_1(k_2 + k_3) + 2k_2k_3,$$

Furthermore, we observe as $\deg(\mathcal{L}_{\text{dom}}) = 2$, $\deg(\mathcal{L}_{\text{low}}) = 1$ and $q = 1$ that

$$(r - q - \ell + 1) \deg(\mathcal{L}_{\text{dom}}) + \ell \deg(\mathcal{L}_{\text{low}}) > n \quad \text{if} \quad 2r - n > \ell. \quad (3.11)$$

We consider the polynomial interpolation given in (3.7) and focus on some cases

- **Case $r = 1$ and $n = 1$:** We obtain

$$\mathcal{H}_{o_2}^{k,1}(G, n)(s) = -i\hat{p}_{0,0}(f, \tau) \Psi_{n,1}^1(\mathcal{L}_{\text{dom}}, 0)(s)$$

$$\begin{aligned}
 &= -i\hat{p}_{0,0}(f, \tau) \int_0^s \xi f(\xi) d\xi \\
 &= \frac{1}{2ik_1^2} \left(se^{2isk_1^2} - \frac{e^{2isk_1^2} - 1}{2ik_1^2} \right) \left(\frac{1 + e^{is\mathcal{L}_{low}}}{2} \right)
 \end{aligned}$$

as condition (3.11) takes for $\ell = 0$ the form $2 - n > 0$.

- **Case $r = 2$ and $n = 2$:** We have that

$$\mathcal{H}_\alpha^{k,2}(G, n)(s) = -i(\hat{p}_{0,1}(g, \tau)\Psi_{n,1}^2(\mathcal{L}_{dom}, 0)(s) + \hat{p}_{1,1}(g, \tau)\Psi_{n,1}^2(\mathcal{L}_{dom}, 1)(s))$$

and condition (3.11) takes the form $4 - n > \ell$.

If $\ell = 1$ we thus obtain

$$\Psi_{n,1}^2(\mathcal{L}_{dom}, 1)(s) = \int_0^s \xi^2 f(\xi) d\xi = \frac{s^2}{2ik_2^2} \left(e^{2isk_1^2} - 2\Psi_{1,1}^1(\mathcal{L}_{dom}, 0) \right).$$

If $\ell = 0$, on the other hand, condition (3.11) holds. Henceforth, we have that

$$\Psi_{n,1}^2(\mathcal{L}_{dom}, 0)(s) = \int_0^s \xi f(\xi) d\xi.$$

Following a similar proof as for [15, Lem. 3.3] by using (3.5), one gets

Lemma 3.4 *We keep the notations of Definition 3.3. We suppose that $q + m \leq r$ then one has for $s \in [0, \tau]$*

$$-i|\nabla|^\alpha(k) \int_0^s \tau^m \xi^q e^{i\xi(\mathcal{L}_{dom} + \mathcal{L}_{low})} d\xi - \mathcal{H}_{o_2}^{k,r}(G, n)(s) = \mathcal{O}(\tau^{r+2} k^{\bar{n}}) \quad (3.12)$$

where $\bar{n} = \max(n, \deg(\mathcal{L}_{low}^{r-q-m+1}) + \alpha)$.

3.2 A forest formula for resonance based schemes

We recall the characters defined now on \mathcal{H} and parametrised by $n \in \mathbf{N}$ where n here the a priori regularity assumed on the initial value, that is $v \in H^n$ where H^n is the periodic Sobolev space of order n . These characters give a low regularity discretisation of some iterated integrals:

$$\begin{aligned}
 \Pi^n(F \cdot \bar{F})(s, \tau) &= (\Pi^n F)(s, \tau)(\Pi^n \bar{F})(s, \tau), \quad (\Pi^n \lambda^\ell)(s, \tau) = s^{\ell_1} \tau^{\ell_2}, \\
 (\Pi^n \mathcal{J}_{o_1}^r(\lambda_k^\ell F))(s, \tau) &= s^{\ell_1} \tau^{\ell_2} e^{isP_{o_1}(k)} (\Pi^n \mathcal{D}^{r-|\ell|}(F))(s, \tau), \\
 (\Pi^n \mathcal{J}_{o_2}^r(\lambda_k^\ell F))(s, \tau) &= \mathcal{H}_{o_2}^{k,r} \left(\Pi^n \left(\lambda^\ell \mathcal{D}^{r-|\ell|-1}(F) \right) (\cdot, \tau), n \right) (s).
 \end{aligned} \tag{3.13}$$

where $o_2 = (t_2, p_2)$ with $t_2 \in \mathfrak{L}_+$ and $o_1 = (t_1, p_1)$ with $t_1 \in \mathfrak{L} \setminus \mathfrak{L}_+$ and $\ell = (\ell_1, \ell_2) \in \mathbf{N}^2$. We will use frequently the notations o_i in the sequel. The main difference with [15] is the use of the polynomial interpolation in Definition 3.3. In the next theorem, we state a forest formula for the resonance scheme in the sense that we exhibit a general formula for the terms $(\Pi^{n,r} F)(t)$ where $\Pi^{n,r}$ is

short hand notation for $\Pi^n \mathcal{D}_r$. This new forest formula is a significant extension of contributions in [15] since it incorporates not just the aforementioned polynomial interpolants but also allows for implicit discretisations in the unknown v . We first need to introduce some notations that are needed for its formulation. We denote by \tilde{E}_T the edges of T associated to an integration in time. They carry a decoration of the type o_2

$$\tilde{E}_T = \{e \in E_T \mid \mathfrak{e}(e) \in \mathfrak{L}_+ \times \{0, 1\}\}.$$

The notation T^e means that we consider the planted tree above the edge e in T . This tree has its root connected to the rest of its nodes by the edge e . By $F_0 \cdot T_1 \dots \cdot T_m \subset F$, we mean that the forest

$$F_0 \cdot T_1 \dots \cdot T_m \subset F \tag{3.14}$$

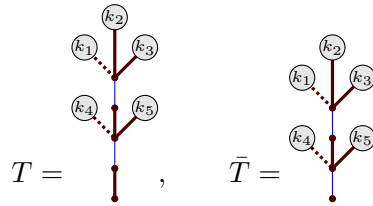
is a splitting of F where :

- The T_i are planted trees with the edge connecting the root decorated by an edge decoration of type o_2 .
- F_0 is a forest either empty or taking the form:

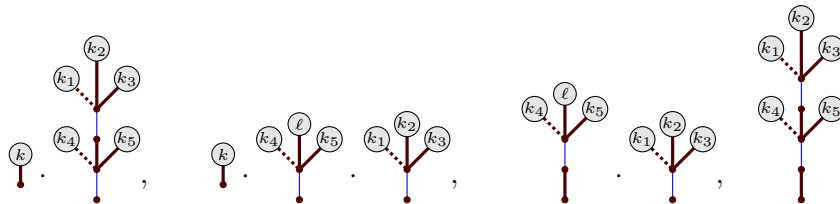
$$F_0 = \prod_{j=1}^{m_0} T_{0,j}$$

where the $T_{0,j}$ are subtrees at the root of some trees appearing in the decomposition of the forest F into product of planted trees.

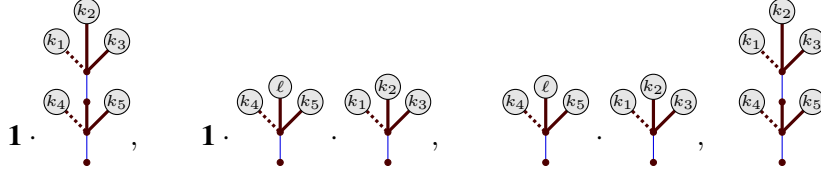
Example 6 We provide an example of the forests such that $F_0 \cdot T_1 \dots \cdot T_m \subset F$. Let us consider F to be the following decorated trees coming from the NLS equation



Because T starts with a brown edge that is an edge decorated by $(t_1, 0)$, F_0 is not empty. Below, we list all the possible splitting respecting this rule and also that the T_i with $i \geq 1$ must be planted trees with a blue edge (decorated by $(t_2, 0)$) at their root.



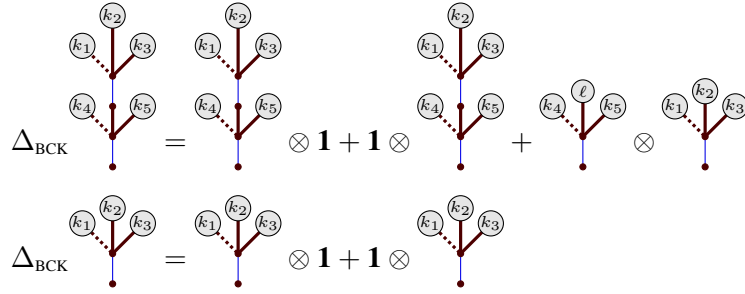
where $\ell = -k_1 + k_2 + k_3$ and $k = -k_4 + \ell + k_5$. We also give below the decomposition for the decorated tree \bar{T} . Notice that now \bar{T}_0 could be empty.



We can obtain these terms by iterating a Butcher-Connes-Kreimer type coproduct $\Delta_{\text{BCK}} : \mathcal{H}_0 \rightarrow \mathcal{H}_0 \otimes \mathcal{H}_0$, a simple version of the one introduced in [15]. It is defined recursively by

$$\begin{aligned}\Delta_{\text{BCK}} \mathcal{J}_{o_1}(\lambda_k^\ell F) &= \left(\mathcal{J}_{o_1}(\lambda_k^\ell \cdot) \otimes \text{id} \right) \Delta_{\text{BCK}} F, \\ \Delta_{\text{BCK}} \mathcal{J}_{o_2}(\lambda_k^\ell F) &= \left(\mathcal{J}_{o_2}(\lambda_k^\ell \cdot) \otimes \text{id} \right) \Delta_{\text{BCK}} F + \mathbf{1} \otimes \mathcal{J}_{o_2}(\lambda_k^\ell F).\end{aligned}$$

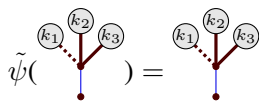
and then extended multiplicatively for the forest product. Below, we provide some examples of computations:



Below, we introduce recursive maps ψ_{BCK} and $\tilde{\psi}_{\text{BCK}}$ that can compute the splitting describe above with the coproduct Δ_{BCK} :

$$\begin{aligned}\psi_{\text{BCK}} &= \left(\text{id} \otimes \tilde{\psi}_{\text{BCK}} \right) \Delta_{\text{BCK}}, \\ \tilde{\psi}_{\text{BCK}} &= \mathcal{M} \left(\tilde{\psi}_{\text{BCK}} \otimes P_{\mathbf{1}} \right) \Delta_{\text{BCK}}, \quad \tilde{\psi}_{\text{BCK}}(\mathbf{1}) = \mathbf{1}\end{aligned}\tag{3.15}$$

where \mathcal{M} is the forest product and $P_{\mathbf{1}} = \text{id} - \mathbf{1}^*$ is the augmentation projector. Here $\mathbf{1}^*$ is the co-unit which is non-zero and equal to one only on the empty forest. The projector $P_{\mathbf{1}}$ forces at least one cut at each iteration and therefore the recursion is well-defined. If we apply ψ to T , we obtain a linear combination of the terms of the form $T_0 \otimes T_1 \cdot \dots \cdot T_m$ that corresponds exactly to the splitting described above. We do not get a forest in the end but a term with a tensor product. This is for distinguishing the root as it is needed in our splitting. As an example of computation of those maps, one has



$$\tilde{\psi}(\text{tree}) = \text{tree} + \tilde{\psi}(\text{tree with dashed line}) \cdot \text{tree} = \text{tree} + \text{tree} + \text{tree} + \text{tree} + \text{tree}$$

Theorem 3.5 For every forest $F \in \hat{H}_0$, $(\Pi^{n,r} F)(t, \tau)$ takes the form:

$$\sum_{\mathbf{a} \in [0,1]^{\tilde{E}_F}} \sum_{F_0 \cdot T_1 \dots T_m \subset F} C_F e^{it \mathcal{F}_{\text{dom}}(F_0)} \prod_{j=0}^m \prod_{e \in \tilde{E}_{T_j}} e^{i\tau a_e \mathcal{F}_{\text{low}}(T_j^e)} \quad (3.16)$$

$$b_{\mathbf{a}, F, F_0 \dots T_m}(t, \tau, i\tau \mathcal{F}_{\text{dom}}(T_j), i\tau \mathcal{F}_{\text{dom}}(T_{0,\bar{j}}))$$

with the convention $T_0 = F_0$. The coefficients C_F depend only on the node decorations of F . The coefficients b are polynomial in t and are non zero only for a finite number of values of \mathbf{a} . They are uniformly bounded in τ . Moreover, they do not depend on the node decorations of the T_i , F_0 and F that correspond to the frequencies.

We recall that in the above notation the parameters n and r in $(\Pi^{n,r} F)(t, \tau)$ denote the regularity requirements and maximum length of trees in the approximation respectively.

Proof. We proceed by induction on the size of the forest F . For the empty forest, the sum is equal to one by convention and

$$(\Pi^{n,r} \mathbf{1})(t, \tau) = 1.$$

Let F_1, F_2 two decorated forests with $F = F_1 \cdot F_2$ for which we have (3.16). We apply the induction hypothesis and get

$$\begin{aligned} (\Pi^{n,r} F)(s, \tau) &= (\Pi^{n,r} F_1)(s, \tau) (\Pi^{n,r} F_2)(s, \tau) \\ &= \sum_{\mathbf{a}_1 \in [0,1]^{\tilde{E}_{F_1}}} \sum_{\mathbf{a}_2 \in [0,1]^{\tilde{E}_{F_2}}} \sum_{F_{1,0} \cdot T_{1,1} \dots T_{1,m_1} \subset F_1} \sum_{F_{2,0} \cdot T_{2,1} \dots T_{2,m_2} \subset F_2} C_{F_1} C_{F_2} \\ &e^{it(\mathcal{F}_{\text{dom}}(F_{1,0}) + \mathcal{F}_{\text{dom}}(F_{2,0}))} \prod_{j=0}^{m_1} \prod_{e \in \tilde{E}_{T_{1,j}}} e^{i\tau a_{1,e} \mathcal{F}_{\text{low}}(T_{1,j}^e)} \times \prod_{j=0}^{m_2} \prod_{e \in \tilde{E}_{T_{2,j}}} e^{i\tau a_{2,e} \mathcal{F}_{\text{low}}(T_{2,j}^e)} \\ &b_{\mathbf{a}_1, F_1, F_{1,0} \dots T_{1,m_1}} \times b_{\mathbf{a}_2, F_2, F_{2,0} \dots T_{2,m_2}}. \end{aligned}$$

By using Definition 3.2, we have

$$\mathcal{F}_{\text{dom}}(F_{1,0}) + \mathcal{F}_{\text{dom}}(F_{2,0}) = \mathcal{F}_{\text{dom}}(F_0), \quad F_0 = F_{1,0} \cdot F_{2,0}.$$

Then, we can perform the disjoint sum of \mathbf{a}_1 and \mathbf{a}_2 :

$$\mathbf{a} = \mathbf{a}_1 + \mathbf{a}_2$$

by extending \mathbf{a}_1 (resp. \mathbf{a}_2) on the edges of F_2 (resp. F_1) by zero. Then, \mathbf{a} is defined on the edges of F . We can gather the sum on the forests by:

$$\begin{aligned} \sum_{F_{1,0} \cdot T_{1,1} \dots T_{1,m_1} \subset F_1} \sum_{F_{2,0} \cdot T_{2,1} \dots T_{2,m_2} \subset F_2} &= \sum_{F_0 \cdot T_{1,1} \dots T_{1,m_1} \cdot T_{2,1} \dots T_{2,m_2} \subset F} \\ &= \sum_{F_0 \cdot T_1 \dots T_m \subset F} \end{aligned}$$

and we can also set

$$\begin{aligned} b_{\mathbf{a}, F, F_0 \dots T_1 \dots T_m} &= b_{\mathbf{a}_1, F_1, F_{1,0} \dots T_{1,m_1}} \times b_{\mathbf{a}_2, F_2, F_{2,0} \dots T_{2,m_2}} \\ C_F &= C_{F_1} \times C_{F_2} \end{aligned}$$

and see that the properties of the coefficient b are preserved by multiplication. Indeed, we have a bijection between partitions of $F = F_1 \cdot F_2$ into a product of trees and the forest product of partitions of F_i . For a tree of the form $\mathcal{J}_{o_1}(\lambda_k^\ell F)$, one has

$$(\Pi^n \mathcal{J}_{o_1}^r(\lambda_k^\ell F))(t, \tau) = t^{\ell_1} \tau^{\ell_2} e^{itP_{o_1}(k)} (\Pi^{n, r-\ell} F)(t, \tau).$$

We multiply the formula for F obtained by the induction hypothesis by $e^{itP_{o_1}(k)}$:

$$\begin{aligned} \sum_{\mathbf{a} \in [0,1]^{\tilde{E}_F}} \sum_{F_0 \cdot T_1 \dots T_m \subset F} C_F e^{it(\mathcal{F}_{\text{dom}}(F_0) + P_{o_1}(k))} \prod_{j=0}^m \prod_{e \in \tilde{E}_{T_j}} e^{i\tau a_e \mathcal{F}_{\text{low}}(T_j^e)} \\ t^\ell b_{\mathbf{a}, F, F_0 \dots T_m}(t, \tau, i\tau \mathcal{F}_{\text{dom}}(T_j), i\tau \mathcal{F}_{\text{dom}}(T_{0,\bar{j}})). \end{aligned}$$

From Definition 3.2, we have

$$\mathcal{F}_{\text{dom}}(F_0) + P_{o_1}(k) = \mathcal{F}_{\text{dom}}(\mathcal{J}_{o_1}(\lambda_k^\ell F_0)).$$

Moreover, for $\mathcal{J}_{o_1}(\lambda_k^\ell F)$, the forest at the root must be of the form $\mathcal{J}_{o_1}(\lambda_k^\ell F_0)$. For the coefficients b , we have

$$t^{\ell_1} \tau^{\ell_2} b_{\mathbf{a}, F, F_0 \dots T_m} = b_{\mathbf{a}, \mathcal{J}_{o_1}(\lambda_k^\ell F), \mathcal{J}_{o_1}(\lambda_k^\ell F_0) \dots T_m}, \quad C_{\mathcal{J}_{o_1}(\lambda_k^\ell F)} = C_F$$

It remains to prove the forest formula for a tree of the form $\mathcal{J}_{o_2}(\lambda_k^\ell F)$. We have

$$\left(\Pi^n \mathcal{J}_{o_2}^r(\lambda_k^\ell F) \right)(t, \tau) = \mathcal{H}_{o_2}^{k,r} \left(\Pi^n \left(\lambda^\ell \mathcal{D}^{r-|\ell|-1}(F) \right)(\cdot, \tau), n \right)(t).$$

We apply the induction hypothesis on $\Pi^{n, r-|\ell|-1}$. Then, the proof boils down to understand how the operator $\mathcal{H}_{o_2}^{k,r}$ acts on the forest formula. This operator

computes first the dominant part of the oscillation. It is given for a fixed forest $F_0 \cdot T_1 \dots \cdot T_m \subset F$ by

$$\mathcal{P}_{\text{dom}}(P_{o_2}(k) + \mathcal{F}_{\text{dom}}(F_0)) = \mathcal{F}_{\text{dom}}(\mathcal{J}_{o_2}(\lambda_k^\ell F_0)).$$

If this dominant part is integrated exactly, we obtain a factor of the form

$$e^{it\mathcal{F}_{\text{dom}}(\mathcal{J}_{o_2}(\lambda_k^\ell F_0))}.$$

This will correspond to forests $\mathcal{J}_{o_2}(\lambda_k^\ell F_0) \cdot \dots \cdot T_m$. In this exact integration, we have terms without this factor which corresponds to the forest $\mathbf{1} \cdot \mathcal{J}_{o_2}(\lambda_k^\ell F_0) \cdot \dots \cdot T_m$ as the forest connected to the root could be the empty forest. For the lower part given by

$$(\text{id} - \mathcal{P}_{\text{dom}})(P_{o_2}(k) + \mathcal{F}_{\text{dom}}(F)) = \mathcal{F}_{\text{low}}(\mathcal{J}_{o_2}(\lambda_k^\ell F_0))$$

we perform an interpolation that produces terms of the form

$$e^{i\tau a \mathcal{F}_{\text{low}}(\mathcal{J}_{o_2}(\lambda_k^\ell F_0))}, \quad a \in [0, 1].$$

The operator $\mathcal{H}_{o_2}^{k,r}$ depends on n which is the a priori regularity assumed on the initial data. With this information, if n is sufficiently big, we can perform a full Taylor expansion via an interpolation that will produce terms of the form:

$$e^{i\tau a \mathcal{F}_{\text{low}}(\mathcal{J}_{o_2}(\lambda_k^\ell F_0))} e^{i\tau a' \mathcal{F}_{\text{dom}}(\mathcal{J}_{o_2}(\lambda_k^\ell F_0))}, \quad a, a' \in [0, 1].$$

These terms will be associated to a forest of the form $\mathbf{1} \cdot \mathcal{J}_{o_2}(\lambda_k^\ell F_0) \cdot \dots \cdot T_m$. The factor $e^{i\tau a' \mathcal{F}_{\text{dom}}(\mathcal{J}_{o_2}(\lambda_k^\ell F_0))}$ will be inside the coefficients b . The interpolation also produces monomials in t and τ which implies the polynomial structure of the coefficients b in t . Also, it produces coefficients bounded in τ such as the $\hat{p}_{j,r}(f, \tau)$ given in (3.6). The choice of the $a \in [0, 1]$ are fixed by the interpolation method and one uses only a finite number of them which implies that the coefficients b are non-zero on a finite set of the \mathbf{a} . Finally, we have

$$C_{\mathcal{J}_{o_2}(\lambda_k^\ell F)} = -i|\nabla|^\alpha(k)C_F.$$

□

Theorem 3.6 For every decorated tree $T = \mathcal{J}_{o_2}(\lambda_k F)$, $(\Pi^{n,r}T)(\tau, \tau)$ takes the form:

$$\sum_{\mathbf{a} \in [0,1]^{\tilde{E}_F}} \sum_{T_0 \cdot T_1 \dots \cdot T_m \subset T} C_T \prod_{j=0}^m \prod_{e \in \tilde{E}_{T_j}} e^{i\tau a_e \mathcal{F}_{\text{low}}(T_j^e)} b_{\mathbf{a}, T, T_0 \dots \cdot T_m}(\tau, i\tau \mathcal{F}_{\text{dom}}(T_j)) \quad (3.17)$$

where the coefficients b are polynomial in τ with bounded coefficient in τ and are non zero for finite values of \mathbf{a} . Moreover, they do not depend on the nodes decorations of the T_i, F_0 and F that correspond to the frequencies.

Proof. The proof works mostly in the same way as for Theorem 3.5 but with $t = \tau$. The main difference is that when we apply the operator $\mathcal{H}_{o_2}^{k,r}$, we put factors of the form $e^{it\mathcal{F}_{\text{dom}}(\mathcal{J}_{o_2}(\lambda_k F_0))}$ in the coefficients b . □

3.3 A more general forest formula

While we will observe that the above forest formula is sufficient for the characterisation of symmetric resonance based schemes, we can actually allow for an even larger number of degrees of freedom in the context of this algebraic structure. This idea leads to a more general forest formula, introduced in the present section, which might be exploited in finding schemes more general than the resonance based methods discussed in the present work. We first introduce a new space of decorated forests with trees having an extra decoration at the root. A tree in \mathcal{T}_+ is of the form

$$\mathcal{F}_o^{(r,m)}(\lambda_k^\ell F), \quad \mathcal{F}_o^r(\lambda_k^\ell F) \in \mathcal{T},$$

with $m \in \mathbf{N}^2$ and the additional constraint that $|m| \leq r + 1$ in order to be non zero. We also assume that λ^ℓ does not appear in \mathcal{T}_+ . We set \mathcal{H}_+ to be the linear span of \mathcal{H} .

We define an extension of Δ_{BCK} using the symbolic notation given by $\Delta : \mathcal{H} \rightarrow \mathcal{H} \otimes \mathcal{H}_+$ and $\Delta^+ : \mathcal{H}_+ \rightarrow \mathcal{H}_+ \otimes \mathcal{H}_+$

$$\begin{aligned} \Delta \mathbf{1} &= \mathbf{1} \otimes \mathbf{1}, \quad \Delta \lambda^\ell = \lambda^\ell \otimes \mathbf{1} \\ \Delta \mathcal{F}_{o_1}^r(\lambda_k^\ell F) &= \left(\mathcal{F}_{o_1}^r(\lambda_k^\ell \cdot) \otimes \text{id} \right) \Delta \mathcal{D}^{r-|\ell|}(F) \\ \Delta \mathcal{F}_{o_2}^r(\lambda_k^\ell F) &= \left(\mathcal{F}_{o_2}^r(\lambda_k^\ell \cdot) \otimes \text{id} \right) \Delta \mathcal{D}^{r-|\ell|-1}(F) + \sum_{|m| \leq r+1} \frac{\lambda^m}{m!} \otimes \mathcal{F}_{o_2}^{(r,m)}(\lambda_k^\ell F) \\ \Delta^+ \mathcal{F}_{o_2}^{(r,m)}(\lambda_k^\ell F) &= \left(\mathcal{F}_{o_2}^{(r,m)}(\lambda_k^\ell \cdot) \otimes \text{id} \right) \Delta \mathcal{D}^{r-|\ell|-1}(F) + \mathbf{1} \otimes \mathcal{F}_{o_2}^{(r,m)}(\lambda_k^\ell F) \end{aligned} \quad (3.18)$$

and it is extended multiplicatively for the forest product. This coproduct is useful for providing a nice factorisation of the discretisation Π^n given in [15]:

$$\Pi^n = \left(\hat{\Pi}^n \otimes A^n \right) \Delta \quad (3.19)$$

where the character $\hat{\Pi}^n$ singles out oscillations and it is recursively defined by

$$\begin{aligned} \hat{\Pi}^n(F \cdot \bar{F})(s, \tau) &= \left(\hat{\Pi}^n F \right)(s, \tau) \left(\hat{\Pi}^n \bar{F} \right)(s, \tau), \quad (\hat{\Pi}^n \lambda^\ell)(s, \tau) = s^{\ell_1} \tau^{\ell_2}, \\ \hat{\Pi}^n(\mathcal{F}_{o_1}^r(\lambda_k^\ell F))(s, \tau) &= s^{\ell_1} \tau^{\ell_2} e^{i\tau P_{o_1}(k)} \hat{\Pi}^n(\mathcal{D}^{r-|\ell|}(F))(s, \tau), \\ \hat{\Pi}^n(\mathcal{F}_{o_2}^r(\lambda_k^\ell F))(s, \tau) &= \mathcal{K}_{o_2,+}^{k,r}(\hat{\Pi}^n(\lambda^\ell \mathcal{D}^{r-|\ell|-1}(F))(\cdot, \tau), n)(s) \end{aligned} \quad (3.20)$$

with

$$\mathcal{K}_{o_2,+}^{k,r} := (\text{id} - \mathbb{Q}) \circ \mathcal{K}_{o_2}^{k,r} \quad (3.21)$$

and \mathbb{Q} is the projection that send to zero functions of the form

$$z \mapsto \sum_j Q_j(z) e^{izP_j(k_1, \dots, k_n)}, \quad P_j \neq 0.$$

The character $A^n : \mathcal{H}_+ \rightarrow \mathbf{C}$ applied to $\mathcal{F}_{o_2}^{(r,m)}(\lambda_k^\ell F)$ is extracting the coefficient of $t^{m_1} \tau^{m_2}$ multiplied by $m!$ in $\Pi^n \mathcal{F}_{o_2}^r(\lambda_k^\ell F)$. In (3.19), we do not need a multiplication because $A^n(F) \in \mathbf{C}$ for every $F \in \mathcal{H}_+$ and \mathcal{C} is a \mathbf{C} -vector space. Therefore, we use the identification $\mathcal{C} \otimes \mathbf{C} \cong \mathcal{C}$. One main property observed in [15] about $\hat{\Pi}^n$ is the following factorisation: For every forest $F \in \tilde{\mathcal{H}}$, there exists a polynomial $B^n(\mathcal{D}^r(F))(\xi, \tau)$ such that

$$\hat{\Pi}^n(\mathcal{D}^r(F))(\xi, \tau) = B^n(\mathcal{D}^r(F))(\xi, \tau) e^{i\xi \mathcal{F}_{\text{dom}}(F)} \quad (3.22)$$

where $\mathcal{F}_{\text{dom}}(F)$ is given in Definition 3.2.

Proposition 3.7 *For every forest $F = \prod_j T_j$ with T_j planted trees, $(\hat{\Pi}^{n,r} F)(t, \tau)$ takes the form:*

$$\sum_{\mathbf{a} \in [0,1]^{\tilde{E}_F}} C_F e^{it \mathcal{F}_{\text{dom}}(F)} \prod_{e \in \tilde{E}_F} e^{i\tau a_e \mathcal{F}_{\text{low}}(F^e)} b_{\mathbf{a},F}(t, \tau, i\tau \mathcal{F}_{\text{dom}}(T_j)). \quad (3.23)$$

We assume the coefficients b are polynomial in t, τ with bounded coefficients in τ and that they are non zero for finite values of \mathbf{a} . They also do not depend on the nodes decorations of F that correspond to the frequencies.

Proof. The proof follows the same lines as for Theorem 3.5 by using the recursive definition (3.20) of the character $\hat{\Pi}^n$. It can be seen as a refinement of (3.22). \square

Theorem 3.8 *For every forest F , $(\Pi^{n,r} F)(t, \tau)$ takes the form:*

$$\sum_{\mathbf{a} \in [0,1]^{\tilde{E}_F}} \sum_{F_0 \cdot T_1 \dots \cdot T_m \subset F} C_F e^{it \mathcal{F}_{\text{dom}}(F_0)} \prod_{j=0}^m \prod_{e \in \tilde{E}_{T_j}} e^{i\tau a_e \mathcal{F}_{\text{low}}(T_j^e)} \quad (3.24)$$

$$b_{\mathbf{a},F,F_0 \dots T_m}(t, \tau, i\tau \mathcal{F}_{\text{dom}}(T_j), i\tau \mathcal{F}_{\text{dom}}(T_{0,\bar{j}}))$$

with the convention $T_0 = F_0$. We assume the coefficients b are polynomial in t, τ with bounded coefficients in τ and that they are non zero for finite values of \mathbf{a} . They also do not depend on the node decorations of the F, F_0 and the T_j that correspond to the frequencies. Now, the forest $F_0 \cdot T_1 \dots \cdot T_m$ correspond to the splitting obtained by iterating Δ and Δ^+ not Δ_{BCK} in (3.15). The forest is produced using the map ψ below:

$$\psi = (\text{id} \otimes \tilde{\psi}) \Delta, \quad \tilde{\psi} = \mathcal{M}(\tilde{\psi} \otimes P_1) \Delta^+, \quad \tilde{\psi}(\mathbf{1}) = \mathbf{1}.$$

Proof. We proceed in the same way as in the proof of Theorem 3.5. The main difference happens on a tree of the form $\mathcal{F}_{o_2}(\lambda_k^\ell F)$. We have

$$\left(\Pi^n \mathcal{F}_{o_2}^r(\lambda_k^\ell F) \right)(t, \tau) = \mathcal{H}_{o_2}^{k,r} \left(\Pi^n \left(\lambda^\ell \mathcal{D}^{r-|\ell|-1}(F) \right) (\cdot, \tau), n \right)(t).$$

We apply the induction hypothesis on $\Pi^{n,r-\ell-1}$. Then, the proof boils down to understand how the operator $\mathcal{H}_{o_2}^{k,r}$ acts on the forest formula. If the dominant part $\mathcal{F}_{\text{dom}}(\mathcal{J}_{o_2}(\lambda_k^\ell F_0))$ is integrated exactly, we obtain a factor of the form

$$e^{it\mathcal{F}_{\text{dom}}(\mathcal{J}_{o_2}(\lambda_k^\ell F_0))}.$$

and this corresponds to forests $\mathcal{J}_{o_2}(\lambda_k^\ell F_0) \cdot \dots \cdot T_m$. In this exact integration, we have terms without this factor and a monomial $t^{q_1} \tau^{q_2}$ which corresponds to the forest $\lambda^q \cdot \mathcal{J}_{o_2}^{(r,q)}(\lambda_k^\ell F_0) \cdot \dots \cdot T_m$. Then, the coefficient b factors out in the following form:

$$\begin{aligned} b_{\mathbf{a}, \mathcal{J}_{o_2}^r(\lambda_k^\ell F), \lambda^q \cdot \mathcal{J}_{o_2}^{(r,q)}(\lambda_k^\ell F_0) \cdot \dots \cdot T_m}(t, \tau, i\tau \mathcal{F}_{\text{dom}}(T_j), i\tau \mathcal{F}_{\text{dom}}(T_{0,\bar{j}})) &= t^{q_1} \tau^{q_2} \\ \tilde{b}_{\mathbf{a}, \mathcal{J}_{o_2}^r(\lambda_k^\ell F), \mathcal{J}_{o_2}^{(r,q)}(\lambda_k^\ell F_0) \cdot \dots \cdot T_m}(\tau, i\tau \mathcal{F}_{\text{dom}}(T_j), i\tau \mathcal{F}_{\text{dom}}(T_{0,\bar{j}})) & \end{aligned}$$

where the term on the right hand side is bounded in τ . The treatment for the lower part is exactly the same. If n is sufficiently big, we can perform a full Taylor expansion via an interpolation that will produce terms of the form:

$$e^{i\tau a \mathcal{F}_{\text{low}}(\mathcal{J}_{o_2}(\lambda_k^\ell F_0))} e^{i\tau a' \mathcal{F}_{\text{dom}}(\mathcal{J}_{o_2}(\lambda_k^\ell F_0))}, \quad a, a' \in [0, 1].$$

These terms will be associated to forests of the form $\lambda^q \cdot \mathcal{J}_{o_2}^{(r,q)}(\lambda_k^\ell F_0) \cdot \dots \cdot T_m$. The factor $e^{i\tau a' \mathcal{F}_{\text{dom}}(\mathcal{J}_{o_2}(\lambda_k^\ell F_0))}$ will be inside the coefficients b . \square

Remark 3.9 The forest formula given in (3.23) contains more terms than the one given in (3.16), and therefore more degrees of freedom that could be exploited for finding new schemes. In the sequel, we will use the first forest formula instead of this one as one can notice that the dominant part $\mathcal{F}_{\text{dom}}(F_0)$ does not change if we change monomial decorations inside F_0 .

Remark 3.10 While the general forest formula (3.37) is suitable for characterising symmetric resonance based schemes (cf. Proposition 4.7) it does not (at the current point) permit a direct analysis of the local error of the scheme, which for a general symmetric resonance based scheme has to be performed on a case-by-case basis. On the other hand, the direct construction of explicit resonance based schemes in [15] automatically allows for local error estimates, which motivates the study of general Duhamel iterates and a description of the midpoint iterates using decorated tree series in the following section. It turns out (cf. Section 4) that these iterations lead to a subclass of symmetric schemes captured by the general formula (3.37) (cf. Theorem 3.15) which allows us to construct and analyse a class of symmetric low-regularity integrators of arbitrary given order in a structured way. We will see in Theorem 3.19 that this iterative approach allows us to derive general estimates on the local error, even in the case of implicit schemes (implicitness is required for symmetry of the scheme).

Example 7 Below, we provide some examples of computations with Δ^+ :

$$\begin{aligned}
 \Delta^+ \begin{array}{c} \textcircled{k_2} \\ | \\ \textcircled{k_1} \textcircled{k_3} \\ | \\ \textcircled{k_4} \textcircled{k_5} \\ | \\ (r, r') \end{array} &= \begin{array}{c} \textcircled{k_2} \\ | \\ \textcircled{k_1} \textcircled{k_3} \\ | \\ \textcircled{k_4} \textcircled{k_5} \\ | \\ (r, r') \end{array} \otimes \mathbf{1} + \mathbf{1} \otimes \begin{array}{c} \textcircled{k_2} \\ | \\ \textcircled{k_1} \textcircled{k_3} \\ | \\ \textcircled{k_4} \textcircled{k_5} \\ | \\ (r, r') \end{array} + \sum_m \frac{1}{m!} \begin{array}{c} \textcircled{k_4} \textcircled{k_5} \\ | \\ \textcircled{k_4} \textcircled{k_5} \\ | \\ (r, r') \end{array} \otimes \begin{array}{c} \textcircled{k_2} \\ | \\ \textcircled{k_1} \textcircled{k_3} \\ | \\ (r-1, m) \end{array} \\
 \Delta^+ \begin{array}{c} \textcircled{k_1} \textcircled{k_3} \\ | \\ \textcircled{k_1} \textcircled{k_3} \\ | \\ (r, r') \end{array} &= \begin{array}{c} \textcircled{k_1} \textcircled{k_3} \\ | \\ \textcircled{k_1} \textcircled{k_3} \\ | \\ (r, r') \end{array} \otimes \mathbf{1} + \mathbf{1} \otimes \begin{array}{c} \textcircled{k_1} \textcircled{k_3} \\ | \\ \textcircled{k_1} \textcircled{k_3} \\ | \\ (r, r') \end{array}
 \end{aligned}$$

where a node of the form $\textcircled{\lambda^m}$ in the example above corresponds to the frequency ℓ and the monomial λ^m . As an example of computation of $\tilde{\psi}$, one has

$$\begin{aligned}
 \tilde{\psi} \left(\begin{array}{c} \textcircled{\lambda^m} \\ | \\ \textcircled{k_4} \textcircled{k_5} \\ | \\ (r, r') \end{array} \right) &= \begin{array}{c} \textcircled{\lambda^m} \\ | \\ \textcircled{k_4} \textcircled{k_5} \\ | \\ (r, r') \end{array} \\
 \tilde{\psi} \left(\begin{array}{c} \textcircled{k_2} \\ | \\ \textcircled{k_1} \textcircled{k_3} \\ | \\ \textcircled{k_4} \textcircled{k_5} \\ | \\ (r, r') \end{array} \right) &= \begin{array}{c} \textcircled{k_2} \\ | \\ \textcircled{k_1} \textcircled{k_3} \\ | \\ \textcircled{k_4} \textcircled{k_5} \\ | \\ (r, r') \end{array} + \sum_m \frac{1}{m!} \tilde{\psi} \left(\begin{array}{c} \textcircled{\lambda^m} \\ | \\ \textcircled{k_4} \textcircled{k_5} \\ | \\ (r, r') \end{array} \right) \cdot \begin{array}{c} \textcircled{k_2} \\ | \\ \textcircled{k_1} \textcircled{k_3} \\ | \\ (r-1, m) \end{array} \\
 &= \begin{array}{c} \textcircled{k_2} \\ | \\ \textcircled{k_1} \textcircled{k_3} \\ | \\ \textcircled{k_4} \textcircled{k_5} \\ | \\ (r, r') \end{array} + \sum_m \frac{1}{m!} \begin{array}{c} \textcircled{\lambda^m} \\ | \\ \textcircled{k_4} \textcircled{k_5} \\ | \\ (r, r') \end{array} \cdot \begin{array}{c} \textcircled{k_2} \\ | \\ \textcircled{k_1} \textcircled{k_3} \\ | \\ (r-1, m) \end{array}
 \end{aligned}$$

3.4 Midpoint general resonance based schemes

In this section, we introduce new resonance based schemes where we iterate Duhamel's formula in slightly different manner. The iteration chosen follows the mid point rule. These schemes turn out to be a subclass of the general forest formula (3.37). In this subclass it is also possible to work with a fairly general framework more closely aligned with [15] which allows for an automatic handle on the local error of these schemes. In particular, in order to incorporate the midpoint iterations and subsequent lower part interpolations we need to add more edge decorations on the trees representing the iterated integrals. For example, we can consider decorated trees of the form $T_{\epsilon, \chi}^{n, o} = (T, n, o, \epsilon, \chi)$ where $\chi : E_T \rightarrow \mathfrak{D}$. Here \mathfrak{D} is a finite set and encodes the following information for an edge $e \in N_T$ decorated by (t, p) :

- For $t \notin \mathfrak{L}_+$, the edge e is associated with a term of the form $e^{iP_{(t,p)}(k_v)}$. Then, $\chi(e)$ corresponds of a way of iterating Duhamel's formula not only using the leftmost point of the interval but a weighted sum of iterations on various points in $[0, \tau]$.
- For $t \in \mathfrak{L}_+$, the edge e is associated with a term of the form $\int_{a\tau}^t e^{iP_{(t,p)}(k_v)} \dots ds$ where $a \in [0, 1]$ and it corresponds to a different Duhamel's iteration. Now, $\chi(e)$ gives a choice of a polynomial interpolation for the lower part of the resonance in the discretisation.

For reasons of presentation we focus on the midpoint rule, however, we could also follow other types of Duhamel iterations. Moreover, in this subclass we take the polynomial interpolation to be fixed.

To illustrate the central idea of a different way of iterating Duhamel's formula, let us first consider the Nonlinear Schrödinger equation. The usual iteration is given by

$$u(t_n + s) = e^{i\tau\Delta}u(t_n) - ie^{i\tau\Delta} \int_0^\tau e^{-is\Delta} (|u(t_n + s)|^2 u(t_n + s)) ds.$$

In Fourier space, we obtain

$$\begin{aligned} u_k(t_n + \tau) &= e^{-i\tau k^2} u_k(t_n) \\ &- ie^{-i\tau k^2} \sum_{k=-k_1+k_2+k_3} \int_0^\tau e^{isk^2} \overline{\hat{u}_{k_1}(t_n + s)} u_{k_2}(t_n + s) u_{k_3}(t_n + s) ds. \end{aligned} \quad (3.25)$$

We can now choose to iterate this expression using two possible ways:

$$\begin{aligned} u_k(t_n + s) &= e^{-isk^2} u_k(t_n) \\ &- ie^{-isk^2} \sum_{k=-k_1+k_2+k_3} \int_0^s e^{i\tilde{s}k^2} \overline{\hat{u}_{k_1}(t_n + \tilde{s})} u_{k_2}(t_n + \tilde{s}) u_{k_3}(t_n + \tilde{s}) d\tilde{s}. \end{aligned} \quad (3.26)$$

and

$$\begin{aligned} u_k(t_n + s) &= e^{-i(s-\tau)k^2} u_k(t_n + \tau) \\ &- ie^{-isk^2} \sum_{k=-k_1+k_2+k_3} \int_\tau^s e^{i\tilde{s}k^2} \overline{\hat{u}_{k_1}(t_n + \tilde{s})} u_{k_2}(t_n + \tilde{s}) u_{k_3}(t_n + \tilde{s}) d\tilde{s}. \end{aligned} \quad (3.27)$$

The iteration (3.26) corresponds to the left end point of the interval $[0, \tau]$ while (3.27) is the right end point. We now have a choice over each term in (3.25) if we want the iteration of Duhamel's formula to begin with (3.26) or (3.27). The average of the two iterations gives the midpoint rule.

There are quite a lot of degrees of freedom as one can choose various linear combinations of Duhamel's formulae in different points. Let us mention that the tree structure is not modified if one changes the iteration but the definition of Π has

to reflect this new formulation. The midpoint rule oscillatory integrals are given by

$$\begin{aligned}\Pi_{\text{mid}}(F \cdot \bar{F})(s, \tau) &= (\Pi_{\text{mid}}F)(s, \tau)(\Pi_{\text{mid}}\bar{F})(s, \tau), \\ (\Pi_{\text{mid}}\mathcal{F}_{O_1}(\lambda_k F))(s, \tau) &= \frac{1}{2}e^{isP_{O_1}(k)}((\Pi_{\text{mid},1}F)(s, \tau) + (\Pi_{\text{mid},2}F)(s, \tau)), \\ (\Pi_{\text{mid},1}\mathcal{F}_{O_2}(\lambda_k F))(s, \tau) &= -i|\nabla|^\alpha(k) \int_\tau^s e^{i\xi P_{O_2}(k)}(\Pi_{\text{mid}}F)(\xi, \tau)d\xi, \\ (\Pi_{\text{mid},2}\mathcal{F}_{O_2}(\lambda_k F))(s, \tau) &= -i|\nabla|^\alpha(k) \int_0^s e^{i\xi P_{O_2}(k)}(\Pi_{\text{mid}}F)(\xi, \tau)d\xi.\end{aligned}\tag{3.28}$$

We notice that, in this definition, we have to keep track of the time step τ in order to remember the interval $[0, \tau]$. In this definition, we have assumed that the Duhamel iteration corresponds to edges decorated by t_1 . Moreover, we have supposed that F is not empty for $(\Pi_{\text{mid}}\mathcal{F}_{O_1}(\lambda_k F))(s, \tau)$ and $s \neq \tau$. If F is empty, we set

$$(\Pi_{\text{mid}}\mathcal{F}_{O_1}(\lambda_k \mathbf{1}))(s, \tau) = e^{isP_{O_1}(k)}.\tag{3.29}$$

If $\tau = s$, we set

$$(\Pi_{\text{mid}}\mathcal{F}_{O_1}(\lambda_k F))(\tau, \tau) = (\Pi_{\text{mid}}\mathcal{F}_{O_1}(\lambda_k F))(\tau) = e^{i\tau P_{O_1}(k)}(\Pi_{\text{mid},2}F)(\tau, \tau).\tag{3.30}$$

The last two specific cases are necessary for building up the scheme. Indeed, (3.29) corresponds to the leaves of our trees or when we terminate on an initial data u_{k_i} . Here, we will apply the midpoint rule in the sequel (see (3.33) in the definition of $\Upsilon_{\text{mid}}^p(T)(v, \tau)$)

$$\frac{1}{2}u_{k_j}(0) + e^{-i\tau P_{O_1}(k_j)}\frac{1}{2}u_{k_j}(\tau).$$

The second condition (3.30) corresponds to the fact that the first is not the midpoint rule approximation as we do not need to perform it as $\tau = s$.

Remark 3.11 This approach also works for the more general scheme given in [2]. The main difference is that now $\Upsilon_{\text{mid}}^p(T)(v, \tau)$ defined in the sequel is part of the definition of Π_{mid} .

The scheme $\Pi_{\text{mid}}^{n,r}$ is defined as the same as for Π_{mid} but now we discretise the time integrals:

$$\left(\Pi_{\text{mid},j}^{n,r}\mathcal{F}_{O_2}(\lambda_k F)\right)(s, \tau) = \mathcal{H}_{O_2,j}^{k,r}(\Pi_{\text{mid}}^{n,r}(F)(\cdot, \tau), n)(s, \tau), \quad j \in \{1, 2\}$$

where the map $\mathcal{H}_{O_2,1}^{k,r}(\cdot)(s, \tau)$ uses the exact integration $\int_s^\tau \dots d\xi$ and $\mathcal{H}_{O_2,2}^{k,r}$ the one given by $\int_0^s \dots d\xi$. We first introduce some notations:

Definition 8 • For a decorated tree $T_\epsilon = (T, \epsilon)$ with only edge decorations, we define the symmetry factor $S(T_\epsilon)$ inductively by $S(\mathbf{1})=1$, while if T is of the form

$$\prod_{i,j} \mathcal{F}_{(t_i, p_i)}(T_{i,j})^{\beta_{i,j}},$$

with $T_{i,j} \neq T_{i,\ell}$ for $j \neq \ell$, then

$$S(T) := \left(\prod_{i,j} S(T_{i,j})^{\beta_{i,j}} \beta_{i,j}! \right). \quad (3.31)$$

We extend this definition to any tree $T_\epsilon^{n,0}$ in \mathcal{T} by setting:

$$S(T_\epsilon^{n,0}) := S(T_\epsilon).$$

Let us stress that the symmetric factor depends only on the edges decorations but not on the nodes decorations given by the frequencies.

- Then, we define the map $\Upsilon_{mid}^p(T)(v, \tau)$ for

$$T = \mathcal{F}_{(t_1,a)} \left(\lambda_k \mathcal{F}_{(t_2,a)} (\lambda_k \prod_{i=1}^n \mathcal{F}_{(t_1,0)} (\lambda_{k_i} T_i) \prod_{j=1}^m \mathcal{F}_{(t_1,1)} (\lambda_{\tilde{k}_j} \tilde{T}_j)) \right), \quad a \in \{0, 1\}$$

by

$$\begin{aligned} \Upsilon_{mid}^p(T)(v, \tau) := & \partial_v^n \partial_{\bar{v}}^m p_a(v, \bar{v}) \prod_{i=1}^n \Upsilon_{mid}^p(\mathcal{F}_{(t_1,0)} (\lambda_{k_i} T_i))(v, \tau) \\ & \prod_{j=1}^m \Upsilon_{mid}^p(\mathcal{F}_{(t_1,1)} (\lambda_{\tilde{k}_j} \tilde{T}_j))(v, \tau) \end{aligned} \quad (3.32)$$

and

$$\begin{aligned} \Upsilon_{mid}^p(\mathcal{F}_{(t_1,0)} (\lambda_k))(v, \tau) &:= \frac{1}{2} v_k(0) + \frac{1}{2} e^{-iP_{o_1}(k)\tau} v_k(\tau) \\ \Upsilon_{mid}^p(\mathcal{F}_{(t_1,1)} (\lambda_k))(v, \tau) &:= \frac{1}{2} \bar{v}_k(0) + \frac{1}{2} e^{iP_{o_1}(k)\tau} \bar{v}_k(\tau). \end{aligned} \quad (3.33)$$

Above, we have used the notation:

$$p_0(v, \bar{v}) = p(v, \bar{v}), \quad p_1(v, \bar{v}) = \overline{p(v, \bar{v})}$$

In the sequel, we will use the following short hand notation:

$$\overline{\Upsilon_{mid}^p(T)}(v, \tau) = \tilde{\Upsilon}_{mid}^p(T)(v, \tau).$$

- We set

$$\begin{aligned} \hat{\mathcal{T}}_0(R) &= \{ \mathcal{F}_{(t_1,0)} (\lambda_k \mathcal{F}_{(t_2,0)} (\lambda_k \prod_{i=1}^N T_i \prod_{j=1}^M \tilde{T}_j)), \mathcal{F}_{(t_1,0)} (\lambda_k) \\ & \quad T_i \in \hat{\mathcal{T}}_0(R), \tilde{T}_j \in \tilde{\mathcal{T}}_0(R), k \in \mathbf{Z}^d \} \\ \tilde{\mathcal{T}}_0(R) &= \{ \mathcal{F}_{(t_1,1)} (\lambda_k \mathcal{F}_{(t_2,1)} (\lambda_k \prod_{i=1}^N T_i \prod_{j=1}^M \tilde{T}_j)), \mathcal{F}_{(t_1,1)} (\lambda_k) \end{aligned}$$

$$T_i \in \tilde{\mathcal{T}}_0(R), \tilde{T}_j \in \hat{\mathcal{T}}_0(R), k \in \mathbf{Z}^d$$

$$\hat{\mathcal{T}}_2(R) = \left\{ \mathcal{J}_{(\mathfrak{t}_2, 0)}(\lambda_k \prod_{i=1}^N T_i \prod_{j=1}^M \tilde{T}_j), T_i \in \hat{\mathcal{T}}_0(R), \tilde{T}_j \in \tilde{\mathcal{T}}_0(R), k \in \mathbf{Z}^d \right\}$$

For a fixed $k \in \mathbf{Z}^d$, we denote the set $\hat{\mathcal{T}}_0^k(R)$ (resp. $\tilde{\mathcal{T}}_0^k(R)$ and $\hat{\mathcal{T}}_2^k(R)$) as the subset of $\hat{\mathcal{T}}_0(R)$ (resp. $\tilde{\mathcal{T}}_0(R)$ and $\hat{\mathcal{T}}_2^k(R)$) whose decorated trees have decorations on the node connected to the root given by k . For $r \in \mathbf{Z}$, $r \geq -1$, we set:

$$\hat{\mathcal{T}}_0^{r,k}(R) = \{T_\epsilon^0 \in \hat{\mathcal{T}}_0^k(R), n_+(T_\epsilon^0) \leq r + 1\}.$$

In the previous space, we disregard iterated integrals which have more than $r + 1$ integrals and will be of order $\mathcal{O}(\tau^{r+2})$. The set $\hat{\mathcal{T}}_2^{r,k}(R)$ is defined as the same from $\hat{\mathcal{T}}_2^k(R)$. In the sequel, we will use the short hand notation for $T \in \hat{\mathcal{T}}_2^k(R)$:

$$\Upsilon_{mid}^p(T)(v, \tau) = \Upsilon_{mid}^p(\mathcal{J}_{(\mathfrak{t}_1, 0)}(\lambda_k T))(v, \tau).$$

This truncation leads exactly to the current local error behaviour as shown in the following proposition which forms the basis of our local error analysis in Theorem 3.19.

Proposition 3.12 *The tree series given by*

$$U_{mid,k}^r(\tau, v) = \sum_{T \in \hat{\mathcal{T}}_0^{r,k}(R)} \frac{\Upsilon_{mid}^p(T)(v, \tau)}{S(T)} (\Pi_{mid} T)(\tau) \quad (3.34)$$

where $o_1 = (\mathfrak{t}_1, 0)$, is the k -th Fourier coefficient of a solution of (3.25) with the midpoint rule expansion up to order $r + 1$.

Proof. The proof follows the same lines as the one given in [15, Prop. 4.3]. \square

We are now able to define the main resonance based scheme:

Definition 3.13 The midpoint resonance based scheme is given by:

$$U_{mid,k}^{n,r}(\tau, v) = \sum_{T \in \hat{\mathcal{T}}_0^{r,k}(R)} \frac{\Upsilon_{mid}^p(T)(v, \tau)}{S(T)} (\Pi_{mid}^{n,r} T)(\tau) \quad (3.35)$$

It is obtained by replacing the character Π_{mid}^r by $\Pi_{mid}^{n,r}$ in (3.34).

The new scheme (3.35) can be described by the same type of forest formula introduced before.

Proposition 3.14 *For every forest F , $(\Pi_{mid}^{n,r} F)(t, \tau)$ is of the form of (3.16). For every decorated tree $T = \mathcal{J}_{o_1}(\lambda_k \mathcal{J}_{o_2}(\lambda_k F))$, $(\Pi_{mid}^{n,r} T)(\tau)$ is of the form (3.17).*

Proof. The proof follow by induction as in Theorem-3,5 and Theorem 3,6. \square

Before stating our main result connecting the midpoint resonance based schemes to our earlier forest formula, we need to introduce a new map

$$\Upsilon_{\chi}^p(T)(u_{k_v}^{n+\chi_v}, v \in L_T, \tau)$$

defined as the same as $\Upsilon_{\text{mid}}^p(T)(v, \tau)$ except that for the leaves we use

$$e^{-i\chi_u \tau P_{o_{e_u}}(k_u)} u_{k_u}^{n+\chi_u}, \quad (3.36)$$

where e_u is the outgoing edge of u in T and o_{e_u} corresponds to the edge decoration of e_u . The map $\Upsilon_{\chi}^p(T)$ allows to parametrise implicit schemes as the scheme given by the midpoint rule.

Theorem 3.15 *The low regularity scheme $U_{\text{mid},k}^{n,r}$ is of the form:*

$$\begin{aligned} u_k^{n+1} &= e^{i\tau P_{o_1}(k)} u_k^n + e^{i\tau P_{o_1}(k)} \sum_{T \in \hat{\mathcal{T}}_2^{r,k}(R)} \sum_{\mathbf{a} \in [0,1]^{\tilde{E}_F}} \sum_{\chi \in \{0,1\}^{L_T}} \sum_{T_0 \cdot T_1 \dots \cdot T_m \subset T} \\ &C_T b_{\mathbf{a}, \chi, T, T_0 \dots T_m}(\tau, i\tau \mathcal{F}_{\text{dom}}(T_j), j \in \{0, \dots, m\}) \\ &\prod_{e \in \tilde{E}_{T_j}} e^{i\tau a_e \mathcal{F}_{\text{low}}(T_j^e)} \frac{\Upsilon_{\chi}^p(T)(u_{k_v}^{n+\chi_v}, v \in L_T, \tau)}{S(T)}, \end{aligned} \quad (3.37)$$

where $\hat{\mathcal{T}}_2^{r,k}(R)$ was introduced in Definition 8.

Proof. First, we notice that

$$U_{\text{mid},k}^{n,r}(\tau, v) = e^{i\tau P_{o_1}(k)} u_k^n + e^{i\tau P_{o_1}(k)} \sum_{T \in \hat{\mathcal{T}}_2^{r,k}(R)} \frac{\Upsilon_{\text{mid}}^p(T)(v, \tau)}{S(T)} (\Pi_{\text{mid}}^{n,r} T)(\tau).$$

Then, the result is just a consequence of Theorem 3,6 applied to each of the $(\Pi_{\text{mid}}^{n,r} T)(\tau)$. Indeed, one multiplies the coefficients for a decorated trees (3.17) with $\Upsilon_{\text{mid}}^p(T)(v, \tau)$. \square

For the local error, we can adapt [15, Def. 3.11].

Definition 3.16 Let $n \in \mathbf{N}$, $r \in \mathbf{Z}$. We recursively define $\mathcal{L}_{\text{low}}^r(\cdot, n)$ as

$$\mathcal{L}_{\text{low}}^r(F, n) = 1, \quad r < 0.$$

Else, when $r \geq 0$, we let:

$$\begin{aligned} \mathcal{L}_{\text{low}}^r(\mathbf{1}, n) &= 1, \quad \mathcal{L}_{\text{low}}^r(F \cdot \bar{F}, n) = \mathcal{L}_{\text{low}}^r(F, n) + \mathcal{L}_{\text{low}}^r(\bar{F}, n) \\ \mathcal{L}_{\text{low}}^r(\mathcal{F}_{o_1}(\lambda_k^\ell F), n) &= \mathcal{L}_{\text{low}}^{r-|\ell|}(F, n) \end{aligned}$$

$$\mathcal{L}_{\text{low}}^r(\mathcal{J}_{o_2}(\lambda_k^\ell F), n) = k^\alpha \mathcal{L}_{\text{low}}^{r-|\ell|-1}(F, n) + \mathbf{1}_{\{r-|\ell|\geq 0\}} \sum_j k^{\bar{n}_j}$$

where

$$\bar{n}_j = \max_m \left(n, \deg \left(P_{(F_j^{(1)}, F_j^{(2)}, m)} \mathcal{F}_{\text{low}}(\mathcal{J}_{(t_2, p)}(\lambda_k^\ell F_j^{(1)}))^{r-|\ell|+1-m} + \alpha \right) \right)$$

with

$$\Delta \mathcal{D}^{r-|\ell|-1}(F) = \sum_j F_j^{(1)} \otimes F_j^{(2)},$$

$$A^n(F_j^{(2)})B^n(F_j^{(1)})(\xi, \tau) = \sum_{|m|\leq r-|\ell|-1} \frac{P_{(F_j^{(1)}, F_j^{(2)}, m)}}{Q_{(F_j^{(1)}, F_j^{(2)}, m)}} \xi^{m_1} \tau^{m_2}$$

and \mathcal{F}_{low} is defined in Definition 3.2.

Remark 3.17 The main difference between the definition above and [15, Def. 3.11] is the fact that we deal with monomials of the form $s^{m_1} \tau^{m_2}$ due to the fact that τ appears in the exact integrations. These modifications are minor from the original structure as the formalism is robust from moving from decorations on the edges in \mathbf{N} to \mathbf{N}^2 .

With the previous definition, one is able to give the local error of the approximations of the oscillatory integrals and for the schemes. The proofs are exactly the same as in [15, Section 3.3].

Theorem 3.18 For every $T \in \mathcal{T}$ one has,

$$(\Pi_{\text{mid}} T - \Pi_{\text{mid}}^{n,r} T)(\tau) = \mathcal{O}(\tau^{r+2} \mathcal{L}_{\text{low}}^r(T, n)).$$

The numerical scheme (3.34) approximates the exact solution locally up to order $r + 2$. More precisely, the following Theorem holds:

Theorem 3.19 (Local error) The numerical scheme (3.34) with initial value $v = u(0)$ approximates the exact solution $U_k(\tau, v)$ up to a local error of type

$$U_{\text{mid},k}^{n,r}(\tau, v) - U_k(\tau, v) = \sum_{T \in \tilde{\mathcal{T}}_0^{r,k}(R)} \mathcal{O}(\tau^{r+2} \mathcal{L}_{\text{low}}^r(T, n) \Upsilon_{\text{mid}}^p(\lambda_k T)(v, \tau))$$

where the operator $\mathcal{L}_{\text{low}}^r(T, n)$, given in Definition 3.16, embeds the necessary regularity of the solution.

Remark 3.20 The local error of the resonance based low regularity schemes does not depend on the choice of the polynomial interpolation and the iteration of Duhamel's formula but only on the structure of the resonances.

Remark 3.21 As in [15, Prop. 3.18], one can always map back to physical space the scheme $U_{\text{mid},k}^{n,r}$. This due to the fact that the structure of the resonances and their exact integration is the same in this context.

4 Symmetric schemes

Having introduced the general forest formula in (3.16) & (3.23) and the general subclass of midpoint general resonance based schemes, we now seek to answer the central question of this manuscript: “Which schemes in these classes are symmetric in the sense of definition 1?” For this we take two routes: Firstly, for the subclass of midpoint general resonance based schemes it turns out that symmetry of the interpolation nodes is sufficient for the symmetry of the schemes. Secondly, for schemes captured by the forest formula (3.16) we can study the form of their adjoint method and find conditions on the coefficients of these schemes under which the methods are symmetric. We recall the adjoint method of a numerical scheme $v^{n+1} = \Phi_\tau v^n$ is defined by $\widehat{\Phi}_\tau := \Phi_{-\tau}^{-1}$ and the method is said to be symmetric if $\widehat{\Phi}_\tau = \Phi_\tau$. We can find the adjoint method of a scheme simply by the operations $n \leftrightarrow n + 1$ and $\tau \leftrightarrow -\tau$. The swapping of n and $n + 1$ corresponds in our case to changing $v_k(0)$ into $v_k(\tau)$. We define $\tilde{\Upsilon}_{\text{mid}}^p(T)(v, \tau)$ as the same as $\Upsilon_{\text{mid}}^p(T)(v, \tau)$ except that we exchange $v_k(0)$ and $v_k(\tau)$ in the definition:

$$\begin{aligned}\tilde{\Upsilon}_{\text{mid}}^p(\mathcal{J}_{(t_1,0)}(\lambda_k))(v, \tau) &:= \frac{1}{2}v_k(\tau) + \frac{1}{2}e^{iP_{o_1}(k)\tau}v_k(0) \\ \tilde{\Upsilon}_{\text{mid}}^p(\mathcal{J}_{(t_1,1)}(\lambda_k))(v, \tau) &:= \frac{1}{2}\bar{v}_k(\tau) + \frac{1}{2}e^{-iP_{o_1}(k)\tau}\bar{v}_k(0).\end{aligned}$$

4.1 Symmetric interpolation

We prove in the next proposition that the Duhamel’s midpoint iteration truncated up to order $r + 1$ gives a symmetric scheme. The proof uses the recursive construction of the iterated integrals.

Proposition 4.1 *The scheme defined by (3.34) is symmetric.*

Proof. We first observe that the scheme is given by

$$u_k(\tau) = e^{i\tau P_{o_1}(k)}u_k(0) + \sum_{T \in \hat{\mathcal{J}}_0^{r,k}(R) \setminus \{\mathcal{J}_{(t_1,0)}(\lambda_k \mathbf{1})\}} \frac{\Upsilon_{\text{mid}}^p(T)(u, \tau)}{S(T)} (\Pi_{\text{mid}} T)(\tau).$$

Now we swap n and $n + 1$, and we also send τ onto $-\tau$, we obtain

$$u_k(\tau) = e^{i\tau P_{o_1}(k)}u_k(0) - e^{i\tau P_{o_1}(k)} \sum_{T \in \hat{\mathcal{J}}_0^{r,k}(R) \setminus \{\mathcal{J}_{(t_1,0)}(\lambda_k \mathbf{1})\}} \frac{\tilde{\Upsilon}_{\text{mid}}^p(T)(u, -\tau)}{S(T)} (\Pi_{\text{mid}} T)(-\tau).$$

Then, one has to show that two sums coincide for proving that the scheme is symmetric. We prove that this is the case for each term of the sum namely, one has:

$$-e^{-i\tau P_{o_1}(k)} \frac{\tilde{\Upsilon}_{\text{mid}}^p(T)(u, -\tau)}{S(T)} (\Pi_{\text{mid}} T)(-\tau) = \frac{\Upsilon_{\text{mid}}^p(T)(u, \tau)}{S(T)} (\Pi_{\text{mid}} T)(\tau). \quad (4.1)$$

We proceed by induction on the construction of the trees for showing (4.1). Decorated trees in $\tilde{\mathcal{T}}_0^{r,k}(R) \setminus \{\mathcal{F}_{(t_1,0)}(\lambda_k \mathbf{1})\}$ are necessarily of the form

$$T = \mathcal{F}_{(t_1,0)}(\lambda_k \mathcal{F}_{(t_2,0)}(\lambda_k F)).$$

We notice that

$$(\Pi_{\text{mid}} T)(-\tau) = -i|\nabla|^\alpha(k) e^{i\tau P_{(t_1,0)}(k)} \int_0^{-\tau} e^{-isP_{(t_1,0)}(k)} (\Pi F)_{\text{mid}}(s, -\tau) ds.$$

By performing the change of variable $s = s + \tau$, one gets

$$(\Pi_{\text{mid}} T)(-\tau) = i|\nabla|^\alpha(k) \int_0^\tau e^{isP_{(t_1,0)}(k)} (\Pi_{\text{mid}} F)(s - \tau, -\tau) ds.$$

It remains to show that

$$\frac{\tilde{\Upsilon}_{\text{mid}}^p(T_j)(u, -\tau)}{S(T_j)} (\Pi_{\text{mid}} T_j)(s - \tau, -\tau) = \frac{\Upsilon_{\text{mid}}^p(T_j)(u, \tau)}{S(T_j)} (\Pi_{\text{mid}} T_j)(s, \tau),$$

where $T_j = \mathcal{F}_{o_1}(\lambda_{k_j} F_j)$ is a decorated tree appearing in the decomposition of F into a product of planted trees. If $F_j = \mathbf{1}$, with loss of generality, we suppose that $o_1 = (t_1, 0)$, then

$$\begin{aligned} \frac{\Upsilon_{\text{mid}}^p(T_j)(u, \tau)}{S(T_j)} (\Pi_{\text{mid}} T_j)(s, \tau) &= \left(\frac{1}{2} e^{-i\tau P_{o_1}(k_j)} u_{k_j}(\tau) + \frac{1}{2} u_{k_j}(0) \right) e^{isP_{o_1}(k_j)} \\ &= \frac{1}{2} e^{i(s-\tau)P_{o_1}(k_j)} u_{k_j}(\tau) + \frac{1}{2} e^{isP_{o_1}(k_j)} u_{k_j}(0) \end{aligned}$$

and

$$\begin{aligned} \frac{\tilde{\Upsilon}_{\text{mid}}^p(T_j)(u, -\tau)}{S(T_j)} (\Pi_{\text{mid}} T_j)(s - \tau, -\tau) &= \left(\frac{1}{2} e^{i\tau P_{o_1}(k_j)} u_{k_j}(0) + \frac{1}{2} u_{k_j}(\tau) \right) e^{i(s-\tau)P_{o_1}(k_j)} \\ &= \frac{1}{2} e^{i(s-\tau)P_{o_1}(k_j)} u_{k_j}(\tau) + \frac{1}{2} e^{isP_{o_1}(k_j)} u_{k_j}(0). \end{aligned}$$

For $(t_1, 1)$, we proceed analogously with the conjugate. For a more general F_j , we have:

$$(\Pi_{\text{mid}} T_j)(s - \tau, -\tau) = \frac{1}{2} e^{i(s-\tau)P_{o_1}(k_j)} ((\Pi_{\text{mid},1} F_j)(s - \tau, -\tau) + (\Pi_{\text{mid},2} F_j)(s - \tau, 0)).$$

Then F_j is of the form $\mathcal{F}_{o_2}(\lambda_{k_j} \hat{F}_j)$. Thus, we have

$$\begin{aligned} \left(\Pi_{\text{mid},1} \mathcal{F}_{o_2}(\lambda_{k_j} \hat{F}_j) \right)(s - \tau, -\tau) &= -i|\nabla|^\alpha(k_j) \int_{-\tau}^{s-\tau} e^{i\xi P_{o_2}(k_j)} (\Pi_{\text{mid}} \hat{F}_j)(\xi, -\tau) d\xi, \\ &= -i|\nabla|^\alpha(k_j) \int_0^s e^{i(\xi-\tau)P_{o_2}(k_j)} (\Pi_{\text{mid}} \hat{F}_j)(\xi - \tau, -\tau) d\xi \end{aligned}$$

and

$$\begin{aligned} \left(\Pi_{\text{mid},2} \mathcal{F}_{o_2}(\lambda_{k_j} \hat{F}_j) \right)(s - \tau, 0) &= -i |\nabla|^\alpha(k_j) \int_0^{s-\tau} e^{i\xi P_{o_2}(k)} (\Pi_{\text{mid}} \hat{F}_j)(\xi, -\tau) d\xi \\ &= -i |\nabla|^\alpha(k_j) \int_\tau^s e^{i(\xi-\tau) P_{o_2}(k)} (\Pi_{\text{mid}} \hat{F}_j)(\xi - \tau, -\tau) d\xi. \end{aligned}$$

We conclude by applying the induction hypothesis on \hat{F}_j that is

$$\frac{\tilde{\Upsilon}_{\text{mid}}^p(F_j)(u, -\tau)}{S(F_j)} (\Pi_{\text{mid}} \hat{F}_j)(s - \tau, -\tau) = \frac{\Upsilon_{\text{mid}}^p(F_j)(u, \tau)}{S(F_j)} (\Pi_{\text{mid}} \hat{F}_j)(s, \tau).$$

□

We recall the scheme given by the midpoint rule (3.35)

$$U_{\text{mid},k}^{n,r}(\tau, v) = \sum_{T \in \hat{\mathcal{T}}_0^{r,k}(R)} \frac{\Upsilon_{\text{mid}}^p(T)(v, \tau)}{S(T)} (\Pi_{\text{mid}}^{n,r} T)(\tau). \quad (4.2)$$

The terms $(\Pi_{\text{mid}}^{n,r} T)(\tau)$ are constructed in a similar way as $(\Pi_{\text{mid}} T)(\tau)$. The main difference happens for the computation of the time integrals. Indeed, $(\Pi_{\text{mid}}^{n,r} T)(\tau)$ performs an approximation with a polynomial interpolation and we need to do it in a symmetric way. We need the following lemma on the polynomial interpolation in order to guarantee this property:

Lemma 4.2 *If the interpolation nodes $a_j \in [0, 1], j = 0, \dots, r$ are symmetrically distributed, i.e. $a_j = 1 - a_{r-j}, j = 0, \dots, r$, then*

$$\tilde{p}_r(s - \tau, -\tau) = \sum_{j=0}^r e^{-ia_j \tau \mathcal{L}_{\text{low}}} p_j(s - \tau, -\tau) = e^{-i\tau \mathcal{L}_{\text{low}}} \tilde{p}_r(s, \tau), \quad (4.3)$$

where we have used the short hand notation

$$\tilde{p}_r(s, \tau) := \tilde{p}_r(\exp(is \mathcal{L}_{\text{low}}), \tau).$$

Proof. To begin with, for any $j = 0, \dots, r$ we have by definition of the interpolating polynomials $\tilde{p}_r(s, \tau)$ and $\tilde{p}_r(s, -\tau)$

$$\tilde{p}_r(a_j \tau, \tau) = e^{ia_j \tau \mathcal{L}_{\text{low}}}, \quad \tilde{p}_r(-a_j \tau, -\tau) = e^{ia_j \tau \mathcal{L}_{\text{low}}}.$$

Thus in particular we have

$$\begin{aligned} \tilde{p}_r(a_j \tau - \tau, -\tau) &= \tilde{p}_r(-a_{r-j} \tau, -\tau) = e^{ia_{r-j} \tau \mathcal{L}_{\text{low}}} \\ &= e^{i\tau \mathcal{L}_{\text{low}}} e^{-ia_j \tau \mathcal{L}_{\text{low}}} = e^{i\tau \mathcal{L}_{\text{low}}} \tilde{p}_r(a_j \tau, \tau), \end{aligned}$$

for each $j = 0, \dots, r$. Thus, for any given τ , $\tilde{p}_r(s - \tau, -\tau)$ and $e^{-i\tau \mathcal{L}_{\text{low}}} \tilde{p}_r(s, \tau)$ are two polynomials in s of degree $\leq r$ which match at $r + 1$ distinct points, so they are identical. □

Theorem 4.3 *The scheme given by (3.35) is symmetric.*

Proof. The proof works in the same manner as for Proposition 4.1. The main difference is the use of the operator $\mathcal{H}_{o_2, j}^{k, r}$. We suppose that

$$\frac{\tilde{\Upsilon}_{\text{mid}}^p(F_j)(u, -\tau)}{S(F_j)}(\Pi_{\text{mid}}^{n, r} \hat{F}_j)(s - \tau, -\tau) = \frac{\Upsilon_{\text{mid}}^p(F_j)(u, \tau)}{S(F_j)}(\Pi_{\text{mid}}^{n, r} \hat{F}_j)(s, \tau) \quad (4.4)$$

and we consider

$$\left(\Pi_{\text{mid}, 1}^{n, r} \mathcal{J}_{o_2}(\lambda_{k_j} \hat{F}_j)\right)(s - \tau, -\tau) = \mathcal{H}_{o_2, 1}^{k_j, r} \left(\left(\Pi_{\text{mid}}^{n, r} \hat{F}_j\right)(\cdot, -\tau), n\right)(s - \tau, -\tau).$$

From (4.4), we know that $\Pi_{\text{mid}}^{n, r} \hat{F}_j$ is of the form

$$\left(\Pi_{\text{mid}}^{n, r} \hat{F}_j\right)(s, \tau) = e^{i(s-\tau)\mathcal{F}_{\text{dom}}(\hat{F}_j)} A(s - \tau) + e^{is\mathcal{F}_{\text{dom}}(\hat{F}_j)} A(s).$$

Now, when we apply the operator $\mathcal{H}_{o_2, j}^{k, r}$, we get among various cases the exact integration

$$\begin{aligned} & \sum_{\ell=0}^r \int_{-\tau}^{s-\tau} e^{i\xi\mathcal{L}_{\text{dom}}} e^{-ia_j\tau\mathcal{L}_{\text{low}}} p_{\ell, r}(\xi, -\tau) \left(e^{i\tau\mathcal{F}_{\text{dom}}(\hat{F}_j)} A(\xi + \tau) + A(\xi) \right) d\xi \\ &= \sum_{\ell=0}^r \int_0^s e^{i(\xi-\tau)\mathcal{L}_{\text{dom}}} e^{-ia_j\tau\mathcal{L}_{\text{low}}} p_{\ell, r}(\xi - \tau, -\tau) \left(e^{i\tau\mathcal{F}_{\text{dom}}(\hat{F}_j)} A(\xi) + A(\xi - \tau) \right) d\xi \\ &= \int_0^s e^{i(\xi-\tau)\mathcal{L}_{\text{dom}}} e^{-i\tau\mathcal{L}_{\text{low}}} \tilde{p}_r(s, \tau) \left(e^{i\tau\mathcal{F}_{\text{dom}}(\hat{F}_j)} A(\xi) + A(\xi - \tau) \right) d\xi \end{aligned}$$

where from the second to the third line, we have used the assumption (4.3) and we have

$$\mathcal{L}_{\text{dom}} + \mathcal{L}_{\text{low}} = P_{o_2}(k_j) + \mathcal{F}_{\text{dom}}(\hat{F}_j).$$

Therefore, we obtain in the end

$$e^{-i\tau P_{o_2}(k_j)} \int_0^s e^{i\xi\mathcal{L}_{\text{dom}}} \tilde{p}_r(s, \tau) \left(A(\xi) + e^{-i\tau\mathcal{F}_{\text{dom}}(\hat{F}_j)} A(\xi - \tau) \right) d\xi$$

which allows us to conclude the symmetry of the method. \square

4.2 Conditions for symmetry

Based on the general expression of the scheme (3.37) we can arrive at sufficient conditions for the methods to be symmetric. The following observation is crucial:

Lemma 4.4 *Let T a decorated tree in $\hat{\mathcal{T}}_0^k(R)$ as introduced in (3.14). We have*

$$\mathcal{F}_{\text{dom}}(T) + \sum_{e \in \hat{E}_T} \mathcal{F}_{\text{low}}(T^e) = \sum_{v \in L_T} P_{o_{e_v}}(k_v)$$

where e_v is the outgoing edge of v in T and o_{e_v} corresponds to the edge decoration of e_v . The k_v are the leaves decorations corresponding to the frequencies. The dominant part $\mathcal{F}_{\text{dom}}(T)$ and the lower parts $\mathcal{F}_{\text{low}}(T^e)$ depend on them.

$$+ \mathcal{F}_{\text{low}}(\mathcal{J}_{(t_2,a)}(\lambda_k F)) + \sum_{e \in \tilde{E}_T \setminus \{\bar{e}\}} \mathcal{F}_{\text{low}}(T^e)$$

where \bar{e} denotes the edge such that $T^{\bar{e}} = \mathcal{J}_{(t_2,a)}(\lambda_k F)$. Now, we use Definition 3.2 to notice that

$$\mathcal{F}_{\text{dom}}(\mathcal{J}_{(t_2,a)}(\lambda_k F)) + \mathcal{F}_{\text{low}}(\mathcal{J}_{(t_2,a)}(\lambda_k F)) = P_{(t_2,a)}(k) + \mathcal{F}_{\text{dom}}(F).$$

By definition, we have also

$$P_{(t_2,a)}(k) + P_{(t_1,a)}(k) = 0. \quad (4.5)$$

We got in the end

$$\begin{aligned} \mathcal{F}_{\text{dom}}(T) + \sum_{e \in \tilde{E}_T} \mathcal{F}_{\text{low}}(T^e) &= \mathcal{F}_{\text{dom}}(F) + \sum_{e \in \tilde{E}_T \setminus \{\bar{e}\}} \mathcal{F}_{\text{low}}(T^e) \\ &= \mathcal{F}_{\text{dom}}(F) + \sum_{e \in \tilde{E}_F} \mathcal{F}_{\text{low}}(F^e). \end{aligned}$$

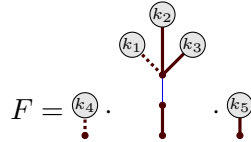
We continue the induction by observing that F is a product of trees in $\tilde{\mathcal{T}}_0^{r,k}(R)$. We apply the induction hypothesis on each of these trees and use the fact that \mathcal{F}_{dom} is additive for the forest product in order to conclude. \square

Lemma 4.5 *Let $T_0 \cdot T_1 \dots \cdot T_m \subset \mathcal{J}_{(t_2,0)}(\lambda_k F) \in \hat{\mathcal{T}}_2^k(R)$ be a splitting of F as introduced in (3.14). Then we have*

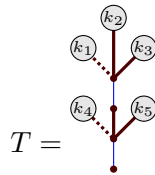
$$\sum_{j=0}^m \left(\mathcal{F}_{\text{dom}}(T_j) + \sum_{e \in \tilde{E}_{T_j}} \mathcal{F}_{\text{low}}(T_j^e) \right) = \sum_{v \in L_F} P_{O_{e_v}}(k_v) + P_{(t_2,0)}(k). \quad (4.6)$$

Proof. This is a consequence of Lemma 4.4 applied to each of the T_j . In the end, we do not get all the leaves of the T_j but only the ones in F because the root of the T_j ($j \geq 0$) is associated with a leaf in a T_i . Indeed, this introduced a cancellation of the type (4.5). \square

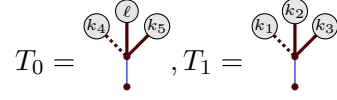
Example 10 Let us consider the following forest



such that $T = \mathcal{J}_{(t_2,0)}(\lambda_k F)$ is identified with



with $k = -k_1 - k_4 + k_2 + k_3 + k_5$. We consider the following forest splitting of T , with $T_0 \cdot T_1 \subset T$:



with $k = k_4 - \ell - k_5$ and $\ell = -k_1 + k_2 + k_3$. Let us compute both sides of the identity (4.6) for this forest splitting: Beginning with the left hand side where we have

$$\mathcal{F}_{\text{dom}}(T_0) = 2k_4^2.$$

Moreover, since the tree has just one single blue edge the sum simplifies and we find

$$\sum_{e \in \tilde{E}_{T_0}} \mathcal{F}_{\text{low}}(T_0) = \mathcal{F}_{\text{low}}(T_0^e) = -k_4^2 - k_5^2 - \ell^2 + k^2,$$

and, similarly for T_1 we have

$$\begin{aligned} \mathcal{F}_{\text{dom}}(T_1) &= 2k_1^2, \\ \sum_{e \in \tilde{E}_{T_1}} \mathcal{F}_{\text{low}}(T_1^e) &= -k_1^2 - k_2^2 - k_3^2 + \ell^2. \end{aligned}$$

For the right hand side on the other hand we obtain

$$\begin{aligned} \sum_{v \in L_F} P_{O_{e_v}}(k_v) &= k_4^2 + k_1^2 - k_2^2 - k_3^2 - k_5^2, \\ P_{(t_2,0)}(k) &= -k^2. \end{aligned}$$

Combining all of the above expressions clearly shows that the identity (4.6) is indeed satisfied in the present example.

Remark 4.6 The appearance of the term $P_{(t_2,0)}(k)$ in (4.6) is due to the fact that here we consider forest splittings of trees inside $\hat{\mathcal{T}}_2^k(R)$. Had we instead chosen to work with trees inside $\hat{\mathcal{T}}_0^k(R)$ this term would disappear from the above identity. Essentially, like in the previous proof, if we want to express the sum of the dominant and lower order parts in a forest splitting we can take advantage of cancellations of the form (4.5), meaning as soon as a blue dotted and brown solid edge are adjacent this leads to cancellation of the contribution from the nodal decoration in the overall identity. This means the only terms left are those which cannot be paired with an edge of conjugate colour, in particular the root and all the leaves of the resulting tree.

Proposition 4.7 *If the coefficients b , satisfy the following simple relation*

$$-\left(\prod_{j=0}^m e^{z_j} \right) b_{\mathbf{a}, \chi, T, T_0 \dots T_m}(-\tau, -z_j) = b_{1-\mathbf{a}, 1-\chi, T, T_0 \dots T_m}(\tau, z_j) \quad (4.7)$$

for every $\mathbf{a} \in [0, 1]^{\tilde{E}_F}$, $\chi \in \{0, 1\}^{L_T}$ and any splitting $T_0 \cdot T_1 \dots \cdot T_m \subset T$, then the method (3.37) is symmetric.

Proof. Let us consider the adjoint method $\widehat{\Phi}_{n \rightarrow n+1} = \Phi_{n+1 \rightarrow n}^{-1}$, which can be expressed as follows

$$\begin{aligned} u_k^{n+1} &= e^{i\tau P_{o_1}(k)} u_k^n - \sum_{T \in \tilde{\mathcal{T}}_2^{\tau, k}(R)} \sum_{\mathbf{a} \in [0, 1]^{\tilde{E}_F}} \sum_{\chi \in \{0, 1\}^{L_T}} \sum_{T_0 \cdot T_1 \dots \cdot T_m \subset T} C_T \\ &\quad b_{\mathbf{a}, \chi, T, T_0 \dots T_m}(\tau, i\tau \mathcal{F}_{\text{dom}}(T_j), j \in \{0, \dots, m\}) \\ &\quad \prod_{e \in \tilde{E}_{T_j}} e^{i\tau a_e \mathcal{F}_{\text{low}}(T_j^e)} \frac{\Upsilon_\chi^p(T)(u_{k_v}^{n+\chi_v}, v \in L_T), \tau}{S(T)}. \end{aligned}$$

By using Lemma 4.5, we have

$$\begin{aligned} u_k^{n+1} &= e^{i\tau P_{o_1}(k)} u_k^n - e^{i\tau P_{o_1}(k)} \sum_{T \in \tilde{\mathcal{T}}_0^{\tau, k}(R)} \sum_{\mathbf{a} \in [0, 1]^{\tilde{E}_F}} \sum_{\chi \in \{0, 1\}^{L_T}} \sum_{T_0 \cdot T_1 \dots \cdot T_m \subset T} C_T \\ &\quad \left(\prod_{j=0}^m e^{i\tau \mathcal{F}_{\text{dom}}(T_j)} \right) b_{\mathbf{a}, \chi, T, T_0 \dots T_m}(-\tau, -i\tau \mathcal{F}_{\text{dom}}(T_j), j \in \{0, \dots, m\}) \quad (4.8) \\ &\quad \prod_{e \in \tilde{E}_{T_j}} e^{i\tau(1-a_e) \mathcal{F}_{\text{low}}(T_j^e)} \frac{\Upsilon_\chi^p(T)(u_{k_v}^{n+1-\chi_v}, v \in L_T, \tau)}{S(T)} \prod_{v \in L_T} e^{-i\tau P_{o_{e_v}}(k_v)}. \end{aligned}$$

Here we have used the fact that

$$\Upsilon_\chi^p(T)(u_{k_v}^{n+1-\chi_v}, v \in L_T, \tau) \prod_{v \in L_T} e^{-i\tau P_{o_{e_v}}(k_v)} = \Upsilon_\chi^p(T)(u_{k_v}^{n+\chi_v}, v \in L_T, \tau)$$

which can be proved easily by induction on T using the recursive definition of Υ_χ^p . We have also used the identity

$$P_{o_1}(k) = -P_{(t_2, 0)}(k).$$

By comparing (3.37) and (4.8) we immediately obtain the conditions (4.7) for symmetry. \square

4.3 Examples

In this section we illustrate the general framework introduced previously on two examples: the nonlinear Schrödinger equation (see Section 4.3.1) and the Korteweg-de Vries equation (see Section 4.3.2).

4.3.1 The Nonlinear Schrödinger equation

As a first example let us consider the cubic nonlinear Schrödinger (NLS) equation

$$i\partial_t u(t, x) + \Delta u(t, x) = |u(t, x)|^2 u(t, x) \quad (t, x) \in \mathbf{R} \times \mathbb{T}^d \quad (4.9)$$

with an initial condition

$$u|_{t=0} = u_0. \quad (4.10)$$

We start with the construction of a first-order symmetric low-regularity scheme for (4.9) and illustrate how our general framework covers both the previous explicit low-regularity schemes [15], [2] and the case of symmetric low-regularity schemes for NLS which was recently introduced and studied in [4], [29], [50]. We then exhibit our new symmetric midpoint rule framework (3.35), which in particular allows for a symmetric second order scheme which is optimal in the sense of regularity.

Note that the Schrödinger equation (4.9) fits into the general framework (1.1) with

$$\mathcal{L}\left(\nabla, \frac{1}{\varepsilon}\right) = \Delta, \quad \alpha = 0 \quad \text{and} \quad p(u, \bar{u}) = u^2 \bar{u}.$$

Here $\mathcal{L} = \{t_1, t_2\}$, $P_{t_1} = -\lambda^2$ and $P_{t_2} = \lambda^2$, and the structure constant $C_T = 1$ for all $T \in \hat{\mathcal{T}}_0^{r,k}(R)$, for any $r \in \mathbf{N}$. Then, we denote by \downarrow an edge decorated by $(t_1, 0)$, $\dot{\downarrow}$ an edge denoted by $(t_1, 1)$ by \downarrow an edge decorated by $(t_2, 0)$ and by $\dot{\downarrow}$ an edge decorated by $(t_2, 1)$. The set $\hat{\mathcal{T}}_0^{0,k}(R)$ is given by:

$$\hat{\mathcal{T}}_0^{0,k}(R) = \{T_0, T_1, k_i \in \mathbf{Z}^d\}, \quad T_0 = \downarrow^k, \quad T_1 = \begin{array}{c} \circlearrowleft k_2 \\ \circlearrowleft k_1 \quad \circlearrowleft k_3 \\ \dot{\downarrow} \end{array}, \quad (4.11)$$

and $\hat{\mathcal{T}}_0^{1,k}(R)$ is given by:

$$\hat{\mathcal{T}}_0^{1,k}(R) = \{T_0, T_1, T_2, T_3, k_i \in \mathbf{Z}^d\}, \quad T_2 = \begin{array}{c} \circlearrowleft k_2 \\ \circlearrowleft k_1 \quad \circlearrowleft k_3 \\ \dot{\downarrow} \\ \circlearrowleft k_4 \quad \circlearrowleft k_5 \\ \dot{\downarrow} \end{array}, \quad T_3 = \begin{array}{c} \circlearrowleft k_2 \\ \circlearrowleft k_1 \quad \circlearrowleft k_3 \\ \dot{\downarrow} \\ \circlearrowleft k_4 \quad \circlearrowleft k_5 \\ \dot{\downarrow} \end{array}, \quad (4.12)$$

If we take all coefficients equal to zero whenever T is not given by

$$T = \begin{array}{c} \circlearrowleft k_2 \\ \circlearrowleft k_1 \quad \circlearrowleft k_3 \\ \dot{\downarrow} \end{array},$$

and we consider only the forest $F = T$, then the general formula (3.37) reduces to a single term of the form:

$$u_k^{n+1} = e^{-i\tau k^2} u_k^n + e^{-i\tau k^2} \sum_{a \in [0,1]} \sum_{\chi \in \{0,1\}^{LT}} b_{a,\chi}(\tau, i\tau \mathcal{F}_{\text{dom}(T)})$$

$$e^{i\tau a \mathcal{F}_{\text{low}}(T)} \frac{\Upsilon_{\chi}^p(T)(u_{k_v}^{n+\chi v}, v \in L_T)}{S(T)}.$$

Note here $|L_T| = 3$ so we can equivalently write the above expression in the following form in Fourier coordinates. Indeed, by noting that $\mathcal{F}_{\text{dom}}(T) = 2k_1^2$, $\mathcal{F}_{\text{low}}(T) = 2k_2k_3 - 2k_1k_2 - 2k_1k_3$ we have

$$u_k^{n+1} = e^{-i\tau k^2} u_k^n + e^{-i\tau k^2} \sum_{k=-k_1+k_2+k_3} \sum_{a \in [0,1]} \sum_{\chi \in \{0,1\}^3} b_{a,\chi}(\tau, 2i\tau k_1^2) e^{i\tau a 2(k_2k_3 - k_1k_2 - k_1k_3)} \widehat{v}_{k_1}^{n+\chi_1} \widehat{v}_{k_2}^{n+\chi_2} \widehat{v}_{k_3}^{n+\chi_3}. \quad (4.13)$$

First of all we note that the first order integrator developed in [55] falls in this category: Take $b_{0,(0,0,0)}(\tau, z) = -i\tau\varphi_1(z)$ and all other coefficients to zero then we find

$$u_k^{n+1} = e^{-i\tau k^2} u_k^n - ie^{-i\tau k^2} \sum_{k=-k_1+k_2+k_3} \tau\varphi_1(2i\tau k_1^2) \overline{u_{k_1}^n} u_{k_2}^n u_{k_3}^n,$$

which is exactly equal to the integrator introduced in [55, (4)]. In physical space the above scheme is given by

$$u^{n+1} = \Phi_{\text{NLS},1}^{\tau}(u^n) = e^{i\tau\Delta} u^n - ie^{i\tau\Delta} ((u^n)^2 \varphi_1(-2i\tau\Delta) \overline{u^n}), \quad (4.14)$$

where the filter function φ_1 is defined as $\varphi_1(\sigma) = \frac{e^{\sigma}-1}{\sigma}$.

Let us now consider symmetric schemes. Following Proposition 4.7 the scheme (3.37) is symmetric if the following equality is satisfied for all $a \in [0, 1]$, $\chi \in \{0, 1\}^3$:

$$-e^z b_{a,\chi}(-\tau, -z) = b_{1-a,1-\chi}(\tau, z). \quad (4.15)$$

Intuitively speaking the above equations provide a sufficient condition relating the coefficients $b_{a,\chi}$ and $b_{1-a,1-\chi}$ therefore allowing us to find symmetric schemes if we specify one of the two for each value of a, χ . There are a large class of first order schemes in this form, but perhaps one of the simplest ones is the following symmetrised version of the integrator from [55] which was recently introduced in [4]: Take $b_{0,(0,0,0)}(\tau, z) = i/2\tau\varphi_1(z/2)$, then by (4.15) we should choose $b_{1,(1,1,1)}(\tau, z) = i/2\tau\varphi_1(-z/2)$. We take all other coefficients equal to zero, which results precisely in the following integrator:

$$u^{n+1} = \Phi_{\text{NLS},2}^{\tau}(u^n) = e^{i\tau\Delta} u^n - i\frac{\tau}{2} e^{i\tau\Delta} ((u^n)^2 \varphi_1(-i\tau\Delta) \overline{u^n}) - i\frac{\tau}{2} ((u^{n+1})^2 \varphi_1(i\tau\Delta) \overline{u^{n+1}}). \quad (4.16)$$

Note this is not the only symmetric first order integrator that can be found in this way. For example we could have taken

$$b_{0,(1,0,0)}(\tau, z) = i/2\tau\varphi_1(z/2), \quad b_{1,(0,1,1)}(\tau, z) = i/2\tau\varphi_1(-z/2),$$

and all other coefficients zero.

Next we choose the coefficients

$$b_{a,(\chi_1,\chi_2,\chi_3)}(\tau, z) = -i \frac{\tau}{16} \varphi_1(z)$$

for every $a, \chi_j \in \{0, 1\}$. The other coefficients are set to be zero which leads to the following symmetric scheme (4.9)

$$\begin{aligned} u^{n+1} &= \Phi_{\text{NLS},3}^\tau(u^n) \\ &= e^{i\tau\Delta} u^n - i \frac{\tau}{16} e^{i\tau\Delta} \left((u^n + e^{-i\tau\Delta} u^{n+1})^2 \varphi_1(-2i\tau\Delta) \left(\overline{u^n} + e^{i\tau\Delta} \overline{u^{n+1}} \right) \right) \\ &\quad - i \frac{\tau}{16} \left((e^{i\tau\Delta} u^n + u^{n+1})^2 \varphi_1(2i\tau\Delta) \left(e^{-i\tau\Delta} \overline{u^n} + \overline{u^{n+1}} \right) \right). \end{aligned} \quad (4.17)$$

The above scheme can also be recursively derived by the general framework of the midpoint rule (3.35) and therefore allows for higher order symmetric counterparts which are optimal in the sense of regularity. Our characterisation of symmetric schemes in Proposition 4.7 immediately confirm this method to be symmetric, since for all a, χ we have

$$-e^z b_{a,\chi}(-\tau, -z) = -i \frac{\tau}{16} e^z \varphi_1(-z) = -i \frac{\tau}{16} \frac{1 - e^z}{-z} = \varphi_1(z) b_{1-a,1-\chi}(\tau, z).$$

Proposition 4.8 *The scheme (4.17) can be derived from the general tree series expansion (3.35).*

Proof. At first order it follows from (3.35) that we have

$$\begin{aligned} U_k^r(\tau, u) &= \sum_{T \in \mathcal{T}_0^{0,k}(R)} \frac{\Upsilon_{\text{mid}}^p(T)(u, \tau)}{S(T)} (\Pi_{\text{mid}}^{n,r} T_0)(\tau) \\ &= \frac{\Upsilon_{\text{mid}}^p(T_0)(u, \tau)}{S(T_0)} (\Pi_{\text{mid}}^{n,r} T_0)(\tau) + \sum_{k=-k_1+k_2+k_3} \frac{\Upsilon_{\text{mid}}^p(T_1)(u, \tau)}{S(T_1)} (\Pi_{\text{mid}}^{n,r} T_1)(\tau) \end{aligned}$$

From the definition of the symmetry factor, one has

$$S(T_0) = 1, \quad S(T_1) = 2$$

for $S(T_1)$ the factor two is due to the fact that we have two solid brown edges \mid attached to the same node in T_1 . Moreover, we have:

$$\begin{aligned} \Upsilon_{\text{mid}}^p(T_0)(u, \tau) &= u_k^\ell \\ \hat{\Upsilon}_{\text{mid}}^p(T_0)(u, \tau) &= \frac{1}{2} (e^{i\tau k^2} u_k^{\ell+1} + u_k^\ell) \end{aligned}$$

where we have used ℓ instead of n such that to not create confusion with $\Pi^{n,r}$. By multiplicativity, for the following tree:

$$\tilde{T}_1 = \begin{array}{c} \textcircled{k_2} \\ \vdots \\ \textcircled{k_1} \textcircled{k_3} \end{array},$$

we have

$$\begin{aligned}\Upsilon_{\text{mid}}^p(T_1)(u, \tau) &= \hat{\Upsilon}_{\text{mid}}^p(\tilde{T}_1)(u, \tau) \\ &= 2\frac{1}{2}(e^{-i\tau k_1^2}\bar{u}_{k_1}^{\ell+1} + \bar{u}_{k_1}^\ell)\frac{1}{2}(e^{i\tau k_2^2}u_{k_2}^{\ell+1} + u_{k_2}^\ell)\frac{1}{2}(e^{i\tau k_3^2}u_{k_3}^{\ell+1} + u_{k_3}^\ell)\end{aligned}$$

On the other hand, we have

$$(\Pi_{\text{mid}}^{n,r}T_0)(\tau) = e^{-i\tau k^2}, \quad (\Pi_{\text{mid}}^{n,r}\tilde{T}_1)(s, \tau) = e^{i(k_1^2 - k_2^2 - k_3^2)},$$

Then,

$$(\Pi_{\text{mid}}^{n,r}T_1)(\tau) = e^{-i\tau k^2}\mathcal{H}_{o_2}^{k,r}((\Pi_{\text{mid}}^{n,r-1}\tilde{T}_1)(\cdot, \tau), n)(\tau)$$

We compute the scheme for $n = 1$ and $r = 0$. We obtain the following term:

$$\mathcal{H}_{o_2}^{k,r}((\Pi_{\text{mid}}^{n,r-1}\tilde{T}_1)(\cdot, \tau), n)(\tau) = -i \int_0^\tau e^{is\mathcal{L}_{\text{dom}}} dS \left(\frac{1 + e^{i\tau\mathcal{L}_{\text{low}}}}{2} \right)$$

where

$$\mathcal{L}_{\text{dom}} = 2k_1^2, \quad \mathcal{L}_{\text{low}} = k^2 - k_1^2 - k_2^2 - k_3^2.$$

In the end, we have

$$(\Pi_{\text{mid}}^{n,r}T_1)(\tau) = -i\tau\varphi_1(2i\tau k_1^2) \left(\frac{e^{-i\tau k^2} + e^{-i\tau(k_1^2 + k_2^2 + k_3^2)}}{2} \right).$$

We note that

$$\varphi_1(2i\tau k_1^2)e^{-2i\tau k_1^2} = \varphi_1(-2i\tau k_1^2).$$

Therefore, we have

$$\begin{aligned}\sum_{k=-k_1+k_2+k_3} \frac{\Upsilon_{\text{mid}}^p(T_1)(u, \tau)}{S(T_1)} (\Pi_{\text{mid}}^{n,r}T_1)(\tau) &= -i \sum_{k=-k_1+k_2+k_3} \frac{e^{-i\tau k^2}}{2} \tau \varphi_1(2i\tau k_1^2) \\ &\frac{1}{2}(e^{-i\tau k_1^2}\bar{u}_{k_1}^{\ell+1} + \bar{u}_{k_1}^\ell)\frac{1}{2}(e^{i\tau k_2^2}u_{k_2}^{\ell+1} + u_{k_2}^\ell)\frac{1}{2}(e^{i\tau k_3^2}u_{k_3}^{\ell+1} + u_{k_3}^\ell) \\ &+ \tau \frac{\varphi_1(-2i\tau k_1^2)}{2} \frac{1}{2}(\bar{u}_{k_1}^{\ell+1} + e^{i\tau k_1^2}\bar{u}_{k_1}^\ell)\frac{1}{2}(u_{k_2}^{\ell+1} + e^{-i\tau k_2^2}u_{k_2}^\ell)\frac{1}{2}(u_{k_3}^{\ell+1} + e^{-i\tau k_3^2}u_{k_3}^\ell).\end{aligned}$$

In physical space this leads to the first order symmetric low regularity integrator for the NLS equation (4.17). \square

Remark 4.9 The derivation of the scheme (4.17) from the general midpoint Duhamel iterations exhibits an interesting recipe for resonance based schemes that are constructed for equations of the form

$$\begin{aligned}i\partial_t u(t, x) + \mathcal{L}\left(\nabla, \frac{1}{\varepsilon}\right)u(t, x) &= |\nabla|^\alpha p(u(t, x), \bar{u}(t, x)), \\ u(0, x) &= v(x).\end{aligned}$$

Indeed, suppose we have already obtained an explicit *first-order* resonance based scheme for the above equation (cf. [55, 39] etc.) of the general form

$$u^{n+1} = \Phi_\tau(u^n),$$

where Φ_τ is a general nonlinear map representing the time step, then this can be easily converted to a second order symmetric method simply by considering instead

$$u^{n+1} = \Phi_\tau \left(\frac{e^{-i\tau\mathcal{L}} \left(\nabla, \frac{1}{\varepsilon} \right) u^{n+1} + u^n}{2} \right).$$

Remark 4.10 In similar vein to Proposition 4.8 we could derive the scheme (4.16) from a generalised tree series expansion. However, instead of using a midpoint iteration of Duhamel's formula as introduced in Section 3.4 we would have to iterate in the following way: By averaging (3.26) and (3.27) we find

$$\begin{aligned} u_k(t_n + s) &= \frac{e^{-isk^2} u_k(t_n) + e^{-i(s-\tau)k^2} u_k(t_n + \tau)}{2} \\ &- \frac{i}{2} e^{-isk^2} \sum_{k=-k_1+k_2+k_3} \underbrace{\int_0^s e^{i\tilde{s}k^2} u_{k_1}(t_n + \tilde{s}) u_{k_2}(t_n + \tilde{s}) u_{k_3}(t_n + \tilde{s}) d\tilde{s}}_{=:\mathcal{F}_1} \\ &- \frac{i}{2} e^{-isk^2} \sum_{k=-k_1+k_2+k_3} \underbrace{\int_\tau^s e^{i\tilde{s}k^2} u_{k_1}(t_n + \tilde{s}) u_{k_2}(t_n + \tilde{s}) u_{k_3}(t_n + \tilde{s}) d\tilde{s}}_{=:\mathcal{F}_2}. \end{aligned}$$

Instead of iterating this midpoint expression throughout all appearances of $u_j(t_n + \tilde{s})$ in the above expression (as we do for the Duhamel midpoint iterates) we could just as well choose to iterate the left endpoint Duhamel formula (3.26) in the terms from \mathcal{F}_1 and the right endpoint Duhamel formula (3.27) in the terms from \mathcal{F}_2 . Repeating this process can be captured with a decorated tree series in analogous manner to the midpoint iterations and truncating such an expansion again leads to symmetric low-regularity schemes, including (after one such iteration and truncation of all terms involving at least double integrals) the scheme (4.16).

Proposition 4.11 *The schemes (4.14), (4.16) and (4.17) have a local error of order $\mathcal{O}(\tau^2 \nabla u)$.*

Proof. First, for the explicit scheme (4.14) the local error directly follows from Theorem (3.19) and can be computed using Definition 3.16 as it is performed in the proof of [15, Cor. 5.1]. In order to obtain the local error bounds of the implicit schemes (4.16), (4.17) one needs to apply Theorem (3.19) and to combine it with a fixed-point argument on the numerical flow. To go further, the first order convergence of these schemes follow by combining the local error bound with a stability argument, we refer to the works [50, 4] which perform this analysis in full detail. \square

Remark 4.12 The symmetric scheme (4.16) was first rigorously analysed in [4]. In particular it was shown in [4] that the local error of the scheme is of order $\mathcal{O}(\tau^2 \nabla u)$, which is optimal in regard of the regularity assumptions. Indeed, the scheme (4.16) does not require more regularity on the solution than previously constructed asymmetric low regularity integrators such as (4.14) introduced in [55, 15]. As the scheme (4.16) is symmetric it is naturally also of second order; however, not under optimal regularity assumptions (see also Remark 2.6). More precisely, by exploiting the tools presented in [4] one can show that the scheme (4.16) (as well as (4.17)) is of second order with a local error of order $\mathcal{O}(\tau^3 \nabla \Delta u)$. This error structure imposes more regularity on the solution than asymmetric low-regularity integrators such as the ones proposed in [15] which only require the boundedness of two additional derivatives instead of three due to the local error of the form $\mathcal{O}(\tau^3 \Delta u)$.

Our new symmetric midpoint rule framework (3.35) allows for a symmetric second order scheme which is optimal in the sense of regularity, i.e., has a local error structure of the form $\mathcal{O}(\tau^3 \Delta u)$, see the scheme (4.18) below.

Proposition 4.13 *The second order scheme coming from (3.35) is given by:*

$$\begin{aligned} u^{n+1} &= \varphi_{NLS,4}^\tau(u^n) = e^{i\tau\Delta} u^n \tag{4.18} \\ &\quad - i\frac{\tau}{8} e^{i\tau\Delta} \left((u^n + e^{-i\tau\Delta} u^{n+1})^2 (\varphi_1(-2i\tau\Delta) - \varphi_2(-2i\tau\Delta)) (\overline{u^n} + e^{i\tau\Delta} \overline{u^{n+1}}) \right) \\ &\quad - i\frac{\tau}{8} \left((e^{i\tau\Delta} u^n + u^{n+1})^2 \varphi_2(-2i\tau\Delta) (e^{i\tau\Delta} \overline{u^n} + e^{2i\tau\Delta} \overline{u^{n+1}}) \right) \end{aligned}$$

with a local error structure of the form $\mathcal{O}(\tau^3 \Delta u)$ and $\varphi_2(\sigma) = \frac{e^\sigma - \varphi_1(\sigma)}{\sigma}$.

Remark 4.14 In practice the computational effort required to compute u^{n+1} in (4.18) is not significantly larger than the solution of (2.11) or other previous symmetric low-regularity methods for the NLSE. In particular, a similar analysis to that presented in [4, Section 3], [7, Appendix A] and [50] shows that the implicit equations can be solved efficiently using fixed point iterations, and that the number of iterations required is independent of the number of spatial discretisation points.

Remark 4.15 One can find the coefficients b for the scheme (4.18) such that it is of the form given by (3.37).

Proof of Proposition 4.13. For the scheme of order two ($r = 1$) and $n = 2$, one has to consider:

$$\begin{aligned} U_k^{n,1}(\tau, u) &= \sum_{T \in \tilde{\mathcal{T}}_0^{1,k}(R)} \frac{\Upsilon_{\text{mid}}^p(T)(u, \tau)}{S(T)} (\Pi_{\text{mid}}^{n,1} T_0)(\tau) \\ &= \frac{\Upsilon_{\text{mid}}^p(T_0)(u, \tau)}{S(T_0)} (\Pi_{\text{mid}}^{n,1} T_0)(\tau) + \sum_{k=-k_1+k_2+k_3} \frac{\Upsilon_{\text{mid}}^p(T_1)(u, \tau)}{S(T_1)} (\Pi_{\text{mid}}^{n,1} T_1)(\tau) \\ &\quad + \sum_{k=-k_1+k_2+k_3-k_4+k_5} \frac{\Upsilon_{\text{mid}}^p(T_2)(u, \tau)}{S(T_2)} (\Pi_{\text{mid}}^{n,1} T_2)(\tau) \end{aligned}$$

$$+ \sum_{k_1 - k_2 - k_3 + k_4 + k_5 = k} \frac{\Upsilon_{\text{mid}}^p(T_3)(u, \tau)}{S(T_3)} \left(\Pi_{\text{mid}}^{n,1} T_3 \right)(\tau).$$

From the definition of the symmetry factor, we have

$$S(T_2) = 1 \times 2 = 2, \quad S(T_3) = 2 \times 2 = 4,$$

for $S(T_2)$ the factor one corresponds to the fact that for the node on top of the first blue edges the symmetry factor is one. Indeed, the trees on top of the brown edges are different: a leaf decorated by k_5 is different from a tree having three leaves. Moreover, we have:

$$\Upsilon_{\text{mid}}^p(T_j)(u, \tau) = \Upsilon^p(T_j) \left(\frac{1}{2} (e^{i\tau k^2} u^{n+1} + u^n) \right), \quad j \in \{2, 3\},$$

where

$$\Upsilon^p(T_2)(u) = 4\bar{u}_{k_1} u_{k_2} u_{k_3} \bar{u}_{k_4} u_{k_5}, \quad \Upsilon^p(T_3)(u) = 4u_{k_1} \bar{u}_{k_2} \bar{u}_{k_3} u_{k_4} u_{k_5}.$$

The factor 4 in both expressions comes from the two brown edges that appear twice inside the decorated trees T_2 and T_3 . For the term $(\Pi_{\text{mid}}^{2,1} T_1)(\tau)$, we proceed with interpolation at two nodes ($a_0 = 0, a_1 = 1$):

$$p_2(s, \tau) = 1 + \frac{s}{\tau} \left(e^{is\mathcal{L}_{\text{low}}} - 1 \right),$$

where

$$\mathcal{L}_{\text{dom}} = 2k_1^2, \quad \mathcal{L}_{\text{low}} = k^2 - k_1^2 - k_2^2 - k_3^2.$$

We obtain

$$\begin{aligned} \mathcal{K}_{o_2}^{k,1} \left((\Pi_{\text{mid}}^{2,0} \tilde{T}_1)(\cdot, \tau), 2 \right)(\tau) &= -i \int_0^\tau e^{is\mathcal{L}_{\text{dom}}} ds - i \int_0^\tau s e^{is\mathcal{L}_{\text{dom}}} ds \left(\frac{e^{i\tau\mathcal{L}_{\text{low}}} - 1}{\tau} \right) \\ &\quad - i\tau\varphi_1(2i\tau k_1^2) - i\tau\varphi_2(2i\tau k_1^2) \left(e^{ik^2 - k_1^2 - k_2^2 - k_3^2} - 1 \right). \end{aligned}$$

Therefore,

$$\begin{aligned} &\sum_{k=-k_1+k_2+k_3} \frac{\Upsilon_{\text{mid}}^p(T_1)(u, \tau)}{S(T_1)} (\Pi_{\text{mid}}^{2,1} T_1)(\tau) \\ &= \left(-i\tau\varphi_1(2i\tau k_1^2) - i\tau\varphi_2(2i\tau k_1^2) \left(e^{ik^2 - k_1^2 - k_2^2 - k_3^2} - 1 \right) \right) \\ &\quad \times \left(e^{-i\tau k_1^2} \bar{u}_{k_1}^{n+1} + \bar{u}_{k_1}^n \right) \frac{1}{2} \left(e^{i\tau k_2^2} u_{k_2}^{n+1} + u_{k_2}^n \right) \frac{1}{2} \left(e^{i\tau k_3^2} u_{k_3}^{n+1} + u_{k_3}^n \right) \end{aligned}$$

For the decorated tree T_2 , we have

$$\left(\Pi_{\text{mid}}^{2,1} T_2 \right)(\tau) = e^{-i\tau k^2} \mathcal{K}_{o_2}^{k,1} \left((\Pi_{\text{mid}}^{2,0} F_2)(\cdot, \tau), 2 \right)(0, \tau) \quad (4.19)$$

where

$$F_2 = \mathcal{J}_{(t_1,1)}(\lambda_{k_4})\mathcal{J}_{(t_1,0)}(\lambda_{k_5})T_1.$$

Then,

$$(\Pi_{\text{mid}}^{2,0}\mathcal{J}_{(t_1,1)}(\lambda_{k_4})\mathcal{J}_{(t_1,0)}(\lambda_{k_5}))(s, \tau) = e^{is(k_4^2 - k_5^2)}$$

and for $\tilde{k} = -k_1 + k_2 + k_3$

$$\begin{aligned} (\Pi_{\text{mid}}^{2,0}T_1)(s, \tau) &= \frac{1}{2}e^{-is\tilde{k}^2} \left(\mathcal{K}_{o_2}^{\tilde{k},0}((\Pi_{\text{mid}}^{2,-1}\tilde{T}_1)(\cdot, \tau), 2)(s, \tau) \right. \\ &\quad \left. + \mathcal{K}_{o_2}^{\tilde{k},0}((\Pi_{\text{mid}}^{2,-1}\tilde{T}_1)(\cdot, \tau), 2)(s, 0) \right), \end{aligned}$$

Now, because of $n = 2$, we perform a direct interpolation of the full operator which gives

$$\mathcal{K}_{o_2}^{\tilde{k},0}((\Pi_{\text{mid}}^{2,-1}\tilde{T}_1)(\cdot, \tau), 2)(s, \tau) = -i \int_{\tau}^s ds \left(\frac{1 + e^{i\tau(\tilde{k}^2 + k_1^2 - k_2^2 - k_3^2)}}{2} \right).$$

We obtain

$$(\Pi_{\text{mid}}^{2,0}T_1)(s, \tau) = -i \frac{(2s - \tau)}{2} e^{-is\tilde{k}^2} \left(\frac{1 + e^{i\tau(\tilde{k}^2 + k_1^2 - k_2^2 - k_3^2)}}{2} \right).$$

Therefore, we find

$$(\Pi_{\text{mid}}^{2,0}F_2)(s, \tau) = -i \frac{(2s - \tau)}{2} e^{is(k_4^2 - k_5^2 - \tilde{k}^2)} \left(\frac{1 + e^{i\tau(\tilde{k}^2 + k_1^2 - k_2^2 - k_3^2)}}{2} \right)$$

and by performing again an interpolation of the full operator:

$$\begin{aligned} \left(\Pi_{\text{mid}}^{2,1}T_2 \right)(\tau) &= - \int_0^{\tau} \frac{(2s - \tau)}{2} ds \\ &\quad e^{-i\tau k^2} \left(\frac{1 + e^{i\tau(k^2 + k_4^2 - k_5^2 - \tilde{k}^2)}}{2} \right) \left(\frac{1 + e^{i\tau(\tilde{k}^2 + k_1^2 - k_2^2 - k_3^2)}}{2} \right) \\ &= 0 \end{aligned}$$

because we have

$$\int_0^{\tau} \frac{(2s - \tau)}{2} ds = 0.$$

A similar computation shows that

$$\left(\Pi_{\text{mid}}^{2,1}T_3 \right)(\tau) = 0.$$

The local error analysis follows from the proof of [15, Cor. 5.3]. \square

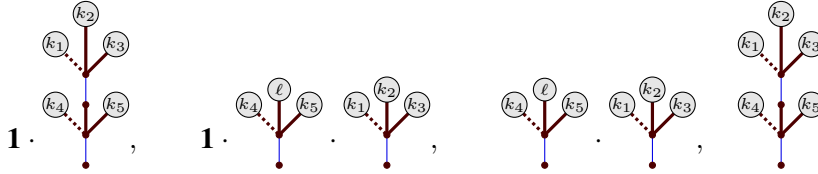
Example 11 To illustrate how the general formula can be used to express more general higher order resonance based schemes, let us consider the following low-regularity integrator

$$\begin{aligned}
u^{n+1} &= e^{i\tau\Delta}u - i\frac{\tau}{2}e^{i\tau\Delta}\left((u^n)^2(\varphi_1(-i\tau\Delta) - \varphi_2(-i\tau\Delta))\overline{u^n}\right) \\
&\quad - i\frac{\tau}{2}\left((u^{n+1})^2(\varphi_1(i\tau\Delta) - \varphi_2(i\tau\Delta))\overline{u^{n+1}}\right) \\
&\quad - i\frac{\tau}{2}e^{i\frac{\tau}{2}\Delta}\left(e^{i\frac{\tau}{2}\Delta}u^n\right)^2\varphi_2(-i\tau\Delta)e^{i\frac{\tau}{2}\Delta}\overline{u^n} \\
&\quad - i\frac{\tau}{2}e^{i\frac{\tau}{2}\Delta}\left(e^{-i\frac{\tau}{2}\Delta}u^{n+1}\right)^2\varphi_2(i\tau\Delta)e^{-i\frac{\tau}{2}\Delta}\overline{u^{n+1}} \\
&\quad - \frac{\tau^2}{8}|u^n|^4e^{-i\tau\Delta}u^{n+1} + \frac{\tau^2}{8}|u^{n+1}|^4e^{i\tau\Delta}u^n
\end{aligned} \tag{4.20}$$

which is motivated from [15, (5.16)] and has a local error of the form $\mathcal{O}(\tau^3\Delta)$. We will see that this scheme is in the form of the general formula (3.37) with $r = 1$. Indeed, we already saw at the beginning of this section that

$$\hat{\mathcal{T}}_0^{1,k}(R) = \left\{T_0, T_1, T_2, T_3, k_i \in \mathbf{Z}^d\right\}$$

where $T_i, i = 0, 1, 2, 3$, were defined in (4.11) and (4.12). In the interest of brevity we will not derive all the coefficients b in the expression of (4.20) in the form (3.37). Instead let us focus on the coefficients arising from the contribution to (3.37) arising from $T = \hat{T}_2$ where \hat{T}_2 is obtained by removing the brown edge attached to the root. To understand this we first recall the forest splittings of this choice of T from Example 6:



Let us now consider the contribution from the second of these splittings, $\tilde{T}_0 \cdot \tilde{T}_1 \cdot \tilde{T}_2$ with

$$\tilde{T}_0 = \mathbf{1}, \quad \tilde{T}_1 = \begin{array}{c} \ell \\ \swarrow \quad \searrow \\ k_4 \quad k_5 \end{array}, \quad \tilde{T}_2 = \begin{array}{c} k_2 \\ \swarrow \quad \searrow \\ k_1 \quad k_3 \end{array}$$

where from Kirchhoff's law we have $k = -k_4 + l + k_5$ and $l = -k_1 + k_2 + k_3$. The dominant and lower order operators arising in these splittings are given by

$$\begin{aligned}
\mathcal{F}_{\text{dom}}(\tilde{T}_0) &= 0, \quad \mathcal{F}_{\text{low}}(\tilde{T}_0) = 0 \\
\mathcal{F}_{\text{dom}}(\tilde{T}_1) &= 2k_4^2, \quad \mathcal{F}_{\text{low}}(\tilde{T}_1) = k^2 - k_4^2 - l^2 - k_5^2 = 2(-k_4l - k_4k_5 + lk_5) \\
\mathcal{F}_{\text{dom}}(\tilde{T}_2) &= 2k_1^2, \quad \mathcal{F}_{\text{low}}(\tilde{T}_2) = l^2 - k_1^2 - k_2^2 - k_3^2 = 2(-k_1k_2 - k_1k_3 + k_2k_3),
\end{aligned}$$

Moreover we have $|\tilde{E}_T|$ (there are only two blue edges in T corresponding to time-integration) and $|L_T| = 5$ (T has 5 leaves), and given the above splitting, $|\tilde{E}_{\tilde{T}_0}| = 0$, $|\tilde{E}_{\tilde{T}_1}| = |\tilde{E}_{\tilde{T}_2}| = 1$. Thus the contribution from this term to the overall sum in (3.37) is of the form (recall that $C_T = 1$ for all T in the NLSE case)

$$\sum_{\mathbf{a} \in [0,1]^2} \sum_{\chi \in \{0,1\}^5} b_{\mathbf{a}, \chi, T, \tilde{T}_0, \tilde{T}_1, \tilde{T}_2}(\tau, i\tau \mathcal{F}_{\text{dom}}(\tilde{T}_0), i\tau \mathcal{F}_{\text{dom}}(\tilde{T}_1), i\tau \mathcal{F}_{\text{dom}}(\tilde{T}_2)) \\ e^{i\tau a_1 \mathcal{F}_{\text{low}}(\tilde{T}_1)} e^{i\tau a_2 \mathcal{F}_{\text{low}}(\tilde{T}_2)} \frac{\Upsilon_\chi^p(T)(u_{k_v}^{n+\chi_v}, v \in L_T, \tau)}{S(T)}$$

From the derivation in the proof of Proposition 4.13 and (3.36) we have that

$$\frac{\Upsilon_\chi^p(T)(u_{k_v}^{n+\chi_v}, v \in L_T, \tau)}{S(T)} \\ = 2e^{-i\tau \chi_1 k_1^2} \bar{u}_{k_1}^{\chi_1} e^{i\tau \chi_2 k_2^2} u_{k_2}^{\chi_2} e^{i\tau \chi_3 k_3^2} u_{k_3}^{\chi_3} e^{-i\tau \chi_4 k_4^2} \bar{u}_{k_4}^{\chi_4} e^{i\tau \chi_5 k_5^2} u_{k_5}^{\chi_5}$$

Thus the contribution to (3.37) equals

$$\sum_{\mathbf{a} \in [0,1]^2} \sum_{\chi \in \{0,1\}^5} b_{\mathbf{a}, \chi, T, \tilde{T}_0, \tilde{T}_1, \tilde{T}_2}(\tau, 0, 2i\tau k_4^2, 2i\tau k_1^2) \\ e^{i\tau a_1 (k^2 - k_4^2 - (-k_1 + k_2 + k_3)^2 - k_5^2)} e^{i\tau a_2 ((-k_1 + k_2 + k_3)^2 - k_1^2 - k_2^2 - k_3^2)} \\ 2e^{-i\tau \chi_1 k_1^2} \bar{u}_{k_1}^{\chi_1} e^{i\tau \chi_2 k_2^2} u_{k_2}^{\chi_2} e^{i\tau \chi_3 k_3^2} u_{k_3}^{\chi_3} e^{-i\tau \chi_4 k_4^2} \bar{u}_{k_4}^{\chi_4} e^{i\tau \chi_5 k_5^2} u_{k_5}^{\chi_5}$$

Let us now show that the quintic terms in (4.20) arise precisely from these contributions: Indeed suppose we choose

$$b_{\mathbf{0}, (0,0,0,0,1), T, \tilde{T}_0, \tilde{T}_1, \tilde{T}_2}(\tau, z_0, z_1, z_2) = -\frac{\tau^2}{16}, \quad (4.21)$$

$$b_{(1,1), (1,0,0,0,0), T, \tilde{T}_0, \tilde{T}_1, \tilde{T}_2}(\tau, z_0, z_1, z_2) = -e^{z_0 + z_1 + z_2} \frac{\tau^2}{16} \quad (4.22)$$

and all other coefficients b in the above expression equal to zero then we arrive precisely at the contributions of the form

$$-\frac{\tau^2}{8} |u^n|^4 e^{-i\tau \Delta} u^{n+1} + \frac{\tau^2}{8} |u^{n+1}|^4 e^{i\tau \Delta} u^n$$

in the overall scheme, corresponding to the quintic terms in (4.20). The remaining terms in the scheme can be expressed similarly from contributions from lower rank trees T_0, T_1 . Moreover, we note that the coefficients as given by (4.21) clearly satisfy (4.7) and that the same holds for the coefficients of lower order contributions, thus confirming that the scheme (4.20) is symmetric.

4.3.2 The Korteweg–de Vries equation

The Korteweg–de Vries (KdV) equation is given by

$$\partial_t u + \partial_x^3 u = \frac{1}{2} \partial_x u^2 \quad (4.23)$$

It fits into the general framework with

$$\mathcal{L} \left(\nabla, \frac{1}{\varepsilon} \right) = i \partial_x^3, \quad \alpha = 1 \quad \text{and} \quad p(u, \bar{u}) = p(u) = i \frac{1}{2} u^2.$$

Here $\mathcal{L} = \{t_1, t_2\}$, $P_{t_1} = -\lambda^3$ and $P_{t_2} = \lambda^3$. Moreover, in this case the structure constant C_T reflects the presence of the Burger's nonlinearity in the iterations of Duhamel's formula, which means

$$C_T = \prod_{\substack{e=(v,u) \in \tilde{E}_T \\ u \in N_T \setminus \{\varrho_T\}}} (-1)^{p(e)} i \sigma(u)$$

where we recall $\epsilon(e) = (t(e), p(e))$ is the edge decoration of e with $t(e) \in \mathcal{L}$ and $p(e) \in \{0, 1\}$. Note by Kirchhoff's law the above definition is invariant under the choice of node u or v for an edge $e = (u, v)$ in the product, so long as the node is an interior one. Then, we denoted by \lfloor an edge decorated by $(t_1, 0)$ and by \lceil an edge decorated by $(t_2, 0)$. Following the formalism given in [12], we can provide the rules that generate the trees obtained by iterating Duhamel's formula:

$$R(\lfloor) = \{(\lfloor, \lfloor)\}, \quad R(\lceil) = \{(\lceil, \lceil)\}.$$

The general framework (3.34) derived in Section 3.4 builds the foundation of the first- and second-order resonance based schemes presented below for the KdV equation (4.23). The structure of the schemes depends on the regularity of the solution.

Corollary 4.16 *For the KdV equation (4.23) the general midpoint scheme (3.34) takes at first order the form*

$$\begin{aligned} u^{\ell+1} &= e^{-\tau \partial_x^3} u^\ell + \frac{1}{24} \left(e^{-\tau \partial_x^3} \partial_x^{-1} u^\ell + \partial_x^{-1} u^{\ell+1} \right)^2 \\ &\quad - \frac{1}{24} e^{-\tau \partial_x^3} \left(\partial_x^{-1} u^\ell + e^{\tau \partial_x^3} \partial_x^{-1} u^{\ell+1} \right)^2 \end{aligned} \quad (4.24)$$

with a local error of order $\mathcal{O}(\tau^2 \partial_x^2 u)$ at first-order and with a local error of order $\mathcal{O}(\tau^3 \partial_x^4 u)$ at second order.

Remark 4.17 Note that this schemes has been obtained in [50]. It was shown that this scheme is of even order for higher regularity in H^4 (see [50, Thm 5.2]). By

embedding this scheme into our general framework, we know that it has the same local error analysis as the second-order scheme introduced in [15].

$$\begin{aligned} u^{\ell+1} &= e^{-\tau\partial_x^3} u^\ell + \frac{1}{6} \left(e^{-\tau\partial_x^3} \partial_x^{-1} u^\ell \right)^2 - \frac{1}{6} e^{-\tau\partial_x^3} \left(\partial_x^{-1} u^\ell \right)^2 \\ &+ \frac{\tau^2}{4} e^{-\tau\partial_x^3} \Psi(i\tau\partial_x^2) \left(\partial_x \left(u^\ell \partial_x (u^\ell u^\ell) \right) \right) \end{aligned} \quad (4.25)$$

with a local error of order $\mathcal{O}(\tau^3 \partial_x^4 u)$ and a suitable filter function Ψ satisfying

$$\Psi = \Psi(i\tau\partial_x^2), \quad \Psi(0) = 1, \quad \|\tau\Psi(i\tau\partial_x^2)\partial_x^2\|_r \leq 1.$$

Proof. The proof follows the line of argumentation to the analysis for the Schrödinger equation. For the first-order scheme, we have

$$\begin{aligned} U_k^{n,0}(\tau, v) &= \frac{\Upsilon_{\text{mid}}^p(T_0)(\tau, v)}{S(T_0)} \Pi_{\text{mid}}^{n,0}(T_0)(\tau) \\ &+ \sum_{k=k_1+k_2} \frac{\Upsilon_{\text{mid}}^p(T_1)(\tau, v)}{S(T_1)} \Pi_{\text{mid}}^{n,0}(T_1)(\tau). \end{aligned} \quad (4.26)$$

where the trees of interest are

$$\hat{\mathcal{J}}_0^{0,k}(R) = \{T_0, T_1, k_i \in \mathbf{Z}^d\}, \quad T_0 = \begin{array}{c} \textcircled{k} \\ \downarrow \end{array} \quad \text{and} \quad T_1 = \begin{array}{c} \textcircled{k_1} \quad \textcircled{k_2} \\ \downarrow \end{array}$$

and in symbolic notation takes the form

$$T_1 = \mathcal{J}_{(t_1,0)}(\mathcal{J}_{(t_2,0)}(\lambda_k F_1)) \quad F_1 = \mathcal{J}_{(t_1,0)}(\lambda_{k_1}) \mathcal{J}_{(t_1,0)}(\lambda_{k_2}) \quad \text{with } k = k_1 + k_2.$$

For the first term we readily obtain that

$$\frac{\Upsilon_{\text{mid}}^p(T_0)(\tau, v)}{S(T_0)} \Pi_{\text{mid}}^{n,0}(T_0)(\tau) = e^{-i\tau k^3} \hat{v}_k.$$

It remains to compute the second term. Note that thanks to (3.13) we have that

$$\begin{aligned} \Pi^{n,0}(T_1)(\tau) &= e^{-i\tau k^3} \Pi^{n,0}(\mathcal{J}_{(t_2,0)}(\lambda_k F_1))(\tau) \\ &= e^{-i\tau k^3} \mathcal{K}_{(t_2,0)}^{k,0}(\Pi^{n,-1}(F_1), n)(\tau) \\ &= e^{-i\tau k^3} \mathcal{K}_{(t_2,0)}^{k,0} \left(e^{i\xi(-k_1^3 - k_2^3)}, n \right)(\tau). \end{aligned} \quad (4.27)$$

where we have used for the third line

$$(\Pi^{n,-1} F_1)(\tau) = (\Pi^{n,-1} \mathcal{J}_{(t_1,0)}(\lambda_{k_1}))(\tau) (\Pi^{n,-1} \mathcal{J}_{(t_1,0)}(\lambda_{k_2}))(\tau) = e^{-i\tau k_1^3} e^{-i\tau k_2^3}.$$

Next we observe that

$$P_{(t_2,0)}(k) - k_1^3 - k_2^3 = k^3 - k_1^3 - k_2^3 = 3k_1 k_2 (k_1 + k_2)$$

such that

$$\frac{1}{P_{(t_2,0)}(k) - k_1^3 - k_2^3}$$

can be mapped back to physical space. Therefore, we set

$$\mathcal{L}_{\text{dom}} = P_{(t_2,0)}(k) - k_1^3 - k_2^3 = 3k_1k_2(k_1 + k_2)$$

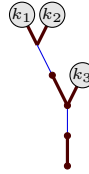
and integrate all frequencies exactly. This implies

$$\begin{aligned} \Pi^{n,0}(T_1)(\tau) &= e^{-i\tau k^3} \frac{i(k_1 + k_2)}{3ik_1k_2(k_1 + k_2)} \left(e^{i\tau(k^3 - k_1^3 - k_2^3)} - 1 \right) \\ &= \frac{1}{3k_1k_2} \left(e^{-i\tau(k_1^3 + k_2^3)} - e^{-i\tau k^3} \right). \end{aligned}$$

Together with (4.26) this yields the scheme (4.24). For the second-order scheme, we first notice that

$$\Pi_{\text{mid}}^{n,0}(T_0)(\tau) = \Pi_{\text{mid}}^{n,1}(T_0)(\tau), \quad \Pi_{\text{mid}}^{n,0}(T_1)(\tau) = \Pi_{\text{mid}}^{n,1}(T_1)(\tau).$$

Indeed, for the tree T_1 , we perform an exact integration without any discretisation. Then, we need to take into account the following trees

$$\hat{\mathcal{J}}_0^{1,k}(R) = \{T_0, T_1, T_2, k_i \in \mathbf{Z}^d\}, \quad T_2 =$$


Then we can proceed as in the second-order schemes for the Schrödinger equation to show its contribution is zero that is

$$\Pi_{\text{mid}}^{4,1}(T_2)(\tau) = 0.$$

□

5 Numerical Experiments

We now test the practical performance of our new symmetric schemes in practical experiments evaluating both their low-regularity convergence properties and their ability to correctly preserve constants of motion in the relevant equations. In fitting with our above construction our spatial discretisation is a Fourier spectral method throughout with M modes. In order to understand the low-regularity convergence properties of our methods we follow [55] and consider the following types of initial data:

1. Smooth initial data,

$$u_0(x) = \frac{\cos(x)}{2 + \sin(x)}. \quad (5.1)$$

2. Low-regularity initial data u_0 of the following form. Firstly we choose a vector sampled from a uniform distribution $U_m \sim U([0, 1] + i[0, 1])$, $m = -M/2 + 1, \dots, M/2$ and then we define

$$u_0(x) := U_0 + \sum_{\substack{m=-M/2+1 \\ m \neq 0}}^{M/2} e^{imx} |m|^{-\vartheta} U_m, \quad (5.2)$$

for a given value of $\vartheta > 0$, which corresponds to $u_0 \in H^\vartheta$.

Both choices of initial data are rescaled such that $u_0 \mapsto u_0 / \|u_0\|_{L^2}$.

5.1 The Nonlinear Schrödinger equation

To begin with we look at our new symmetric integrators for the NLSE ((4.17) and (4.18)). In the following numerical experiments we compare the performance of our new schemes to the following state-of-the-art reference schemes for the NLSE:

- The Strang splitting [51], as an example of a classical symmetric numerical technique;
- The first and second order resonance based integrators introduced by Ostermann & Schrätz [55] and Bruned & Schrätz [15, Section 5.1.2] respectively, as examples of asymmetric low-regularity schemes;
- The symmetrised low-regularity integrator introduced by Alama Bronsard [4], as an example of previous structure preserving low-regularity schemes.

In the following numerical experiments we focus on the 1d case, i.e. the NLSE formulated on \mathbb{T} , but our methods equally apply to higher dimensional settings where their favourable performance can also be observed.

In the first instance we consider the long-time structure preservation properties of our newly designed symmetric low-regularity integrators. For this we consider two first integrals of the cubic NLSE, the normalisation

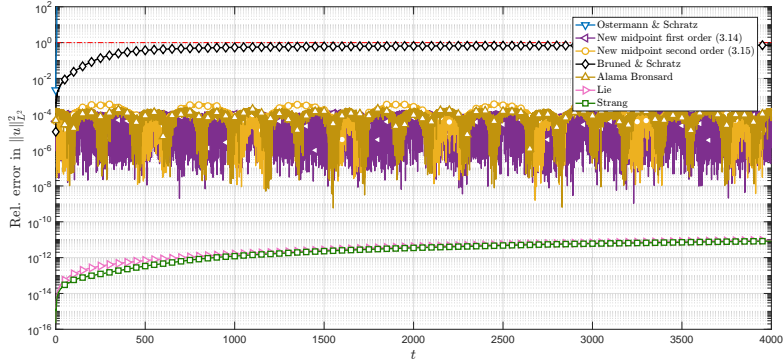
$$I_0^{[NLSE]}[u] = \int_{\mathbb{T}} |u|^2 dx,$$

and the energy

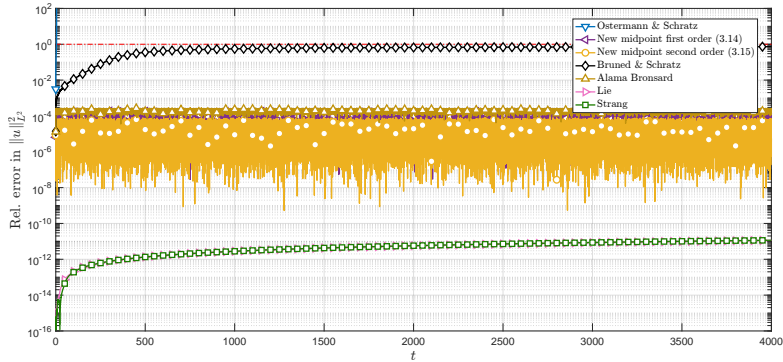
$$I_1^{[NLSE]}[u] = \int_{\mathbb{T}} |\nabla u|^2 + \frac{1}{2} |u|^4 dx.$$

Symmetric numerical schemes are typically unable to preserve such conservation laws exactly, however it is known for the ODE case [36, Chapter XI] (and also observed numerically for the PDE case, for example in [19]) that symmetric methods can exhibit very good approximate long-time preservation of such first integrals. In the following numerical experiments we test this behaviour by looking at the error in these quantities for a fixed time step $\tau = 0.02$ and highest frequency $M = 1024$, over a long time interval, much larger than $\mathcal{O}(1/\tau)$. Firstly, in figures 4&5 we

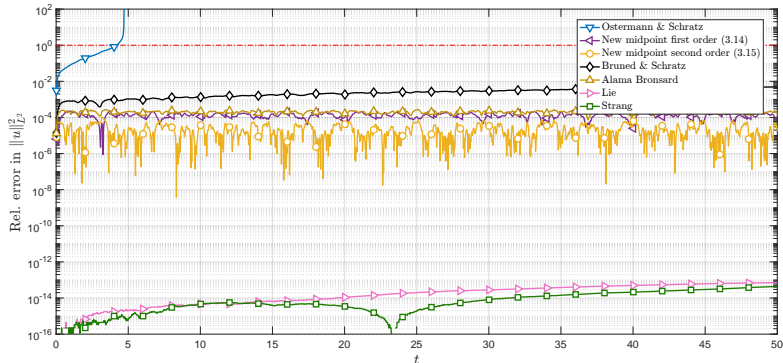
observe that the normalisation appears to be preserved really well, in particular (the example is representative of a host of numerical experiments for various time steps which we performed) the preservation is much better than previous asymmetric resonance based schemes. We note that the Strang splitting conserves quadratic first integrals, i.e. the normalisation, to machine accuracy and thus undoubtedly outperforms our schemes on the level of normalisation preservation.



(a) Long-time interval $t = n\tau \in [0, 4000]$, $M = 128$.

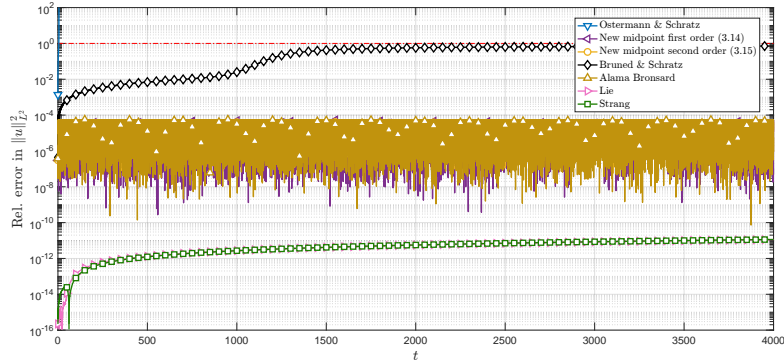


(b) Long-time interval $t = n\tau \in [0, 4000]$, $M = 1024$.

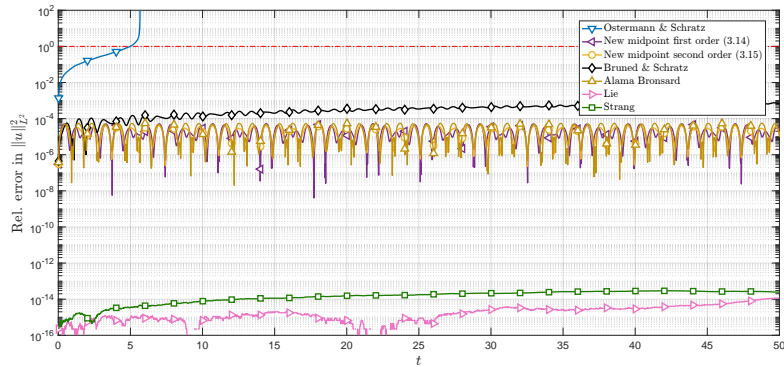


(c) Magnification of $t = n\tau \in [0, 50]$, $M = 1024$.

Figure 4: Error in the normalisation $\|u^n\|_{L^2}$, for time step $\tau = 0.02$ and H^2 data.



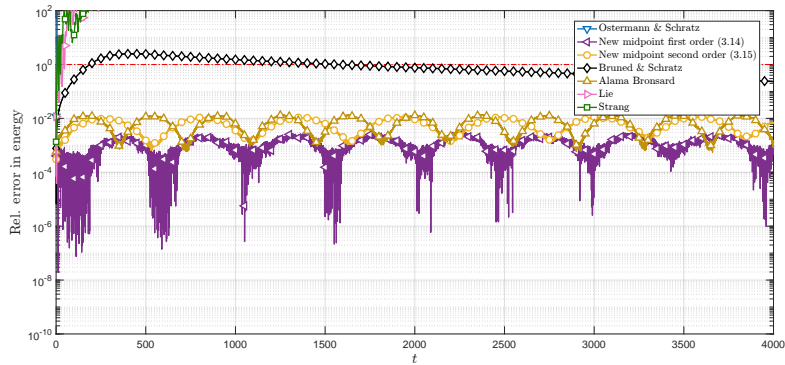
(a) Long-time interval $t = n\tau \in [0, 4000]$, $M = 1024$.



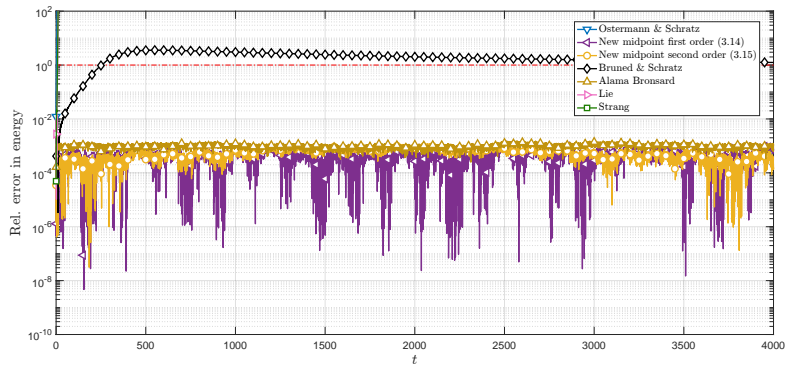
(b) Magnification of $t = n\tau \in [0, 50]$, $M = 1024$.

Figure 5: Error in the normalisation $\|u^n\|_{L^2}$, for time step $\tau = 0.02$ and C^∞ data.

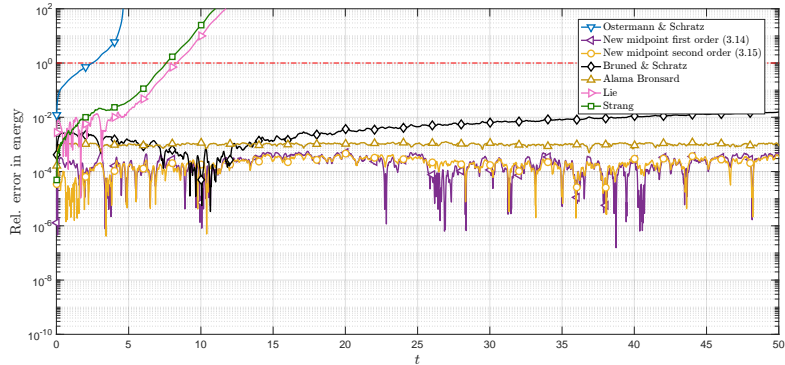
Our next numerical result for the NLSE, presented in Figure 6&7, shows the error in the NLSE energy over a long time interval, for a fixed time step $\tau = 0.02$. Albeit rigorous theory exists for the ODE case [36], there is again no theoretical guarantee for the long-time preservation of the energy under symmetric methods. Indeed in practical experiments it can be seen that symmetric schemes are able to clearly outperform asymmetric integrators in the long-time approximate energy preservation. For the Strang splitting this behaviour was rigorously analysed in [28] where a CFL condition was necessary to guarantee long-time approximate energy preservation beyond the realms of forward error analysis. This CFL condition is indeed observed even for smooth data in our experiments. Perhaps somewhat surprisingly our new symmetric resonance based scheme do not appear to suffer from comparable CFL conditions and, as expected, perform well for both smooth and low-regularity solutions.



(a) $M = 128$.



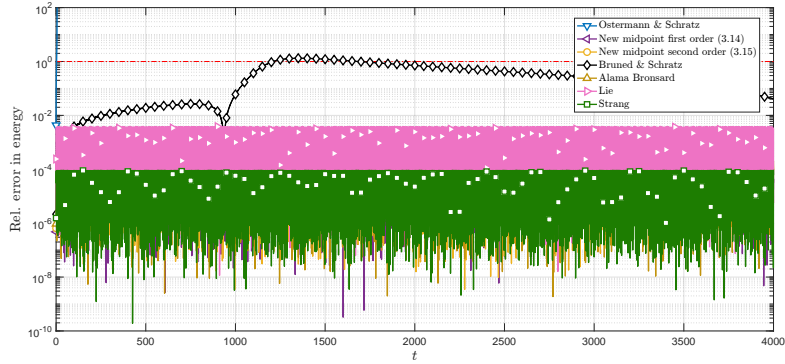
(b) $M = 1024$.



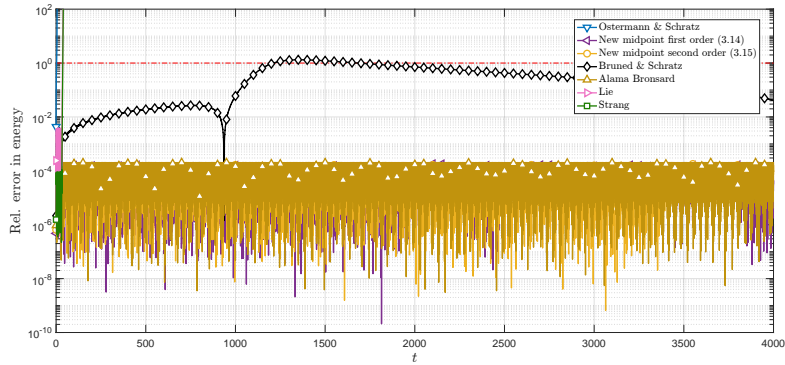
(c) $M = 1024$.

Figure 6: Error in the Hamiltonian, for time step $\tau = 0.02$ and H^2 data.

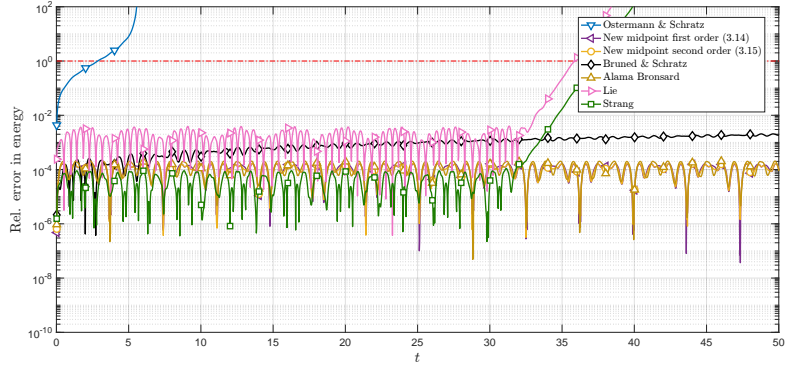
Finally, we performed experiments to confirm that the low-regularity convergence properties of our symmetric schemes are at least as good as in prior asymmetric methods. In the following numerical experiments our reference solutions were computed with $M = 2^{14}$ Fourier modes and a time step $\tau = 10^{-6}$ with the symmetrised method from [4]. In Figures 8 & 9 we choose to measure the error in H^1 -norm, and observe the convergence properties of our methods for initial data



(a) $M = 128$.



(b) $M = 1024$.



(c) $M = 1024$.

Figure 7: Error in the Hamiltonian, for time step $\tau = 0.02$ and C^∞ data.

of various levels of regularity. In all of these experiments the number of spatial discretisation modes was taken to be $M = 1024$ and the initial data chosen according to (5.2) & (5.1). In Figure 8 we observe that our new methods have exactly the predicted convergence properties at those levels of regularity: The integrator (4.17) is optimal for first order convergence in the sense of regularity, meaning it converges at first order in H^1 with H^2 data, while the integrator (4.18) is optimally convergent

in the sense of regularity up to second order meaning it converges at $\mathcal{O}(\tau)$ in H^1 for data in H^2 and at $\mathcal{O}(\tau^2)$ in H^1 for data in H^3 . For smaller values of τ the error forms a plateau around 10^{-4} and 10^{-7} in Figures 8a and 8b respectively. This is due to the error made by the pseudo-spectral space discretisation, which decreases as the regularity of the initial data is increased.

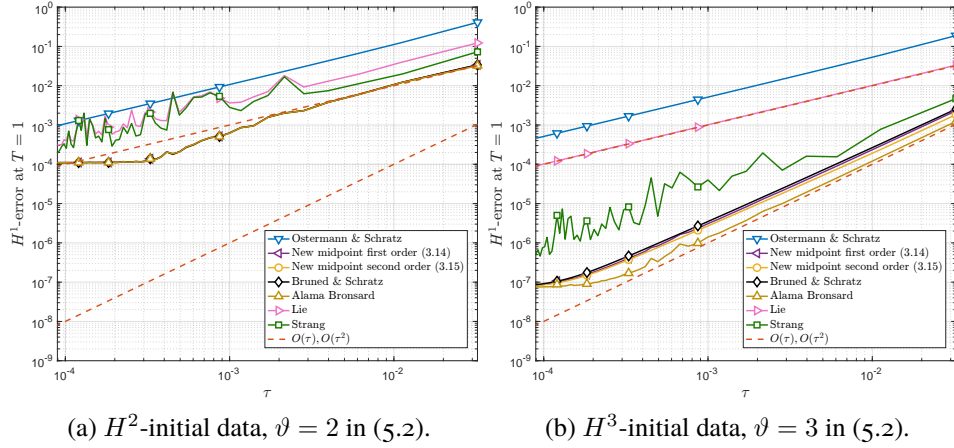


Figure 8: H^1 -error at $T = 1$ as a function of the timestep τ for low-regularity initial data.

The behaviour of the splitting methods observed in these experiments matches exactly with the convergence analysis given by [49, 60] and suffers from significant order reduction in low-regularity regimes.

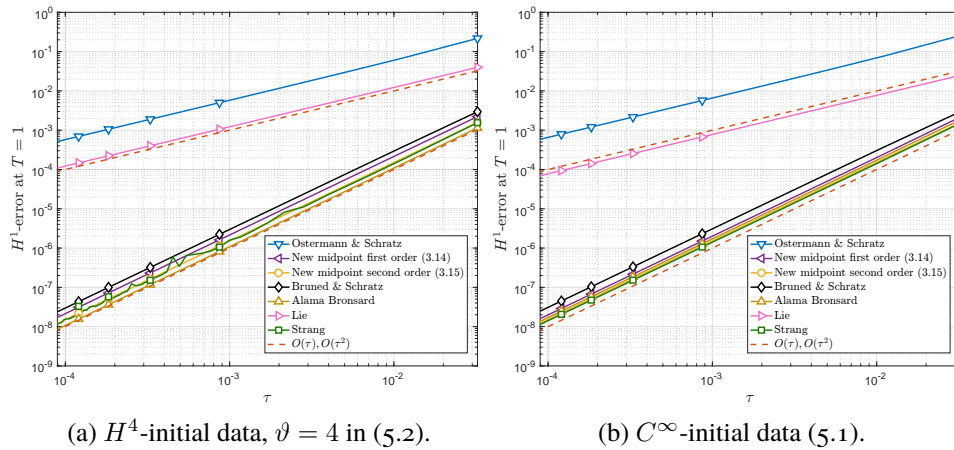


Figure 9: H^1 -error at $T = 1$ as a function of the timestep τ for more regular initial data.

5.2 The Korteweg–de Vries equation

As a final numerical example we consider the resonance based midpoint rule (4.24) introduced in [50] which our midpoint iterates (section 3.4) are able to recover. This rule has excellent low-regularity convergence properties and at the same time is able to conserve momentum and energy of the KdV equation over long times even in the low-regularity regime. With permission we reproduce some of the numerical results presented in [50] to recall the favourable properties of the method (4.24), for further evaluation and results the interested reader is referred to [50]. Here we compare the performance of our new schemes to the following state-of-the-art reference schemes for the KdV:

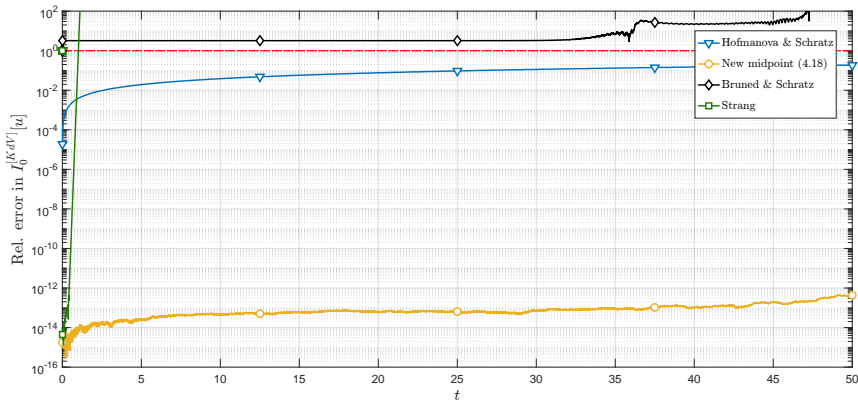
- The Strang splitting [51], as an example of a classical symmetric numerical technique, by splitting the KdV equation into the two subproblems $\partial_t u = -\partial_x^3 u$ and $\partial_t u = u\partial_x u$. In our implementation the resulting Burgers equation is solved using an explicit RK4 scheme with small time step $\tau_{RK4} = \tau 10^{-3}$ such that in essence the error observed in the following experiments is only due to the splitting of the problem.
- The first and second order low-regularity schemes introduced by Hofmanova & Schratz [39] and Bruned & Schratz [15, Section 5.2] respectively, as examples of asymmetric low-regularity integrators.

To begin with, we can consider the momentum, which is a quadratic first integral in the flow.

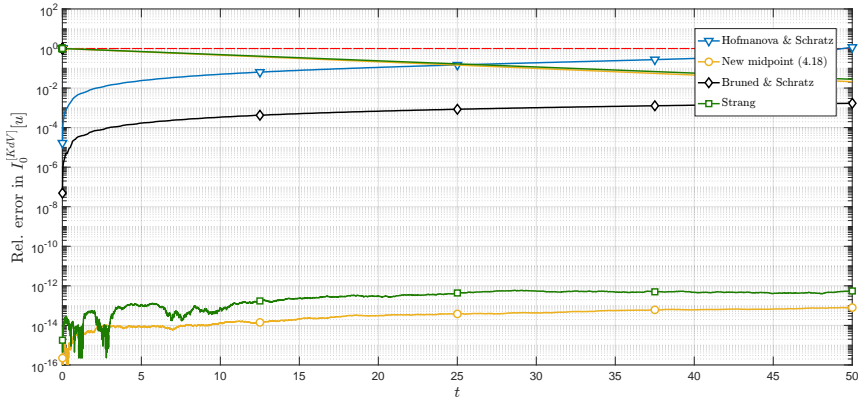
$$I_0^{[KdV]}[u] = \int_{\mathbb{T}} u^2 dx.$$

Seeing as the Strang splitting is a symplectic integrator we expect the momentum to be preserved to machine precision for C^∞ solutions which is indeed observed in Figure 10b. Note in [50] it was actually shown that the method (4.24) is symplectic and preserves the momentum exactly, which explains the preservation of momentum to machine accuracy in that same graph. On the other hand, for low-regularity data we see in Figure 10a that this preservation is lost in the Strang splitting for rougher data, but that the symmetric scheme (4.24) is able to deal with rough solutions as well.

In addition to this favourable long-time behaviour, in Figures 11&12 we observe the excellent low-regularity convergence properties of our method. For this example all reference values were computed with $M = 2^{14}$ Fourier modes and a time step $\tau = 10^{-6}$ with the second order method from [15]. The classical Strang splitting suffers in this case from a CFL condition, which requires $\tau \lesssim 1/M$ in order to resolve the Burgers nonlinearity, as a result we chose to include numerical results with only a small number of Fourier modes, since the classical integrator was found to be unstable whenever the aforementioned CFL condition is not satisfied. Perhaps somewhat surprisingly we see that in practice the integrator (4.24) appears

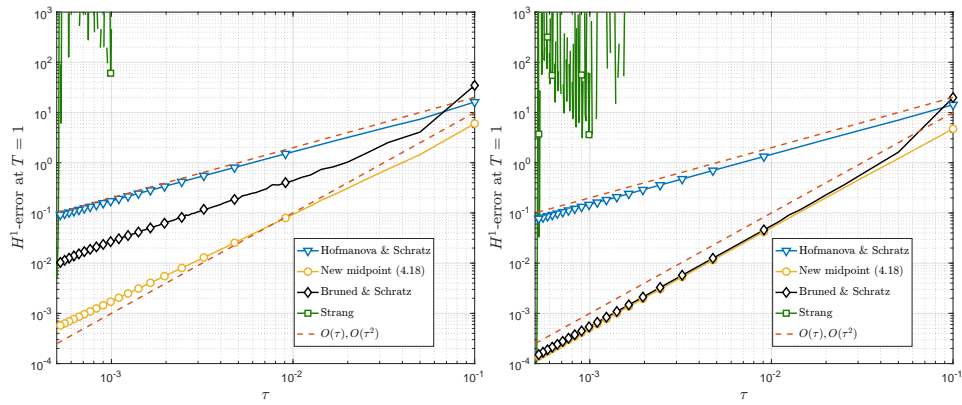


(a) H^5 -initial data, $\vartheta = 5$ in (5.2).



(b) C^∞ -initial data (5.1).

Figure 10: Error in the momentum $I_0^{[KdV]}[u]$ for $\tau = 0.005$ and $M = 64$.



(a) H^3 -initial data, $\vartheta = 3$ in (5.2).

(b) H^5 -initial data, $\vartheta = 5$ in (5.2).

Figure 11: H^1 -error at $T = 1$ as a function of the timestep τ for low-regularity initial data.

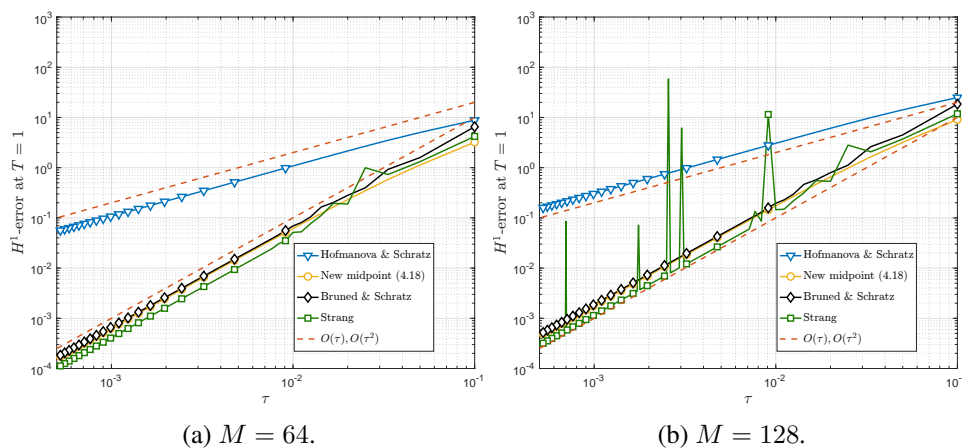


Figure 12: H^1 -error at $T = 1$ as a function of the timestep τ for C^∞ -initial data (5.1).

to converge even faster than the method introduced by Bruned & Schratz for solutions in H^3 , this was also observed in [50].

References

- [1] Y. Alama Bronsard, Y. Bruned, K. Schratz, *Approximations of dispersive PDEs in the presence of low-regularity randomness*. To appear in Foundations of Computational Mathematics. [arXiv:2205.02156](https://arxiv.org/abs/2205.02156).
- [2] Y. Alama Bronsard, Y. Bruned, K. Schratz, *Low regularity integrators via decorated trees*. [arXiv:2202.01171](https://arxiv.org/abs/2202.01171).
- [3] Y. Alama Bronsard, *Error analysis of a class of semi-discrete schemes for solving the Gross-Pitaevskii equation at low regularity*. *J. Comput. Appl. Math.*, **418**, (2023), 114632. doi:10.1016/j.cam.2022.114632
- [4] Y. Alama Bronsard, *A symmetric low-regularity integrator for the nonlinear Schrödinger equation*. *IMA J. Numer. Anal.*, drad093, 2023. doi.org/10.1093/imanum/drad093.
- [5] I. Ampatzoglou, C. Collot, P. Germain, *Derivation of the kinetic wave equation for quadratic dispersive problems in the inhomogeneous setting*. [arXiv:2107.11819](https://arxiv.org/abs/2107.11819).
- [6] G. Bai, B. Li, and Y. Wu. *A constructive low-regularity integrator for the 1d cubic nonlinear Schrödinger equation under the Neumann boundary condition*. *IMA J. Numer. Anal.* doi:10.1093/imanum/drac075
- [7] V. Banica, G. Maierhofer, K. Schratz, *Numerical integration of Schrödinger maps via the Hasimoto transform*. To appear in *SIAM J. Numer. Anal.* [arXiv:2211.01282](https://arxiv.org/abs/2211.01282).
- [8] G. Benettin and A. Giorgilli, *On the Hamiltonian interpolation of near-to-the identity symplectic mappings with application to symplectic integration algorithms*. *J. Stat. Phys.*, **74**, (1994), 1117–1143. doi:10.1007/BF02188219.
- [9] P. B. Bochev and C. Scovel, *On quadratic invariants and symplectic structure*. *BIT Numer. Math.*, **34**, no. 3, (1994), 337–345. doi:10.1007/BF01935643.

- [10] Y. Bruned, A. Chandra, I. Chevyrev, M. Hairer, *Renormalising SPDEs in regularity structures*. J. Eur. Math. Soc. (JEMS), **23**, no. 3, (2021), 869–947. doi:10.4171/JEMS/1025.
- [11] Y. Bruned, K. Ebrahimi-Fard, *Bogoliubov type recursions for renormalisation in regularity structures*. arXiv:2006.05284.
- [12] Y. Bruned, M. Hairer, L. Zambotti. *Algebraic renormalisation of regularity structures*. Invent. Math. **215**, no. 3, (2019), 1039–1156. doi:10.1007/s00222-018-0841-x.
- [13] Y. Bruned, M. Hairer, L. Zambotti. *Renormalisation of Stochastic Partial Differential Equations*. EMS Newsletter **115**, no. 3, (2020), 7–11. doi:10.4171/NEWS/115/3.
- [14] Y. Bruned, D. Manchon. *Algebraic deformation for (S)PDEs*. To appear in J. Math. Soc. Japan. arXiv:2011.05907.
- [15] Y. Bruned, K. Schratz. *Resonance based schemes for dispersive equations via decorated trees*. Forum of Mathematics, Pi, **10**, E2. doi:10.1017/fmp.2021.13.
- [16] N. N. Bogoliubow, O. S. Parasiuk. *Über die Multiplikation der Kausalfunktionen in der Quantentheorie der Felder*. Acta Math. **97**, (1957), 227–266. doi:10.1007/BF02392399.
- [17] J. C. Butcher, *An algebraic theory of integration methods*. Math. Comp. **26**, (1972), 79–106. doi:10.2307/2004720.
- [18] J. Cao, B. Li, and Y. Lin, *A new second-order low-regularity integrator for the cubic nonlinear Schrödinger equation*, IMA Journal of Numerical Analysis (2023). doi:10.1093/imanum/drad017.
- [19] E. Celledoni, D. Cohen, B. Owren, *Symmetric exponential integrators with an application to the cubic Schrödinger equation*. Found. Comput. Math. **8**, (2008), 303–317. doi:10.1007/s10208-007-9016-7.
- [20] P. Chartier and A. Murua, *Preserving first integrals and volume forms of additively split systems*. IMA J. Numer. Anal. **27**, (2007), 381–405. doi:10.1093/imanum/dri000.
- [21] D. Cohen, L. Gauckler, *One-stage exponential integrators for nonlinear Schrödinger equations over long times*. BIT **52**, (2012), 877–903. doi:10.1007/s10543-012-0385-1.
- [22] A. Chandra, M. Hairer. *An analytic BPHZ theorem for regularity structures*. arXiv:1612.08138.
- [23] A. Connes, D. Kreimer, *Hopf algebras, renormalization and noncommutative geometry*. Comm. Math. Phys. **199**, no. 1, (1998), 203–242. doi:10.1007/s002200050499.
- [24] A. Connes, D. Kreimer, *Renormalization in quantum field theory and the Riemann-Hilbert problem I: the Hopf algebra structure of graphs and the main theorem*. Commun. Math. Phys. **210**, (2000), 249–73. doi:10.1007/s002200050779.
- [25] M. Christ, *Power series solution of a nonlinear Schrödinger equation*. In Mathematical aspects of nonlinear dispersive equations, volume 163 of Ann. of Math. Stud., pages 131–155. Princeton Univ. Press, Princeton, NJ, 2007.
- [26] Y. Deng, Z. Hani, *Full derivation of the wave kinetic equation*. To appear in Invent. Math. arXiv:2104.11204.
- [27] Y. Deng, Z. Hani, *On the derivation of the wave kinetic equation for NLS*. Forum of Mathematics, Pi, **9**, (2021), e6. doi:10.1017/fmp.2021.6.

- [28] E. Faou, *Geometric Numerical Integration and Schrödinger Equations*. European Math. Soc. Publishing House, Zürich 2012.
- [29] Y. Feng, G. Maierhofer, K. Schratz, *Long-time error bounds of low-regularity integrators for nonlinear Schrödinger equations*. To appear in Math. Comput. arXiv: 2302.00383.
- [30] L. Gauckler and C. Christian, *Splitting integrators for nonlinear Schrödinger equations over long times*, Found. Comput. Math. **10**, no. 3, (2010), 275–302. doi:10.1007/s10208-010-9063-3.
- [31] Z. Guo, S. Kwon, T. Oh, *Poincaré-Dulac normal form reduction for unconditional well-posedness of the periodic cubic NLS*, Comm. Math. Phys. **322**, no. 1, (2013), 19–48. doi:10.1007/s00220-013-1755-5.
- [32] M. Gubinelli, *Rough solutions for the periodic Korteweg-de Vries equation*. Comm. Pure Appl. Anal. **11**, no. 4, (2012), 709–733. doi:10.3934/cpaa.2012.11.709.
- [33] M. Hairer, *A theory of regularity structures*. Invent. Math. **198**, no. 2, (2014), 269–504. doi:10.1007/s00222-014-0505-4.
- [34] K. Hepp, *On the equivalence of additive and analytic renormalization*. Comm. Math. Phys. **14**, (1969), 67–69. doi:10.1007/BF01645456
- [35] E. Hairer, C. Lubich, *Symmetric multistep methods over long times*. Numer. Math. **97**, (2004), 699–723. doi:10.1007/s00211-004-0520-2.
- [36] E. Hairer, C. Lubich, G. Wanner, *Geometric Numerical Integration. Structure-Preserving Algorithms for Ordinary Differential Equations*. Second edition, Springer, Berlin 2006.
- [37] M. Hochbruck, A. Ostermann, *Exponential integrators*. Acta Numer. **19**, (2010), 209–286. doi:10.1017/S0962492910000048.
- [38] M. Hochbruck, J. Leibold, A. Ostermann, *On the convergence of Lawson methods for semilinear stiff problems*. Numer. Math. **145**, (2020), 553–580. doi:10.1007/s00211-020-01120-4.
- [39] M. Hofmanová, K. Schratz, *An exponential-type integrator for the KdV equation*. Numer. Math. **136**, (2017), 1117–1137. doi:10.1007/s00211-016-0859-1.
- [40] H. Holden, K. H. Karlsen, K.-A. Lie, N. H. Risebro, *Splitting for Partial Differential Equations with Rough Solutions*. European Math. Soc. Publishing House, Zürich 2010.
- [41] A. Iserles, G. R. W. Quispel and P. S. P. Tse, *B-series methods cannot be volume-preserving*. BIT Numer. Math. **47**, (2007), 351–378. doi:10.1007/s10543-006-0114-8.
- [42] A. Iserles, A. Zanna, *Preserving algebraic invariants with Runge–Kutta methods*. J. Comp. Appl. Math. **125**, no. 1-2, (2000), 69–81.
- [43] G. Y., Kulikov, *Symmetric Runge–Kutta methods and their stability*. Russian Journal of Numerical Analysis and Mathematical Modelling **18**, no. 1, (2003), 13–41.
- [44] J. D. Lawson, *Generalized Runge–Kutta processes for stable systems with large Lipschitz constants*. SIAM J. Numer. Anal. **4**:372–380 (1967).
- [45] B. Leimkuhler, S. Reich, *Simulating Hamiltonian dynamics*. Cambridge Monographs on Applied and Computational Mathematics 14. Cambridge University Press, Cambridge, 2004.

- [46] B. Li, S. Ma, K. Schratz, *A semi-implicit low-regularity integrator for Navier-Stokes equations* arXiv:2107.13427.
- [47] B. Li, Y. Wu, *An unfiltered low-regularity integrator for the KdV equation with solutions below H^1* . arXiv:2206.09320.
- [48] V.T. Luan, A. Ostermann, *Exponential B-series: The stiff case* SIAM J. Numer. Anal. **51**, no. 6, (2013), 3431–3445. doi:10.1137/130920204
- [49] C. Lubich, *On splitting methods for Schrödinger-Poisson and cubic nonlinear Schrödinger equations*. Math. Comp. **77**, no. 4, (2008), 2141–2153. doi:10.1090/S0025-5718-08-02101-7.
- [50] G. Maierhofer, K. Schratz, *Bridging the gap: symplecticity and low regularity in Runge–Kutta resonance-based schemes*. arXiv:2205.05024.
- [51] R.I. McLachlan, G.R.W. Quispel, *Splitting methods*. Acta Numer. **11**, (2002), 341–434. doi:10.1017/S0962492902000053.
- [52] H. Z. Munthe-Kaas, A. Lundervold, *On post-Lie algebras, Lie-Butcher series and moving frames*. Found. Comput. Math. **13**, (2013), 583–613.
- [53] A. Ostermann, F. Rousset, K. Schratz, *Error estimates of a Fourier integrator for the cubic Schrödinger equation at low regularity*. Found. Comput. Math. **21**, (2021), 725–765. doi:10.1007/s10208-020-09468-7.
- [54] A. Ostermann, F. Rousset, K. Schratz, *Fourier integrator for periodic NLS: low regularity estimates via discrete Bourgain spaces*. To appear in J. Eur. Math. Soc. (JEMS), DOI10.4171/JEMS/1275.
- [55] A. Ostermann, K. Schratz, *Low regularity exponential-type integrators for semilinear Schrödinger equations*. Found. Comput. Math. **18**, (2018), 731–755 doi:10.1007/s10208-017-9352-1.
- [56] F. Rousset, K. Schratz, *A general framework of low regularity integrators*, SIAM J. Numer. Anal. **4**, (2022) 127–152 10.2140/paa.2022.4.127.
- [57] F. Rousset, K. Schratz, *Convergence error estimates at low regularity for time discretizations of KdV*. To appear in Pure and Applied Analysis arXiv:2102.11125.
- [58] J.M. Sanz-Serna, M.P. Calvo, *Numerical Hamiltonian Problems*. Chapman and Hall, London, 1994.
- [59] J.M. Sanz-Serna, *Runge-Kutta schemes for Hamiltonian systems*. BIT Numer. Math. **28**, (1988), 877–883 doi:10.1007/BF01954907.
- [60] M. Thalhammer, *Convergence analysis of high-order time-splitting pseudospectral methods for nonlinear Schrödinger equations*. SIAM Journal on Numerical Analysis, 50(6):3231–3258, 2012. doi.org/10.1137/12086637.
- [61] Y. Wang, X. Zhao, *A symmetric low-regularity integrator for nonlinear Klein-Gordon equation*, Math. Comp. **91**, (2022) 2215–2245 10.1090/mcom/3751.
- [62] Y. Wu, F. Yao, *A first-order Fourier integrator for the nonlinear Schrödinger equation on \mathbb{T} without loss of regularity*, Mathematics of Computation 91.335 (2022): 1213–1235 10.1090/mcom/3705.
- [63] Y. Wu, X. Zhao, *Embedded exponential-type low-regularity integrators for KdV equation under rough data*, BIT Numer. Math. **62**, (2022) 1049–1090 10.1007/s10543-021-00895-8.

- [64] W. Zimmermann. *Convergence of Bogoliubov's method of renormalization in momentum space*. *Comm. Math. Phys.* **15**, (1969), 208–234. doi:10.1007/BF01645676.